The role of 14-3-3 proteins in spinal cord commissural neuron axon guidance and oligodendrocyte differentiation

Ricardo Alchini

A thesis submitted to McGill University in partial fulfillment of the requirements of the degree of

Doctor of Philosophy in Neurosciences

Integrated Program in Neuroscience

McGill University, Montreal

August 2017

List of contents

Acknowledgements

This thesis is the result of a long journey that literally started in the other side of the world and became more than just its academic achievements, but also a self-learning experience. First of all, I have to thank Dr Alyson Fournier, my supervisor, for giving me the opportunity to learn so much during my PhD. Thank you for allowing me to try so many techniques and for teaching me the importance of building trust between supervisor and students. Thank you also to the members of my advisory committee, Dr Ed Ruthazer and Dr Tim Kennedy, for the patience and creative insights given during these years.

I want to express also my deepest appreciation and admiration to Dr Josephine Nalbantoglu. Thank you for believing in me and constantly motivating me with your wise advice. Thank you for being such an approachable person and an example of an engaging leader. Thank you, Jo! And also, thank you to the IPN staff for their support and diligence in your work (and for listening to me when I had to vent =)).

Many thanks to the current and past members of the Fournier lab, especially Camille (easy, breezy, beautiful, Flower Girl), R Sanz and MP. I'm happy I had the chance to start my PhD with such great people, and grow together with you after these years. It will sound like a cliché if I say that you taught me so much, but it's true. Thanks also to Isabel, Angie, Mardja, Barbara, Simon, Alexandra, Julia, Tadayuki, Chris and Gino! My lab experience would not have been the same without each one of you.

And for the company during the late-night experiments, the lunch/linner/lupper/dunch time and random conversations, thank you so much to my other

IPN/BTRC people Ian, Elena, Zahraa, Mina, Daniel, Farin, Marie-Claude, Ana, Jeanne, Daryan.

I'd like to acknowledge how much I owe these last 6 years to my (natural or acquired) family. My coolest feelings to the coolest scientists of Montreal, Omar, Cecilia and Luisa (and by extension Luciana, Joao Victor and Shawn, and the coolest babies Theo, Arthur and Sophia). Really cool. Cool.

To my parents and sister, Vergilio, Liliana and Rebeca, "muito obrigado". For your trust, even though all the doctoral story sounded alien and Canada is so far from home. Thank you for keeping wishing me the best in this long journey. Thank you also to my Quebec family, Pierre-Luc and Phylippe, and to all the friends I made here in Montreal (you are all included in thought here).

And to conclude, my most special thanks to Ronan, my husband and partner for life. Thank you for being always there, despite the late hours of work, the stressful deadlines, and the uncertainties about the future. Thank you for being this understanding and caring person. I wouldn't have made this far without you, and I'm so glad we made it together. Everything is more fun with your bubbly attitude. ;)

Contributions of authors

Abstract and Résumé:

Ricardo Alchini: wrote the text.

Alyson Fournier: edited the text.

Marie-Claude Bélanger: edited the French language (Résumé).

Chapter 1: Introduction

Ricardo Alchini: wrote the text.

Alyson Fournier: edited the text.

Chapter 2:

Ricardo Alchini: designed and performed the experiments. Performed the analysis. Wrote the text.

Timothy Kennedy: designed the ectopic Netrin-1 expression experiment.

Alyson Fournier: Edited the text.

Chapter 3:

Ricardo Alchini: designed and performed the experiments. Analyzed the results and made the figures. Wrote the text.

Christopher Kent: co-designed and performed some of the turning assays on figure 3.2.

Luyang (Simon) Hua: performed the co-immunoprecipitations for figure 3.3C and analyzed the data for the turning assays on figure 3.7.

Andrew Kaplan: performed the 14-3-3ζ co-immunoprecipitation for figure 3.3C.

Jonathan DeGeer: performed the CRIB pulldown experiments in figures 3.6A and 3.6B.

Isabel Rambaldi: performed the Rac G15A pulldowns in figure 3.6C.

Timothy Kennedy: supplied Netrin-1 related reagents and contributed to the rationale of the project.

Nathalie Lamarche-Vane: co-designed the CRIB pulldowns in figure 3.6A, B.

Quenten Schwarz: provided the 14-3-3ζ knockout embryos.

Alyson Fournier: co-designed the experiments and edited the text.

Chapter 4:

Ricardo Alchini: designed and executed the experiments. Analyzed the data and wrote the manuscript.

Ana Amaral: performed some of the cell culture experiments in the figures 4.3 and 4.4.

Mark Kotter: contributed to the rationale of the project.

Alyson Fournier: co-designed the research and edited the text.

Chapter 5:

Ricardo Alchini: wrote the text.

Alyson Fournier: edited the text.

Abstract

The current work seeks to understand some of the molecular mechanisms that act regulating the development of the central nervous system (CNS). We focus on the role of a family of adaptor proteins called 14-3-3s. The first two chapters are devoted to the field of axon guidance. During development, neurons must project their axons towards appropriate targets in order to establish physiologically relevant connections. To navigate properly they must interpret a complex molecular environment, a role that is fulfilled by the growth cone. Our group has previously identified 14-3-3 proteins, a family of adaptor proteins, as being major constituents of growth cones. Their importance for axonal repulsion has been described linking these proteins to the modulation of repulsion responses via antagonism to the protein kinase A. First, we describe the local ex utero electroporation technique we designed to observe axonal development in organotypic cultures of the spinal cord, and then we offer examples of its use. Next, we present this use of *ex utero* electroporation as a starting point to study the role of 14-3-3 proteins in the development of the spinal cord circuitry, which is further explained through the investigation of the downstream signaling. We show that 14-3-3 loss of function leads to disorganization of spinal cord commissural fibers *ex vivo.* This phenotype is attributed to an impairment in responsiveness to Netrin, an important attractant expressed by the floorplate. We implicate 14-3-3 loss of function results in abnormal activation of the small GTPase Rac1. We describe the 14-3-3ζ isoform as a key player in this process and demonstrate that a lack 14-3-3ζ results in guidance errors of commissural fibers projecting to the floorplate. Finally, we wanted to explore the role of 14-3-3s in different

cell types of the CNS. Chapter 3 examines the expression pattern of 14-3-3 proteins in differentiating oligodendrocytes, the myelinating cells of the CNS. We show that most 14-3-3 isoforms are expressed by oligodendrocytes in vitro, and that 14-3-3 loss of function improves their differentiation. Further studies will define the molecular mechanisms involved in this process. Together we describe the importance of 14-3-3 proteins in the guidance of pre-crossing commissural neurons and show that 14-3-3 proteins are potential targets for future remyelination therapies.

Résumé

Le travail actuel vise à comprendre certains des mécanismes moléculaires qui agissent sur la régulation du développement du système nerveux central (SNC). Nous nous concentrons sur le rôle d'une famille de protéines adaptatrices qui s'appelent 14-3-3. Les deux premiers chapitres sont consacrés au guidage axonal. Au cours du développement, les neurones doivent projeter leurs axones vers les cibles appropriées afin d'établir des connexions physiologiquement pertinentes. Pour se faire, les neurones doivent interpréter l'environnement moléculaire complexe dans lequel ils se trouvent, rôle qui est accompli par les cônes de croissance. Notre groupe a déjà identifié 14-3-3s, une famille de protéines adaptatrices, comme étant un constituant majeur des cônes de croissance. Leur importance dans la répulsion axonale a été montrée dans différents modèles, associant ces protéines à la modulation des réponses de répulsion via l'inhibition de la protéine kinase A. Premièrement, nous décrivons la technique d'électroporation *ex utero* que nous avons conçu pour observer le développement axonal dans des cultures organotypiques de la moelle épinière, et nous proposons des exemples de son utilisation. Prochainement, nous présentons cette utilisation de l'électroporation *ex utero* comme point de départ pour étudier le rôle des protéines 14-3-3 dans le développement du circuit de la moelle épinière, rôle étant élucidé par l'étude de la signalisation moléculaire en aval de ces protéines. Nous montrons que la perte de fonction des 14-3-3s conduit à une désorganisation des fibres commissurales de la moelle épinière *ex vivo*. Ce phénotype est attribué à une altération de la signalisation de Netrin, une molécule chemoattractive importante exprimée par la plaque du plancher.

Cette altération est le résultat d'une activation anormale de la petite GTPase Rac1. La protéine 14-3-3ζ est fortement impliquée dans ce processus, et son absence atténue l'attraction des fibres commissurales par la plaque du plancher. Finalement, nous voulions explorer le rôle des 14-3-3 dans différents types cellulaires du SNC. Le chapitre 3 examine l'expression des protéines 14-3-3 durant la différenciation des oligodendrocytes, les cellules qui produisent de la myéline, une substance qui isole les axones et améliore la transmission des potentiels d'action dans le SNC. Nous montrons que la plupart des isoformes de14-3-3 sont exprimées par des oligodendrocytes *in vitro*, et que la perte de la fonction des 14-3-3 améliore leur différenciation. De futures études décriront les mécanismes moléculaires impliqués dans ce processus. En conclusion, nous avons confirmé l'importance de 14-3-3s durant le stade de développement précédant la traversée des axones commissuraux au niveau de la ligne médiane, et nous avons identifié les protéines 14-3-3s comme étant des cibles potentielles pour de futures thérapies remyélinantes.

Abbreviation list

AKAP: A-kinase anchoring protein

ANOVA: Analysis of variance

AMP: Adenosine monophosphate

ATP: Adenosine triphosphate

cAMP: Cyclic adenosine monophosphate

β-Pix: β-PAK interacting exchange factor

Boc: Brother of CDO

BMP: Bone morphogenic protein

CaMK: Calcium/ calmodulin-dependent kinase

Cdc42: Cell division controlling protein 42

CMV: Cytomegalovirus

CNP: 2'3' -Cyclic Nucleotide 3' Phosphodiesterase

Comm: Commissureless

CRIB: Cdc242- and Rac-interactive binding domain

DBE: Dibenzyl ether

Dbx2: Developing brain homeobox

DCC: Deleted in colorectal cancer

DIV: Days *in vitro*

DMSO: Dimethyl sulfoxide

DNA: Deoxyribonucleic acid

DOCK-180: Dedicator of cytokinesis

DSCAM: Down syndrome cell adhesion molecule

ECL: Enhanced chemiluminescence substrate

EDTA: Ethylenediaminetetracetic acid

EGTA: Ethylene glucol-bis(β-aminoethyl ether)- N,N,N',N'-tetraacetic acid

EGF: Endothelial growth factor

Erk: External signal-regulated kinase

FAK: Focal adhesion kinase

FGF: Fibroblast growth factor

FLIM: Fluorescence lifetime imaging microscopy

FLK: Flagellar regulator

FoxO: Forkhead box

FRET: Fluorescence resonance energy transfer

GAP: GTPase-activating proteins

GAPDH: Glyceraldehyde 3-phosphate dehydrogenase

GC: Growth cone

GCN1: General control of amino-acid synthesis

GDI: Guanine nucleotide dissociation inhibitor

GDP: Guanine diphosphate

GEF: Guanine exchange factors

GFP: Green fluorescent protein

Gpr17: G protein coupled-protein receptor

GST: Glutathione S transferase

GTP: Guanine triphosphate

HDAC: Histone deacetylase

HEK293T: Human embryonic kidney 293T (cells)

HRP: Horseradish peroxidase

HSV: Herpes-simplex virus

iDisco: Immunolabelling enabled three-dimensional imaging of solvent cleared organs

Id2/4: Inhibitor of DNA binding

IGF: Insulin-like growth factor

IgG: Immunoglobulin G

IPTG: Isopropyl β-D-1-thiogalactopyranoside

Lhx: Lim homeobox protein

LIM: Lin11, Isl-1 & Mec-3

LIMK: Lim domain kinase

MAPK: Mitogen-activated protein kinase

MAP2: Microtubule associated protein 2

Mash1: Mammalian achaete-scute homolog-1

MS: Multiple sclerosis

Math-1: Mouse athonal 1

mTOR: Molecular target of rapamycin

MBP: Myelin basic protein

mRNA: Messenger ribonucleic acid

NG2: Neuron-glial antigen 2

Olig2: Oligodendrocyte transcription factor 2

OPC: Oligodendrocyte progenitor cell

PAK: p21 activated kinase

Pax7: Paired box protein 7

PBS: Phosphate buffer solution

PDGF: Platelet derived growth factor

PFA: Paraformaldehyde

PIP2: Phosphatidylinositol 4,5-biphosphate

PI3K: Phosphoinositide 3-kinase

PKA: Protein kinase A

PKC: Calcium dependent kinase

PMSF: Phenylmethane sulfonyl fluoride

PVDF: Polyvinylidene fluoride

PSA-NCAM: Polysialylated-neural cell adhesion molecule

Rac: Ras-related c3 botulinum toxin substrate

Raf: Rapidly accelerated fibrosarcoma (protein)

RIPA: Radioimmunoprecipitation assay (buffer)

RNA: Ribonucleic acid

RNAi: Interference RNA

Robo: Roundabout

SCN: Spinal cord commissural neuron

SDK: Protein sidekick precursor

SDS-PAGE: Sodium duodocyl sulfate – polyacrylamide gel electrophoresis

Shh: Sonic hedgehog

shRNA: Short hairpin ribonucleic acid

Src: Sarcoma (used to name a protein)

Tag-1: Transient axonal glycoprotein 1

TAT: Trans-activator of transcription

Tcf4: Transcriptional factor 4

Tgf: Transforming growth factor

THF: Tetrahydrofuran

TIAM1: T-lymphoma invasion and metastasis-inducing protein 1

tPA: Tissue-type plasminogen activator

TRIO: Triple functional domain protein

WASP: Wiskott–Aldrich syndrome protein

WAVE: WASP-family verprolin-homologous protein

YY1: Yin Yang 1 transcription factor

Figure list

Introduction

Chapter 1 – Introduction

During development neurons must project their axons to target domains and establish physiologically relevant connections. Axons extend through a complex environment requiring the axon to modify cell surface expression of receptor molecules and intracellular signalling pathways with tight spatial and temporal control. Switching molecular signalling on and off can by regulated by members of the 14-3-3 family of adaptor proteins. Upon reaching their targets, some nerve fibers are myelinated to allow for efficient transmission of nerve impulses. The myelination depends on the proper differentiation of cells called oligodendrocytes, and the wrapping of the mature axons by their processes. Similar to neurons, cell signalling in oligodendrocytes is regulated spatially and temporally by a number of 14-3-3 client proteins to affect the final myelination process. In the current work, we sought to analyze the role of 14-3-3 proteins as regulators of axon guidance and oligodendrocyte differentiation.

1.1 – Historic background of axon guidance

1.1.1 – The axon guidance field through the years

The field of axon guidance originated in the late XIXth century when Santiago Ramon y Cajal obtained the clearest CNS superstructure images for the period and demonstrated that the CNS was formed by cells and not a reticulum (Finger, 1994). While trying to perfect Golgi's technique for neuronal staining, Cajal examined several stages of brain

development to produce high resolution preparations of neuronal projections. He later discovered that his staining technique was more efficient at stages that preceded the formation of the myelin sheaths that wrap the axons. By comparing different developmental stages Cajal described the morphology of the cells in the CNS and described the development of several patterns of neuronal projections in the cerebellum, retina, olfactory bulb, cerebral cortex, spinal cord and brainstem (Cajal, 1889). This work can be considered the first in the field of axon guidance, which studies the development of the neuronal projections.

While observing spinal cord sections at different stages of chick embryonic development, Cajal described the existence of specializations on the tips of some of the neuronal processes (Cajal, 1890). These were the growth cones, dynamic structures that are responsible for guiding growing neuronal processes. Cajal developed the hypothesis that the growth cones have in their constitution some property to sense the environment and, based on cues that are present in the milieu, project to the correct regions. Hence, the growth cones should be the cellular structures responsible for promoting axonal outgrowth and pathfinding.

1.1.2 - The discovery of the chemotaxis

In spite of Cajal's limited tools to investigate the molecular mechanisms of axon guidance, he compared different retina sections and based on the morphological progression of the axonal outgrowth, he hypothesized that gradients of molecules guided axons to reach their target (Cajal, 1892). He proposed that the molecular cues would be

expressed at the target, where they reach their highest concentration, and gradually diffuse through the tissues to the location of the growth cones.

The neuronal population used for most of the project in this thesis, the dorsal spinal cord commissural neurons (SCNs), was also accurately described by Cajal, who suggested that neurons in the dorsal spinal cord project their axons towards the ventral midline attracted by diffusible factors expressed at the floor plate (Cajal, 1899). However, no molecular gradient was identified in the nervous system at that time.

The idea that neurons responded to gradients of molecules was reinforced in the 1940's when Roger Sperry studied axonal projections from the retina and concluded that the axons were guided to specific locations. He rotated newt eyes and saw that the retinal cells in specific regions of the retina would always project to the same region of the tectum, independently of the orientation of the eye (Sperry, 1943). Sperry would later define the term chemoaffinity as the ability of the neuronal axons to be attracted by their future targets (Sperry, 1963; Sperry and Miner, 1949).

In the following decades, the extensive work of Rita Levi-Montalcini identified NGF as a chemoattractant and neurotrophic factor. She initially observed that deprivation of peripheral tissue provoked a reduction in the number of cells of the lateral motor column of the spinal cord and concluded that their target nerve cells secreted a substance that affected the survival of the cells in the spinal cord (Hamburger, 1934, 1939; Levi-Montalcini and Levi, 1942). To further understand the nature of the substance she co-cultured nerve explants with tumor cells that released the unidentified molecule and discovered the tumor cells attracted nerve fibers (Levi-Montalcini and Hamburger, 1953). Levi-Montalcini named the substance as "Nerve Growth Factor", the first growth factor to

be described and the first “substance” to be shown to have a role in directing axons. With the help of Stanley Cohen she would isolate NGF as a single protein, later confirming that NGF alone was able to promote neuronal survival and chemotaxis (Cohen et al., 1954; Levi-Montalcini, 1964).

1.1.3 – The axon guidance field in the present

Following the discovery and isolation of NGF, the search for guidance molecules and their receptors accelerated. Commissural neurons became a popular model to identify molecular mechanisms underlying axon guidance because of their stereotypical projection pattern and relatively accessible anatomical location. By studying their projection pattern, some of the first chemoattractants were discovered and the concept of chemorepulsion, where a protein can guide the growth cones away from a target, was better established (Kennedy et al., 1994; Parra and Zou, 2010; Placzek et al., 1990a; Placzek et al., 1990b; Serafini et al., 1994; Shirasaki et al., 1995; Tessier-Lavigne et al., 1988). The contemporary axon guidance field continues to use this system to identify the guidance receptors that a cell expresses on the surface of the growth cone, in relation to the total pool of receptor expressed by a neuron. It has been demonstrated that individual guidance cues can trigger different responses by neurons, depending on the cell surface receptors they express (Keino-Masu et al., 1996; Long et al., 2004; Shirasaki et al., 1995).

1.2 – Function and specification of SCNs

SCNs have been widely studied in the axon guidance field as they can be readily obtained from the developing spinal cord (Moore and Kennedy, 2001; Shekarabi et al., 2005). Further, their trajectory through the developing spinal cord relies on a range of guidance cues and cognate receptors that are expressed in a carefully regulated temporal and spatial manner. The details of its development will be discussed in the following sections.

The commissural circuits form a complex network of projections interconnecting both sides of the CNS. Commissures are present at all levels of the CNS, where neurons extend their axons across the midline to build circuits that are essential for the biological integration of CNS functions (Vulliemoz et al., 2005). In the spinal cord, the SCNs form the circuitry in charge of the coordination of bilateral motor behaviors, which is fundamental for alternate and synchronized activities. This integrated information is transmitted as a somatosensory relay to the upper brain regions. SCNs are part of a mixed neuronal population that is located in the dorsal level comprising the classes of neurons named from dI1 to dI6 (Chizhikov and Millen, 2005).

The proprioceptive dI1 class is located at the dorsal most position of the spinal cord, close to the roof plate, and projects to the cerebellum via the spinocerebellar and the cuneocerebellar tracts. They are derived from Math1 expressing progenitors, and can be identified by two LIM transcription factors, Lhx2 and Lhx9 (Helms and Johnson, 1998; Lee et al., 1998). Ngn1/2-expressing progenitors give rise to dI2 interneurons, which project towards the sensory regions of the brain (Gowan et al., 2001). Mash1-positive progenitors originate the dI3–5 cells that are relay neurons or the somatosensory pathway (Qian et al., 2002). The dI6 inhibitory neurons are likely to be born from

Pax7+/Dbx2+/Mash1 cells (Helms and Johnson, 2003; Müller et al., 2002). Among these, the dI1 cells are the ones that have been most commonly used as a model for SCN development.

1.2.1 – SCN pre-crossing navigation

After the dI1 neuron is specified, its axon is oriented towards the ventral aspect of the spinal cord by a series of well-orchestrated guidance responses (Fig 1.1). Chemorepulsion of SCN axons away from the dorsal roof plate is a key first step for SCN axon guidance mediated by repellents including Bone Morphogenetic Proteins (BMPs) BMP7 and Draxin (Fig 1.1A) (Augsburger et al., 1999; Islam et al., 2009). This roof plate repulsion is thought to direct the axons towards the midline and to serve as a pushing force to increase their elongation rate (Phan et al., 2010).

Pushed away by these dorsal repellents, SCNs axons project ventrally in compact bundles until they start perceiving guidance signals emanating from the floor plate. The development of *ex vivo* models in which spinal cord tissue was co-cultured with pieces of floor plate in three-dimensional collagen gels was essential for the investigation of SCN axon navigation. Netrin-1 was the first guidance cue identified as a floor-plate-derived chemoattractant for SCNs (Fig 1.1B) (Kennedy et al., 1994), signaling through a receptor, DCC (Keino-Masu et al., 1996). Netrin-1 mRNA can be detected in spinal cords during the navigation of SCNs, forming a high ventral to low dorsal gradient, which has also been suggested by immunostainning of the protein (Kennedy et al., 1994; Kennedy et al., 2006). DCC-deficient mice have misprojections in the majority of the SCNs, and die within

a few hours from birth, while very few commissural axons reach the midline in Netrin-1 null animals (Fazeli et al., 1997). This indicates a crucial role for Netrin-1/ DCC signaling in the development of the organism, but also opened questions about the existence of other receptors for Netrin-1.

The Down syndrome cell adhesion molecule (DSCAM) was shown to be another receptor to Netrin-1 (Ly et al., 2008). *In ovo* knockdown of DSCAM with RNAi disturbed commissural axon guidance (Liu et al., 2009; Ly et al., 2008), although the spinal commissures were observed to form normally in DSCAM knockout mice, suggesting that DSCAM has only a secondary role in SCN axon guidance. The G protein-coupled adenosine receptor A2b was also shown to bind to Netrin1 and regulate SCN axon outgrowth (Palmesino et al., 2012). More recently, the amyloid precursor protein (APP) was shown to interact with DCC and act as a co-receptor for netrin-dependent attraction of SCNs (Rama et al., 2012). Thus, several Netrin-1 receptors seem to participate in the guidance of SCN axons towards the midline. The extent of their contribution remains to be further investigated.

In addition to Netrin-1 a number of other attractive cues synergistically direct SCN axons towards the midline. Shh functions as an attractant by engaging the receptor Boc while VEGF attracts Flk1-positive axons (Charron et al., 2003; Okada et al., 2006; Ruiz de Almodovar et al., 2011). Absence of these other guidance cues in animal models has suggested that they play less pronounced roles as attractants, since their phenotypes are somewhat mild, with the animals being postnatally viable and their SCNs reaching the ventral midline. This collaborative role for different guidance cues has been recently reinforced by *in vitro* studies utilizing shallow gradients of netrin and Shh (Sloan et al.,

2015). Sloan and colleagues showed that dissociated SCNs respond to steep but not shallow gradients of Shh or Netrin-1, which would be similar to the gradients *observed in vivo*. When the axons were presented to a combination of shallow Shh and Netrin-1 gradients, their sensitivity to the resulting gradient was heightened and the cells turned towards gradients that separately would be ineffective.

1.2.2 – Midline-mediated switches in sensitiveness to guidance cues

Upon reaching the floor plate, SCNs selectively cross the midline and then acquire sensitivity to repellents in the midline including members of the Slit, Ephrin, and Semaphorin families to impede recrossing (Black and Zipursky, 2008; Evans and Bashaw, 2010; Shirasaki et al., 1998). These repellents also mediate repulsion and targeting of ipsilaterally projecting neurons.

Of these repellent mechanisms, Roundabout (Robo)/Slit signaling is one of the best studied. An abundance of work has been performed in the *Drosophila* model, where glial cells at the midline of the ventral chord act orthologously to the vertebrate floor plate (Kidd et al., 1998a; Kidd et al., 1998b). In *Drosophila,* pre-crossing neurons express Comm, a molecule that restricts expression of the Slit receptor Robo to the late endocytic pathway and prevents the receptor from reaching the cell surface. Thus, the sensitivity of pre-crossing commissural growth cones to repellent Slit is silenced and allows midline crossing (Keleman et al., 2002; Keleman et al., 2005). After midline crossing Comm is downregulated, Robo trafficking to the growth cone surface is restored mediating sensitivity to Slit and preventing recrossing (Kidd et al., 1999; Kidd et al., 1998a).

Frazzled, the *Drosophila* ortholog of the Netrin receptor DCC, is implicated in the regulation of Comm expression and this function is Netrin-independent, which suggests an interplay between netrin-signaling and sensitivity to repellents (Yang et al., 2009).

In vertebrates, three Slits combine their effect to regulate SCN axon guidance at the midline, acting via the synergistic receptors Robo1 and Robo2 (Long et al., 2004). The temporal regulation of SCNs responsiveness to Slits between pre-crossing and post-crossing stages follow a similar pattern than in *Drosophila*, although a vertebrate homologue to Comm has only recently been described (Evans and Bashaw, 2010; Justice et al., 2017). Robo3, with its several splice variants has been suggest to regulate Robo 1 and 2 sensitivity (Black and Zipursky, 2008). Robo3.1 is expressed in pre-crossing SCNs rendering them insensitive to Slit, while Robo3.2 expression substitutes for it after it in post-crossing SCNs. How the switch between Robo 3.1 and Robo 3.2 is regulated and their effects on Robo 1 and 2 remains vastly unexplained.

Simultaneously to their gain in sensitivity to midline repellents, SCN axons lose their responsiveness to Netrin-1 after reaching the floor plate (Shirasaki et al., 1998). Spinal cord openbooks from rat embryos were co-cultured with grafted floor plate tissue at lateral position, either at pre-crossing position or at post-crossing position, observing that pre-crossing SCN axons were re-routed towards the ectopic floor plate, while post-crossing axons were not. In *Xenopus* SCNs, netrin-attraction can be silenced in the presence of Slit. Slit induces the formation of a complex between Robo and DCC, resulting in inhibition of DCC signaling activity (Stein and Tessier-Lavigne, 2001).

1.2.3 – Longitudinal projection of SCNs

After crossing the midline and changing their responsiveness to the aforementioned guidance cues, SCNs project their axons towards the encephalon. The rostrocaudal extension of these SCN axons is oriented by gradients of two proteins, Wnt and Shh, which form two opposite gradients that act synergistically (Fig 1.1C) (Lyuksyutova et al., 2003; Yam et al., 2012). Several members of the Wnt family form attractive high rostral to low caudal gradients in the neural tube (Lyuksyutova et al., 2003). In contrast, Shh forms a repellent high caudal to low rostral gradient (Yam et al., 2012). A cooperative effect between these two gradients was initially hypothesized, but an interplay between Shh and Wnt signaling has only been shown in other systems (Briggs et al., 2016; Domanitskaya et al., 2010; Zhou et al., 2015).

1.3 – Cellular and molecular basis of axon guidance

1.3.1 – Growth cone: the cellular structure responsible for axon guidance

Axons recognize their complex environment thanks to highly motile structures called growth cones. The motility of growth cones is highly due to the dynamic regulation of their cytoskeleton, which is mostly constituted by microtubules and filamentous actin (Dent et al., 2011). Microtubules are polarized polymers that elongate through the axon shaft and the central domain of the growth cone. They are formed by innumerous repetitions of 13 protofilaments of α and β-tubulin organized around a hollow center. Anchored to the central domain, there is a network of finer fibers, the actin cytoskeleton, which is

composed by an ensemble of globular actin monomers. Actin cytoskeleton forms the peripheral domain of the growth cone, which is responsible for providing its shape and motility.

The dynamic rate of assembly and disassembly of the actin cytoskeleton can confer its ability to remodel into sheet-like and rod-like protrusions, respectively called lamellipodia, and filopodia. While filopodia bear several axon guidance receptors at their tips, lamellipodia are responsible for controlling the growth cone area through their expansion movements (Pacheco and Gallo, 2016).

1.3.2 – Rho GTPases

The Rho GTPase family plays an essential role in the remodeling of the growth cone cytoskeleton. This family is part of the Ras superfamily and consists, in mammalians, of 22 different members that can be subclassified into 8 groups (Ridley, 2006). Among these proteins, Rho, Rac and Cdc42 are the best studied members and have been associated with the formation of stress fibers, lamellipodia and filopodia, respectively. Their functions were largely studied in fibroblasts via the microinjection of mutant proteins and the observation of the actin cytoskeletal phenotypes (Nobes and Hall, 1995; Ridley and Hall, 1992; Ridley et al., 1992). These proteins are also known for their roles in regulating cell motility, cell polarity, axon guidance, vesicle trafficking and cell cycle.

Rho GTPases cycle between an active GTP-bound conformation and an inactive GDP-bound conformation (reviewed in Hodge and Ridley, 2016). Such cycling is dependent on 3 types of proteins. Guanine exchange factors (GEFs) activate the function

of small GTPases by promoting by exchanging GDP for GTP; GTPase -activating proteins (GAPs) suppress the activity of small GTPases by increasing the GTP hydrolysis rate of the GTPase; and guanine nucleotide dissociation inhibitors (GDIs) lock small GTPases in an inactive conformation and regulate the subcellular localization of the GTPases, impeding them from reaching the membrane domains where they would be activated by GEFs (Cherfils and Zeghouf, 2013; Huang et al., 2017; Rossman et al., 2005).

Rho GTPases are activated by various cell-surface receptors, such as integrins cadherins, cytokine, tyrosine kinase and G-coupled receptors. Downstream to Rho GTPases, we can find a number of effector proteins including kinases, actin regulators and adaptor proteins. These pathways evoke cell responses that vary according to cell type and the stimulus received. The spatiotemporal regulation of different Rho GTPases are important to determine their activity.

There are also proteins called atypical GTPases, which do not depend on GTP-GDP cycling, hence not requiring also GEFs and GAPs for their activity (Chardin, 2006). They are constitutively bound to GTP, either due to mutations on the GTPase domain that prevent such activity or due to their high intrinsic nucleotide exchange activity.

In the current work, I focus on the classical Rho GTPase Rac1. Genetic studies in C. elegans showed that Unc-40 (the homologue of DCC) acts upstream to Rac in response to Unc-6 (Netrin) (Gitai et al., 2003). These studies corroborate work in cultured vertebrate cells (Li et al., 2002b; Shekarabi and Kennedy, 2002; Shekarabi et al., 2005). In this context, Rac1 and Cdc42 activation and Rho inhibition are required for DCC mediated attraction (Li et al., 2002b; Moore et al., 2008; Shekarabi et al., 2005). The mechanism underlying DCC activation of Rac involves different GEFs: TRIO, DOCK 180,

TIAM1 and β-Pix, as well as activation of the p120RasGAP (Antoine-Bertrand et al., 2016; Briançon-Marjollet et al., 2008; DeGeer et al., 2015; Demarco et al., 2012; Lai Wing Sun, 2015; Li et al., 2008). In addition to the direct effects of Rho GTPases on actin regulation, Rac can play a role in the guidance receptors subcellular localization and Rho acts in the trafficking of DCC to the membrane (Moore et al., 2008; Norris et al., 2014; Watari-Goshima et al., 2007) .

1.3.3 – Additional molecules that regulate growth cone morphology and axon guidance

Other key regulators of the cytoskeleton dynamics are the phosphoinositides, which are involved in many signal transduction pathways related to membrane trafficking and chemotaxis (Quinn et al., 2008; Wu et al., 2014). Lipid enzymes, such as phosphoinositol 3-kinase (PI3K), phosphorylate the lipid phosphatidylinositol at different positions generating distinct phosphoinositides, therefore conferring them specificity. Many phosphoinositides associate with actin binding proteins, modulating their activity or subcellular localization (Wu et al., 2014). For instance, phosphatidylinositol 4,5-bisphosphate (PIP2) typically inhibits proteins involved in actin filament disassembly such as cofilin, and activates proteins that induce actin polymerization such as WASP (Wiskott–Aldrich syndrome protein) (Hilpela et al., 2004; Rohatgi et al., 2000; van Rheenen et al., 2007).

PI3K can act downstream to DCC in response to netrin (Chang et al., 2006). 3`-phosphoinosidites can show a polarized distribution in the presence of chemoattractants,

being localized to the region closest to the source, therefore establishing a gradient of signalling in the growth cone.

There is also an interplay between PI3K and Rho GTPases. Phosphoinositides can modulate the activation/inactivation of GTPases by interacting with several GEFs and GAPs (Campa et al., 2015; Ko et al., 2014). One of these is DOCK180, a GEF that can act downstream to DCC, and also function as an effector for 3'phosphoinositides (Cote et al., 2005; Cote and Vuori, 2007). In addition, Rho kinase and Rac1 induce the synthesis of PIP2 in neurons (Halstead et al., 2010; Taoufiq et al., 2013).

1.4 – 14-3-3s role in SCN axon guidance

14-3-3 proteins are a family of highly homologous adaptor proteins. Seven 14-3-3 isoforms are encoded by separate mammalian genes and named with Greek letters α/β, ε, γ, η, σ, τ/θ, δ/ζ (Ichimura et al., 1988; Martin et al., 1993). α and δ are the phosphorylated forms of β and ζ, which were initially thought to be different isoforms because of their biochemical characteristics (Aitken et al., 1995b). The 14-3-3 proteins exist mainly as hetero- or homodimers, with the exception of 14-3-3ζ, which can also form monomers (Woodcock et al., 2003; Yang et al., 2006). 14-3-3 proteins bind to client proteins affecting their stability and subcellular localization.

In a growth cone proteomics screen 14-3-3 proteins were found to be remarkably abundant in growth cones prompting Kent and colleagues (2010) to investigate the role of this protein family in axon guidance. The group determined that the expression of 14-3-3 proteins is developmentally regulated and that 14-3-3 proteins could bind and stabilize

the PKA holoenzyme to switch the polarity of the neuronal response to guidance cues (Kent et al., 2010; Yam et al., 2012). Bourikas et al. (2005) had already demonstrated a repulsive role for Shh during the longitudinal projection of SCN fibers. However, how Shh would transition from an attractant for pre-crossing commissural neurons to a repellent for post crossing commissural neurons was unknown. Yam et al. (2012) observed that rat SCN axons exposed to Shh gradient switched their response from attraction to repulsion after 3 to 4 days in culture, suggesting a cell-intrinsic and time-dependent underlying mechanism. The authors identified a key contribution of 14-3-3 proteins. *In vivo*, 14-3-3β and 14-3-3γ are enriched as SCNs cross the midline, whereas *in vitro* their expression increases over time. SCNs treated with R18, a 14-3-3 antagonist, failed to change their attractive behavior to repulsion after 3 days in culture, a phenotype that is replicable by the knockdown of 14-3-3β and 14-3-3γ. Conversely, overexpression of 14-3-3s at 2 DIV switched SCN attraction to repulsion. The authors demonstrated that interfering with 14-3-3 proteins in chick embryos resulted in aberrant rostrocaudal choices, which were attributed to a loss of Shh repulsion. The investigation of downstream signaling demonstrated that 14-3-3 proteins act by decreasing PKA activity, which is corroborated by our group's previous report that 14-3-3s stabilize the PKA holoenzyme, causing it to be inactivated (Kent et al., 2010).

These two reports (Kent et al., 2010; Yam et al., 2012), have brought 14-3-3s to attention in the axon guidance field. Their role in regulating intrinsic states of cells and modulating guidance responses is an example of the broad range of functions that these proteins can exert, which will be discussed throughout this thesis.

1.4.1 – 14-3-3 discovery

Initially, the 14-3-3 proteins were described as an acidic brain protein (Moore, 1967). Their name derives from the combination of their fraction number on DEAE-cellulose chromatography and their migration position in the subsequent starch–gel electrophoresis. First described as brain-specific, they later came to be identified as a family of ubiquitous eukaryotic proteins (Celis et al., 1990; Fu et al., 2000; Sun et al., 2009). 14-3-3s have emerged as a group of multifunctional proteins that bind and modulate the function of a myriad of cellular proteins and regulate a wide range of physiological functions.

14-3-3s comprise approximately 1.0 % of the total content of soluble protein in the brain, and approximately 6.5 % of the proteins in the axonal growth cone (Boston et al., 1982; Kent et al., 2010). These proteins may be present in different cell compartments, highlighting their multifunctional character (Celis et al., 1990; Grozinger and Schreiber, 2000; McKinsey et al., 2000). The identification of 14-3-3 functionality was initially based on studies aimed at identifying regulatory proteins for several different pathways. 14-3-3 functions can be grouped into three major clusters: occluding certain domains on its target proteins, scaffolding protein interactions or acting as an allosteric co-factor (Celis et al., 1990; Fu et al., 2000; Johnson et al., 2010; Yaffe et al., 1997). Thus, the understanding of the regulation of 14-3-3 binding can give us substantial information on their roles for the biology of the cell.

1.4.2 – 14-3-3 recognition sequences

The vast majority of the interactions between 14-3-3s and their targets happen at the phospho-serine residue of the mode 1 consensus binding motifs RSXpS(XP), which was deduced from a 15-mer Raf-1 peptide containing RQRS257TS259TP (Muslin et al., 1996). The study of the interaction between 14-3-3s and Raf-1 has provided numerous insights into the dynamics of 14-3-3 binding. This peptide, when phosphorylated on S259, directly binds 14-3-3ζ in a specific manner. The proline residue at +2 is important to stabilize the interaction between its target and the 14-3-3 of interest, but it is observed in only 50.0 % of all known 14-3-3 interactions (Johnson et al., 2010). Screens of phospho-serine-oriented peptide libraries identified alternative consensus motifs with one (mode 1) closely related to the RSXpSXP motif (Yaffe et al., 1997). The second identified motif (mode 2) uses the optimal sequence RX[aromatic residues][positively charged residue]pS[L/ E/A/M]P, yielding a high affinity 14-3-3 interaction. These consensus binding domains do not allow for substitutions of the phospho-serine residue, with the exception of phospho-threonines (Brunet et al., 1999). Mode 3 binding motifs are characterized as a serine-rich motif (Liu et al., 1997). They are defined by the formula RX1–2SX2–3S, where at least one of the serines is phosphorylated.

It is clear that 14-3-3s predominantly bind to phosphorylated proteins (Fu et al., 2000), although *in vitro* studies have indicated that they are also capable of interacting with unphosphorylated ligands. An example is a Raf-1 14-3-3 binding site located between residues 139–184, a cysteine-rich domain (McPherson et al., 1999; Winkler et al., 1998). These interactions of 14-3-3 with unphosphorylated ligands can be of high

affinity, similar to those with phosphorylated proteins, some of them following an RSXSXP-like motif, RSESEE (Campbell et al., 1997).

14-3-3 isoforms have very similar protein structures (Liu et al., 1995; Xiao et al., 1995). The molecules form a cup-like shape with a highly conserved, inner, concave surface and a variable outer surface. Inside of its concave surface lies an amphipathic groove in each monomer, which mediates the binding of 14-3-3 to its target proteins (Liu et al., 1995).

1.4.3 – 14-3-3 antagonists

Notably, the high conservation of the amphipathic groove led to the isolation of R18, a peptide that binds to the groove and has been used to antagonize 14-3-3-client protein binding. Initially selected from a phage display library for its high affinity for 14-3-3 proteins (Wang et al., 1999), R18 competes with other 14-3-3 targets to prevent their binding (Kent et al., 2010; Yam et al., 2012). R18's core WLDL sequence can be mutated to produce control peptides (WLRL or WLKL), which will be used in this thesis. R18 can be applied to the cells by viral transduction, plasmid transfection or through a cell permeable form, tagged with the viral peptide sequence "TAT" (Kent et al., 2010; Yam et al., 2012).

The production of peptidic antagonists for 14-3-3s was initially anticipated as a potential source for therapeutic use in a number of 14-3-3 related disorders (for review, refer to Fu et al., 2000 and Shimada et al., 2013). However, difficulties in delivering R18 in subclinical settings has led to the development of a second generation of 14-3-3 inhibitors, which are small molecules of non-peptidic nature that also sit in the

amphipathic groove of 14-3-3s (Mancini et al., 2011). One of these inhibitors, an aromatic compound called BV02, has been recently made commercially available, and is used for some of the experiments in this project.

1.4.4 – Regulation of 14-3-3 activity

The interaction of 14-3-3s with their client proteins is controlled at the level of target protein phosphorylation as well as at the level of 14-3-3 itself. Mechanisms that regulate 14-3-3 include isoform specificity, posttranslational modifications, and expression levels in cells. The presence of seven 14-3-3 isoforms in mammalian cells suggests a role for isoform-specific interactions with different targets. Isoform specificity for client proteins has been empirically demonstrated several times in spite of a lack of structural basis, since the amphipathic groove is highly conserved.

Phosphorylation of 14-3-3 also modulates the function of 14-3-3 isoforms, as in the aforementioned isoforms α, τ and δ (Aitken et al., 1995b). S184 phosphorylation of 14-3-3ζ regulates its ligand binding (Liu et al., 1995) and phosphorylated 14-3-3β and ζ show increased potency in the inhibition of PKC (Aitken et al., 1995a).

In addition to the regulation of the interactions between 14-3-3s and their target, phosphorylation of specific residues can modulate the formation of 14-3-3 dimers. Examples of such regulation include the S60 of 14-3-3β, the S59 of 14-3-3η and the S58 of 14-3-3ζ which can be phosphorylated by the sphingosine-dependent protein kinase 1 (SDK1) (Megidish et al., 1998; Megidish et al., 1995).

1.4.5 – Perspectives for 14-3-3s for the development of the CNS circuitry

The ability of 14-3-3s to bind to other proteins, regulating their activities implicates this family of adaptor proteins in a number of intracellular signaling pathways. Their contribution for axon guidance has already been demonstrated in several examples of axon repulsion via PKA (Fig 1.1) (Kent et al., 2010; Yam et al., 2012; Yang and Terman, 2012). However, whether they can play a direct role on axon guidance, independently of PKA, remains unknown. The presence of a large number of guidance receptors that contain 14-3-3 consensus binding regions is an indication of the potential to find novel partners for these proteins.

A recent report in which a 14-3-3 stabilizing drug has been used to promote spinal cord and optic nerve regeneration has linked these adaptor proteins to the ability of the CNS to regenerate (Kaplan et al., 2017). In this report, a small molecule that stabilizes interactions between 14-3-3s and client proteins with select binding motifs has been used to promote axon regrowth after injury. The authors implicate the transcriptional regulator GCN1 in this pathway, but due to the broad spectrum of such drug, we can infer that other client proteins are also involved in 14-3-3 function on axon regeneration. An example is the class IIa HDACs, which have been shown to be an important pre-conditioning response to axonal injury, and also important proteins for axonal development (Alchini et al., 2017; Cho et al., 2013). HDAC5, a class IIa HDAC, shuttles from the nucleus to the cytoplasm in dorsal root ganglion (DRG) neurons, and this shuttling is required for the effectiveness of this first injury to pre-condition neurons to a second injury, in which the regeneration potential is enhanced (Cho and Cavalli, 2012; Cho et al., 2013). HDAC9,

another class IIa HDAC, is exported from the nucleus during the early postnatal development of the thalamus, nucleocytoplasmic translocation that is required for the activity dependent axon branching in these cells (Alchini et al., 2017). The nucleocytoplasmic shuttling of both proteins is mediated by 14-3-3, and mutations to their 14-3-3 binding sites have been used to manipulate their function, suggesting that 14-3-3 plays a central role in the regulation of these transcription factors.

Therefore, the current work will focus on 14-3-3 role in axon guidance and will probe the underlying molecular mechanisms responsible for any effects. We expect to find novel mechanisms to explain the events involved in the development of axonal circuits, which might have important implications for the knowledge in the field as well as other related areas, such as neuronal regeneration.

1.5 – Oligodendrocyte role and differentiation

Once the circuitry of the CNS is established, many projecting axons must be wrapped by myelin, specialized lipid-rich membrane ensheathments (reviewed in Sherman and Brophy, 2005). Myelin is a living structure, formed by processes of oligodendrocytes in the CNS or Schwann cells in the peripheral nervous system (PNS). Myelin wraps the axons in multiple layers with regular gaps, the nodes of Ranvier. This way, myelin sheaths insulate axonal membranes and restrict action potentials to the nodes of Ranvier, to mediate saltatory conduction, i.e. nerve pulses that jump from node to node (Nelson and Jenkins, 2017; Simons and Nave, 2015).

Saltatory conduction significantly decreases the time and energy required for signal transduction. Myelinated axons conduct nerve impulses orders of magnitude faster than unmyelinated axons, allowing for much more complex brain functions to evolve (Nave and Werner, 2014; Simons and Nave, 2015). Also, since nodes of Ranvier occupy a small fraction of the axonal surface, saltatory conduction avoids the necessity of continuous energy regeneration along the axon, reducing the metabolic burden that the synapses would cause to cells (Simons and Nave, 2015). Finally, oligodendrocytes play an important role in the maintenance of axonal structure. Animal models lacking myelin proteins, such as proteolipid protein (PLP) or 2'3'-cyclic-nucleotide 3'-phosphodiesterase (CNP) 1, show only mild myelin phenotypes, despite developing progressive axonal degeneration (Griffiths et al., 1998; Lappe-Siefke et al., 2003). These major axonal phenotypes are attributed to disruptions in axonal transport and metabolic processes (Fruhbeis et al., 2013; Funfschilling et al., 2012).

These mechanisms are thought to play a role in the progression of some neurodegenerative diseases, such as multiple sclerosis (MS) (Domingues et al., 2016). In this context, either malformation or degeneration of myelin affects axon integrity, causing a number of neurological symptoms.

Finding new targets to improve myelin function in neurodegenerative diseases can be an important venue to therapeutics. Further in this work we will attempt to analyse the potential of 14-3-3s for remyelinating therapies in the CNS. Thus, we will review the differentiation of the oligodendrocyte, and the myelination process in the CNS in the next sections.

1.5.1 – The discovery of oligodendrocytes

Pio Del Rio-Hortega described the existence of oligodendrocytes in 1921 (Del Rio-Hortega, 1921). Using a combination of different tissue stainings and metal impregnations, Del Rio-Hortega developed a silver carbonate procedure that enabled him to efficiently observe the existence of the "third element", the brain cells that were discovered after the first (neurons) and second (astrocytes) elements described by Ramon y Cajal (Pérez-Cerdá et al., 2015). This "third element" was initially split into the microglia, cells with an ectodermal origin and later found to play an immune role in the CNS, and then named "interfascicular cells", the oligodendroglia (Del Rio-Hortega, 1920, 1921). Ramon y Cajal was among the researchers who discredited Del Rio-Hortega's findings delaying research in the field for a few years until his findings were accepted (Pérez-Cerdá et al., 2015). Still, Del Rio-Hortega devoted his career to the description of oligodendrocytes in their morphological variety and provided invaluable information on the role of oligodendrocytes in the production of myelin (Del Rio-Hortega, 1928).

The physiological relevance of different oligodendrocyte subtypes is still unclear to date, although oligodendrocytes are now classified in two groups based on the diameter of the fibers that they myelinate, an inheritance from Del Rio-Hortega's studies.

Presently there are many open questions related to the biology and molecular identity of oligodendrocytes (reviewed in Buttermore et al., 2013). Much of the current research on these cell types focuses on the differentiation of the oligodendrocyte progenitor cells (OPCs), a pool of cells that is capable of differentiating into oligodendrocytes and producing myelin.

1.5.2 – Origin of oligodendrocytes

Although oligodendrocytes are widespread in the CNS, they originate from OPCs restricted to specific regions of the spinal cord and brain. In the rodent spinal cord, the first wave of differentiating OPCs share a common origin with motor neurons. Both cell types originate from Olig2-positive cells in the ventral portion of the neural tube at E12.5 in mice and E14 in rats (Richardson et al., 2000). A second wave of OPCs is generated about 3 days later in the dorsal ventricular zone (Cai et al., 2005; Fogarty et al., 2005; Vallstedt et al., 2005). In the brain, the first pool of OPCs is formed in the ventricular zone close to the medial ganglionic eminence and anterior entopeduncular area, with the dorsal progenitors arising from the ganglionic eminence and cortex (Kessaris et al., 2006).

These pools of cells migrate across the CNS to their target regions before becoming myelinating cells (Simons and Nave, 2015). A schematic of the factors involved in the differentiation of oligodendrocytes can be found in Figure 1.2. Some secreted growth factors, such as platelet derived growth factor (PDGF)-A, fibroblast growth factor (FGF)-2 and tissue-type plasminogen activator (tPA), act as chemokinetic cues, promoting OPC motility and serving as chemoattractants, together with more traditional guidance cues semaphorin 3F, Shh and neuregulin-1 (Armstrong et al., 1990; Leonetti et al., 2017; Merchan et al., 2007; Milner et al., 1997; Ortega et al., 2012; Zhang et al., 2004; Zhang et al., 2003). Conversely, proteins such as netrin-1, semaphorin 3A, BMPs, and transforming growth factor (Tgf) β1 direct the cells away from their birth region (Choe et al., 2014; Jarjour et al., 2003; Spassky et al., 2002). Many of the aforementioned

chemoattractants play an additional role promoting OPC proliferation, which happens throughout their migratory phase (Colognato et al., 2004; Noble et al., 1988; Zeger et al., 2007). The balance of these trophic factors is extremely important for the maintenance of OPCs, since there are estimates that approximately 50% of OPCs might undergo apoptosis due to lack of growth factors (Barres et al., 1992).

In addition, extracellular matrix molecules play an important role in OPC migration, e.g. tenascin-C, laminin, fibronectin, anosmin-1, integrins, polysialylated-neuron cell adhesion molecule (PSA-NCAM), ephrins, and N-cadherin, control their motility and help direct them along the axons (Bribian et al., 2008; Kiernan et al., 1996; Milner et al., 1996; Payne et al., 1996; Prestoz et al., 2004; Wang et al., 1994).

1.5.3 – Oligodendrocyte differentiation

Upon reaching their targets, OPCs differentiate into post-mitotic, O4 positive premyelinating oligodendrocytes, regulated by proteins like leucine rich repeat and Immunoglobin-like domain-containing protein (Lingo) 1, Wnt, G-protein coupled receptor (Gpr) 17, Notch-1/Jagged1, triiodothyronine, and insulin-like growth factor (IGF) 1 (Barres et al., 1994; Carson et al., 1993; Chen et al., 2009; Durand and Raff, 2000; Fancy et al., 2009; Mi et al., 2005; Sommer and Schachner, 1981; Wang et al., 1998). These factors provoke epigenetic modifications and regulation of transcription factors, which activate a set of genes that promote differentiation and inhibit genes that repress OPC differentiation (reviewed in Emery and Lu, 2015).

Transcription factors such as Id4 and Tcf4, as well as Wnt signalling, naturally repress the differentiation of OPCs, hence the activity of histone deacetylases (HDACs), like HDAC1 and HDAC2, is required to stop these self-renewing mechanisms and allow for OPC differentiation (He et al., 2007a; Shen et al., 2005; Ye et al., 2009). The downregulation of OPC-like genes happens simultaneously to an increase of the activity of the transcription factor Olig2, which acts in collaboration to Sox 10 and Nkx 2.2, to promotes ATP-dependent chromatin remodeling (Liu et al., 2007; Yu et al., 2013).

Interestingly, myelin gene regulatory factor (Myrf) is to date the only transcription factor that has been reported to be expressed in immature oligodendrocytes, while completely absent from OPCs (Emery et al., 2009). Expression of Myrf is required for OPC differentiation, and its maintenance is essential for the expression of myelin related proteins such as myelin basic protein (MBP), myelin oligodendrocyte (MOG), myelin-associated glycoprotein (MAG), proteolipid protein (PLP) 1 through adulthood (Emery et al., 2009; Koenning et al., 2012).

MicroRNAs (miRs) also play a crucial role for OPC differentiation, which is supported by the failure of OPCs to differentiate upon deletion of Dicer1, a miR processing enzyme (Dugas et al., 2010; Zhao et al., 2010). mir146a, miR-219 and miR-338, among others, are upregulated during OPC differentiation, often working through repression of genes that maintain OPCs in an undifferentiated state (Dugas et al., 2010; Santra et al., 2014; Zhao et al., 2010).

The differentiation of OPCs into immature oligodendrocytes is accompanied by cell remodelling, in which the maturing cells produce complex branched processes, so that the cells can sense the axons that require myelination (Hardy and Friedrich, 1996).

Signaling through integrins, contactins and DCC have all been implicated in the promotion of the cell remodelling, acting by the activation of Fyn (Chun et al., 2003; Rajasekharan et al., 2009; Relucio et al., 2009).

1.5.4 – Myelin production

Myelination is a postnatal process in rodents and humans, that continues through early adulthood (Simons and Nave, 2015). Adult myelination is thought to replace dead oligodendrocytes, remodel myelinated fibers, or occasionally myelinate new fibers (Gibson et al., 2014; Young et al., 2013). The existence of mechanisms for myelination in adults is of special interest for the development of new therapies for neurodegenerative diseases, in order to restore damaged myelin. However, the process of CNS myelination is yet to be fully unveiled.

Schwann cells decide to myelinate axons based on the level of neuregulin-1 expressed by them, however a similar, single axonal signal has not been described for the CNS (Simons and Lyons, 2013; Taveggia et al., 2005). Neuregulin-1 overexpression can lead to myelination of otherwise unmyelinated small caliber axons (Brinkmann et al., 2008). Also, while Schwann cells choose to ensheath axons wider than 1 μm, CNS axons between 200 nm to 1 μm might be myelinated or not (Simons and Lyons, 2013). There is increasing evidence that neuronal activity drives CNS myelination, however it remains unclear whether activity stimulation leads to myelination of new, unmyelinated fibers or to the addition of new sheaths on top of the pre-existing ones (Gibson et al., 2014; Makinodan et al., 2012; Sampaio-Baptista et al., 2013; Zatorre et al., 2012). *In vitro*

studies showed that neural activity regulates Fyn activity in oligodendrocytes, promoting myelin synthesis, and increases expression of neuregulin-1 (Liu et al., 2011; Wake et al., 2011)

1.5.5 – Axonal wrapping by oligodendrocytes

Oligodendrocytes start producing myelin upon finding their target axons. Upon axonal contact, oligodendrocytes begin flattening the tips of their processes, wrapping around the axon and expanding to up to 2 x 10^6 μm^2 (Pfeiffer et al., 1993). While each Schwann cell forms one internode, a single oligodendrocyte can form 80 internodes, on multiple axons, starting from the axons with larger caliber (Almeida et al., 2011; Snaidero and Simons, 2014). The formation of internodes seems to be regulated by an axonal signal, despite all internodes of an oligodendrocyte being produced within a few hours time frame (Czopka et al., 2013; Watkins et al., 2008).

Oligodendrocytic membrane keeps being added to the region closest to the axon, rather than in the outer region of the internodes, at the same time it expands laterally, occupying the whole space between nodes of Ranvier (Snaidero et al., 2014). The number of wraps and the thickness of the myelin internode is constant in the CNS and follows a g-ratio, which is the relationship between the axon diameter and the thickness of the myelinated fiber (Hildebrand and Hahn, 1978; Murray and Blakemore, 1980; Snaidero and Simons, 2014).

This process is at least partially regulated by Fyn kinase, since Fyn activity peaks during the initiation of myelination and Fyn loss of function leads to myelination

deficiencies in the forebrain (Kramer-Albers and White, 2011; Sperber et al., 2001). Myelin protein synthesis is also promoted by activation of the PI3K/AKT/mTOR pathway (Flores et al., 2008; Narayanan et al., 2009; Norrmen and Suter, 2013). PI3K, an enzyme already discussed in the growth cone section, recruits and activates Akt, a serine/threonine kinase with a number of downstream targets. One downstream target is “molecular target of rapamycin” (mTOR), a kinase responsible for the regulation of a variety of biological processes. Animal models have shown that constitutively active AKT results in thicker myelin sheaths throughout the CNS, whereas mTOR loss reduces myelination, suggesting that these pathways can play an alternative role to Fyn kinase (Flores et al., 2008; Narayanan et al., 2009). Erk1/2 is another pathway that controls myelin production, where Erk activity is increased during OPC proliferation and myelin production, its sustained expression is required for myelin health and repair in adults (Fyffe-Maricich et al., 2013; Ishii et al., 2013; Ishii et al., 2014; Ishii et al., 2012). Calcium/ calmodulin-dependent kinase (CaMK) IIβ has also been implicated in the expansion of myelin membranes, as CamK IIβ is expressed by neurons and oligodendrocytes, and CamK IIβ null mice have defective myelination, indicating that this is another potential pathway to regulate myelin biogenesis (Waggener et al., 2013).

Membrane compaction starts as soon as a few wraps are completed, starting from the outer layers (Simons and Lyons, 2013; Snaidero and Simons, 2014). Myelin compaction involves the removal of cytoplasm from myelin internodes and the adhesion of adjacent myelin membrane wraps by bringing together their extracellular membranes, which can be visualized by electron microscopy as alternating electron dense and less dense layers (Sherman and Brophy, 2005). MBP is required for this process as it binds

and bring together opposing cytoplasmic leaflets of the myelin bilayer (Readhead et al., 1987). Thus, MBP also blocks sequences larger than 20-30 amino acids from entering the compact myelin (Aggarwal et al., 2011). MBP can be locally synthesized in the oligodendrocyte processes, and it is considered as being a marker of fully differentiated oligodendrocytes (Colman et al., 1982). After this point of myelin production, the myelin must still further specialize in its functional domains, such as the juxtanodes, paranodes, and nodes of Ranvier. These are complex processes that go beyond the scope of the current work (further reviewed in Sherman and Brophy, 2005; Simons and Nave, 2015).

1.5.6 – Considerations for the study of 14-3-3s in the development of oligodendrocytes

Little is known about the role of 14-3-3s in the development of the oligodendrocytes. Reports of 14-3-3 expression in white matter tracts have suggested that 14-3-3s might be required for myelin maintenance in adults, however whether these are axonal or oligodendrocytic proteins, as well as their physiological function, remains unclear (Saia-Cereda et al., 2015; Umahara et al., 2007).

The expression of 14-3-3s during the differentiation of OPCs is unexplored, although 14-3-3s have already been shown to regulate many pathways that are required in this process, e.g. CaMK, mitogen-activated protein kinase (MAPK)/ Erk, Akt downstream signalling (Davare et al., 2004; McPherson et al., 1999; Morrison, 1995; Tzivion et al., 2011).

Hence, we will focus on this early stage of the development of oligodendrocytes to explore whether 14-3-3s play a biological role in the myelin production.

1.6 – Thesis rationale and objectives

The current work seeks to understand how 14-3-3 proteins affect axon guidance and oligodendrocyte development. Building from our group's previous work, which showed that 14-3-3s are key regulators of switches in the polarity of the responses to guidance cues, I focused on the physiological role of this family of proteins before such switches occur.

In chapter 2, I develop and characterize a system for the study of pre-crossing spinal cord commissural axons.

In chapter 3, I perform the detailed description of 14-3-3 role in the pre-crossing stage of spinal cord commissural axon development.

For chapter 4, starting from the rationale that much of the molecular signalling activated during axon guidance is recapitulated in the differentiation of oligodendrocytes, I perform one of the first reports of the expression of 14-3-3s by oligodendrocytes and perform a cursory study on its implications for the differentiation of oligodendrocyte progenitor cells.

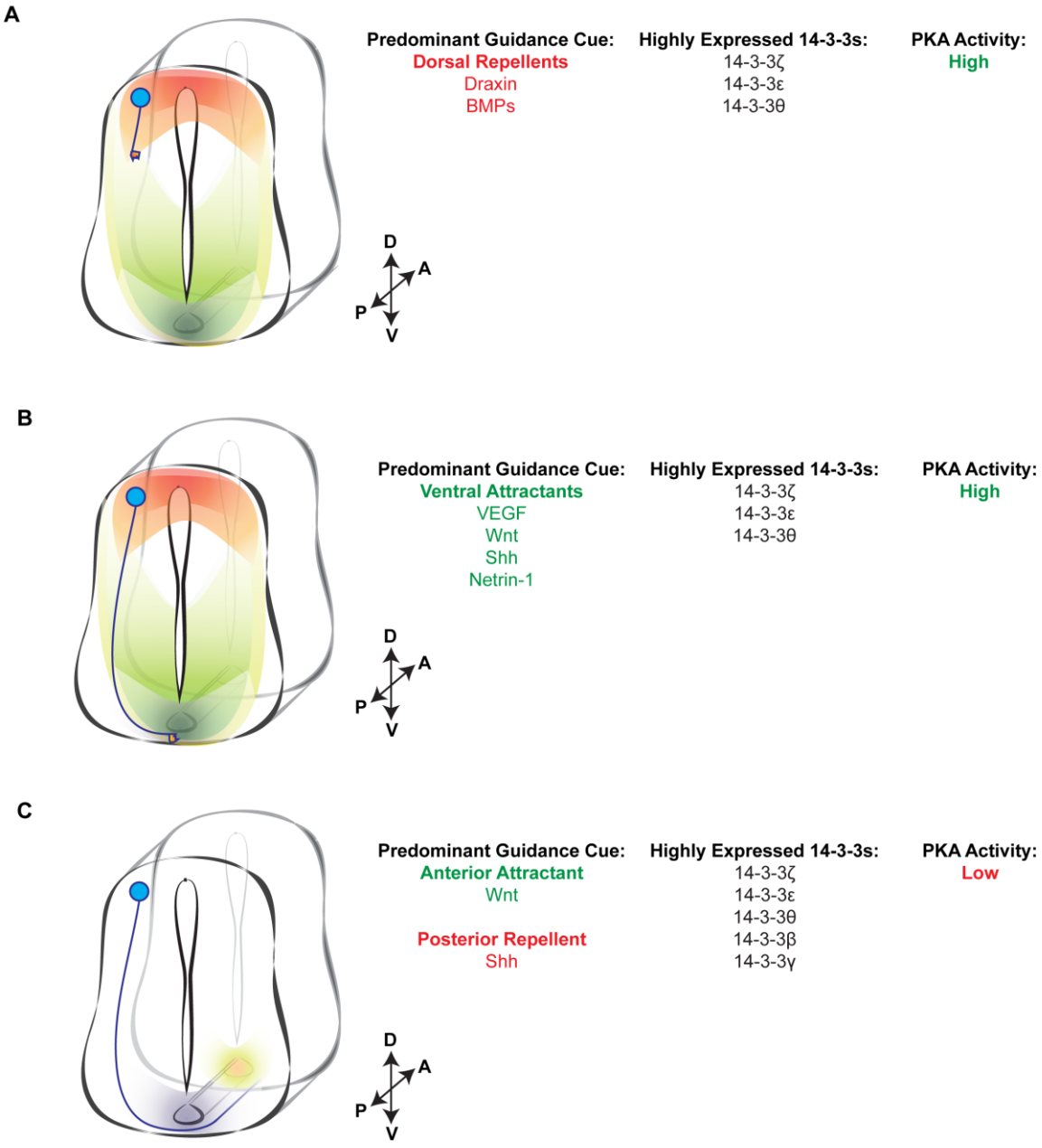

Figure 1.1: Guidance cues and 14-3-3 expression during SCN development. A. Initial projection of the SCN axons, when the predominant response is evoked by dorsal repellents. B. Axial projection affected by ventral midline derived attractants. C. Longitudinal projection, guided by rostrocaudal gradients in the floorplate. DV axis: Dorsoventral axis. AP axis: Anteroposterior (rostrocaudal) axis.

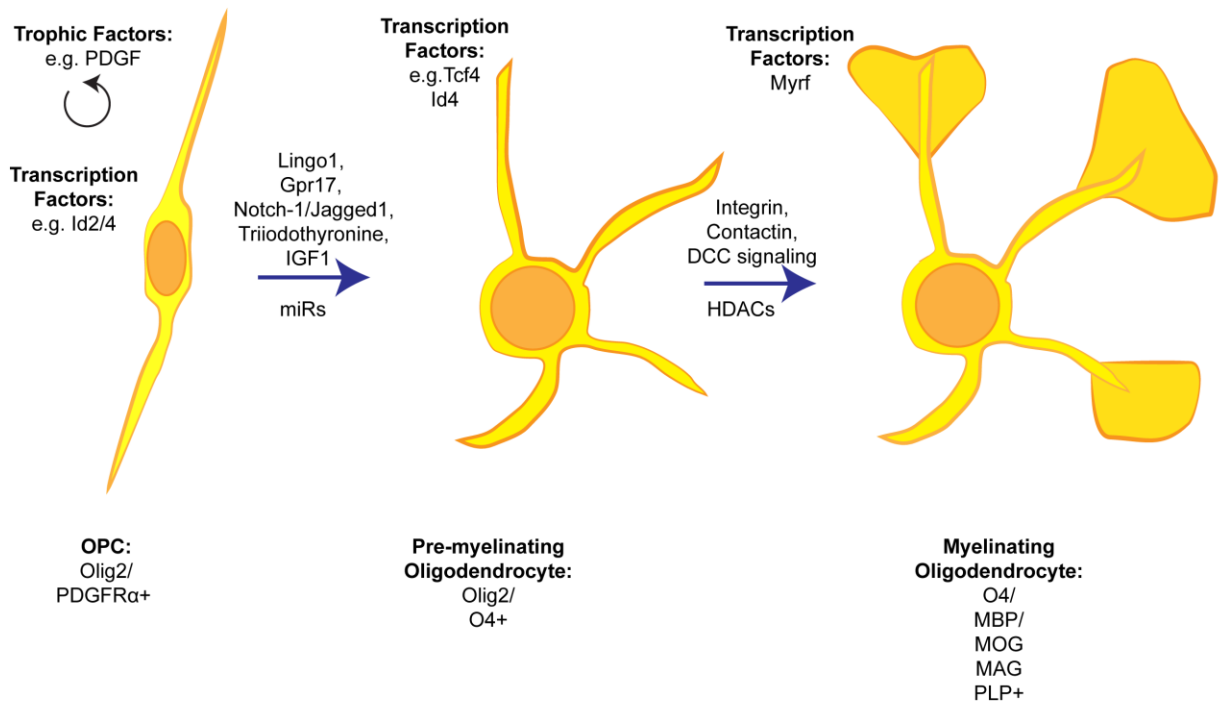

Figure 1.2: Differentiation of oligodendrocytes. The differentiation of OPCs into pre-myelinating and then myelinating oligodendrocytes depends on the regulation of several signaling pathways (indicated by the blue arrows) and result in the activity of cell-type specific transcription factors (upper left side) and cell markers (bottom).

Results

Chapter 2 – Preface

In this first result chapter, I developed a protocol to analyse spinal cord commissural neuron *ex vivo.* The necessity for this protocol started in the early stage of the research for chapter 3, when we were still trying to find a suitable *in vivo* (or *in vivo*-like) model to describe the function of 14-3-3s in the development of pre-crossing commissural neuron guidance.

This technique is described in detail here and could be used in the following chapter as well, in the figure 3.1. With this method, we offer and a new tool for people who study different aspects of spinal cord axon guidance, which is further discussed in this chapter.

Chapter 2 – *Ex utero* electroporation of rodent spinal cords as a method to study commissural axon guidance

Ricardo Alchini, Timothy Kennedy, Alyson Fournier.

Montreal Neurological Institute, McGill University, Montreal, Canada.

2.1 – Abstract

Proper synchronization of bodily functions depends on the communication between the two sides of the body, a role that is fulfilled by commissural neurons. The study of commissural axon guidance has produced many important insights into the molecular underpinnings of axon guidance in general. A system that successfully recapitulates commissural axon development *ex vivo* and permits the manipulation of gene expression with tight temporal and spatial precision would be of great value in understanding how axon projections are formed in the organism. Here, we describe a method to culture spinal cord tissue and to transduce it with a gene of interest. Transduction of fluorescent proteins enabled the tracing of single commissural axons. Spinal cords can be kept in culture for several days for stationary studies, or subjected to live imaging. As proof of principle we demonstrate that commissural neuron axons project directly to the ventral midline and that overexpression of ectopic Netrin-1 disrupts their proper targeting.

2.2 – Introduction

Neurons must project their axons to their physiologically relevant targets in order to be fully functional. Developing axons sense their paths through complex environments of guidance cues that are expressed in stereotypical manners. Reverse engineering the environment to allow for accurate observation of axonal development can be a challenging task (for review, refer to Chédotal, 2011). The developing spinal cord is one of the most widely studied systems in the field of axon guidance. Spinal cord commissural neurons (SCNs) are dorsally born interneurons that connect both sides of the body, and participate in processes such as proprioception, movement coordination and sensorimotor reflexes (Bellardita and Kiehn, 2015; Bermingham et al., 2001; Thiry et al., 2016). At the neural tube stage, SCNs project their axons radially, being repelled by guidance molecules expressed in the roof plate and attracted by the floorplate (Chédotal, 2011; Martinez and Tran, 2015; Placzek et al., 1990a). After reaching the floorplate, these axons cross towards the opposite side of the body, and project towards the upper brain areas. Understanding the molecular mechanisms that are involved in the regulation of SCN projections has provided valuable insights to the axon guidance field, being transposed to the development of other brain regions (Martinez and Tran, 2015).

Such molecular studies depend on the usage of techniques that allow for the genetic and pharmacological manipulations of the growing axons, for later tracing. Several methods have been used for the observation of different types of developing neurons, such as dye injections, biolistic gene gun, lipofection, viral vectors, genetic models and electroporation (Ehrengruber et al., 2001; Feng et al., 2000; Itasaki et al., 1999; Ma et al., 2002; O'Brien et al., 2001; Uesaka et al., 2007). The application of these gene transduction techniques to mammalian SCNs has been restricted to *in vitro* studies, in

which the tissue structure is disrupted. Therefore, a method to efficiently transduce SCNs in *ex vivo*, organotypic preparations can be of great use.

Here, we take advantage of the relative simplicity of the neural tube morphology to develop a system in which the backs of rat embryos are cut open and fluorescent proteins are locally transduced into a small portion of the cells, using a SCN-specific reporter. These axons can be carefully traced and analyzed in stationary studies or followed in time lapse experiments. This way, by combining local electroporation and spinal cord openbook techniques, we developed a simple technique to trace and follow genetically manipulated SCN axons that allows for *ex vivo* observation.

2.3 – Methods

2.3.1 – Reagents

The DNA constructs utilized in this work were purified from transduced bacteria using a HiSpeed Plasmid Maxi Kit (Qiagen, Waltham, MA). After purification, DNA was precipitated in 0.3 M sodium acetate, 70% isopropanol by 13200 rpm centrifugation for 10 min at 4º C. DNA was resuspended in DMEM (Invitrogen, Carlsband, CA) to the stock concentration of 5.0 µg / µL and stored at 4º C.

The Math-1-GFP plasmid was a generous gift from Dr. Jane E. Johnson (University of Texas Southwestern Medical Center). The CMV-GFP and myc- Netrin-1 constructs were previously described (Goldman et al., 2013).

2.3.2 – Animals

All animal care and use were performed in accordance with the McGill University guidelines and approved by the Montreal Neurological Institute Animal Care Committee. Staged pregnant Sprague–Dawley rats were acquired from Charles River (St. Constant, Canada). Noon of the day on which the vaginal plug was detected in the morning was designated embryonic day 0 (E0). In this manuscript, E11.5 (Witschi 19 - 22), E12.5 (Witschi 25-26) and E13.5 (Witschi 27-28) embryos have been utilized for comparison (Altman and Katz, 1962).

2.3.3 - Spinal cord dissection

Neural tubes were isolated and cultured following a previously described protocol (Moore and Kennedy, 2001). For the experiments in which the tissue was electroporated with commissural neuron specific promoters, the dorsal tissue of the embryo was kept intact, i.e. after removal of the head and the viscera, the neural tube was open using 5SF forceps (FST, Dumont, Switzerland) without the removal of the surrounding tissue. Damage to the spinal cord was minimized and the environment of the spinal cord was kept as similar as possible to the *in vivo.*

Embryonic spinal cords were dorsally open and placed with the central canal facing down on Type I rat tail collagen (BD Biosciences,) coated Millicell (Millipore, Bedford, MA) culture inserts (Fig.1A). With the central canal facing down, the SCNs are closer to the electroporated surface, easing their transduction.

Approximately 800 µL of culture media formulated from Neurobasal medium (Invitrogen, Carlsbad, CA) supplemented with 10% heat-inactivated fetal bovine serum (FBS, Sigma, St-Louis, MO) were placed under the culture insert and the openbook organotypic preparations were left recovering for approximately 2 to 4 hours until the electroporation procedure.

2.3.4 – Spinal cord *ex vivo* gene transduction

The electroporation set up (Fig. 2.1B) consisted of a stereoscopic microscope (CPSC, Nikon, Tokyo, Japan), a square pulse stimulator (Grass SD9, Grass Telefactor, West Warwick, RI) and two micromanipulators (M132, Narishige, Tokyo, Japan), illuminated by a NCL150 illumination system (Volpi, Auburn, NY).

The micropipettes used were prepared using an electrode puller (PC10, Narishige, Tokyo, Japan), from glass capillaries (OD 1 mm, ID 0.78 mm, 100 mm - Harvard Apparatus, Edenbridge, UK). 20 µm tip injection pipettes were attached to standard tubing and a 1.0 mL syringe. 200 µm tip electrode pipettes were fire polished and a 0.25 mm silver wire (World Precision Instruments, Sarasota, FL) was placed inside of the electrode pipette to transfer electrical current to the biological samples. A second wire was prepared to be used as a ground electrode, to be placed inside the culture dish in contact with the culture medium. All materials were carefully sterilized with 70% ethanol before use.

Solutions with the plasmid of interest were used at 2.0 µg/µl, and backloaded to both pipettes. Approximately 0.5 – 1.0 µL of the DNA solution were either poured on the surface of the tissue or microinjected through the space in between dorsal root

ganglia. The electrode pipette was placed on the same injected site and the electrical pulses (7-10 trains of 1 ms pulses at 200 Hz, 50 V) were delivered.

The procedure was repeated to 3 sites in each explant. 750 µL of the culture medium were added to the dish and the samples were allowed to grow until further usage.

For the live imaging experiments, confocal micrographs were obtained using a Quorum WaveFX-X1 spinning disk system on a Leica DMI6000B inverted microscope equipped with 10x objective lens and the appropriate filters. Constant 37º C temperature, 5% CO_2 and humidified air were supplied to the cultures via a Live Cell Instruments Chamlide TC environmental control system. Z-series of 20-30 optical sections were sampled at 5 µm step size, covering the whole surface of the cord.

2.3.5 – Fixation and staining

Samples were used at the indicated time points, when fixed using 4 % paraformaldehyde (Electron Microscopy Sciences, Hatfield, PA) in PBS, and immersed in 50% formamide/ 20 % poly ethylene glycol, following the ClearT2 protocol (Kuwajima et al., 2013). When described, tissue samples were stained for Tag-1 (1:300, Goat IgG, R&D Systems) of myc (in the myc-Netrin-1 electroporated group, 1:500, Rabbit IgG, R& D Systems), and the appropriated species-specific anti-IgG secondary antibodies were used following a standard protocol. For the Netrin-1 staining experiments, GFP electroporated cords were used as control, and the same staining as the myc-Netrin-1 electroporated samples. Fluorescence signals were acquired using a spinning disk

system (Quorum WaveFX-X1, on a Leica DMI6000B inverted microscope) equipped with 10x objective lens and the appropriate filters. Z-series of 10-20 optical sections.

The angle formed by the cell body, the axonal tip and the midline was measured for individual axons. Their averages and distribution were plotted and statistical analysis (Student t-test or Chi-squared) was performed using Prism 7.0 (GraphPad).

2.4 – Results

2.4.1 – Math-1 promoter can be used to follow SCN development

In this work, we sought to develop a versatile method that would allow us to observe SCN development *ex vivo.* We started performing openbook preparations of E11.5 spinal cord tissue, an age in which the dividing spinal cords are still naïve to the ventral midline and the stage that is often used for openbook preparations (Moore and Kennedy, 2001; Moore and Kennedy, 2006). By transducing a GFP construct under the control of the general promoter CMV (Supplementary Fig 2.1), we observe that after 2 days in culture many cells have not yet extended neurites. Staining for Tag-1, a protein that is highly expressed in SCN axons, revealed that visible neurites did not overlap with the electroporated fibers (Supplementary Fig 2.1A). When performing the analysis of the cells that produced neurites we observed that these cells grew in different directions, not representing the phenotype that would be expected from SCNs, suggesting that a varied population of spinal cord cells was electroporated, possibly including but not limited to SCNs. Therefore, it seemed fundamental to utilize a promoter that selected only SCNs.

We utilized a specific reporter for SCNs to trace commissural axons. The promoter Math-1 (Atoh-1) was chosen to drive the expression of GFP in this study because of its expression in the latest developing commissural population in the spinal cord, the dI1 neurons, which are also the prominent cell type in *in vitro* dissociated cultures (Bermingham et al., 2001; Helms and Johnson, 1998; Yam et al., 2012).

We found that *ex utero* electroporation of GFP driven by a Math-1 promoter failed to transduce cells at stage E11.5 perhaps as a result of insufficient Math-1 expression. We thus electroporated explants at E12.5, the stage where Math-1 expression was first shown (Bermingham et al., 2001) and E13.5, a stage often used to assess SCN guidance *in vitro*. Cells were successfully electroporated at both stages (Fig 2.2A-C). Fluorescent cells could be observed in both groups, and the average number of successfully electroporated sites did not significantly differ (Fig 2.2C, E12.5= 57.14% ± 15.79%, E13.5= 47.62% ± 17.6%, n= 7 explants each condition, 3 electroporated sites each). However, at approximately 48 h after electroporation, the number of electroporated cells was visibly different (Fig 2.2D, E12.5=41.8 ± 7.72 cells/ electroporated site, E13.5= 16.5 ± 3.15 cells/site, n= 10 electroporated sites). The GFP signal intensity and the growth rate of neurons in E12.5 explants was also visibly increased (Fig 2.2B, E-G) compared to E13.5. All of the successfully electroporated sites from E12.5 explants revealed cells with long axons even reaching the ventral midline. Interestingly the E12.5 fibers that reached the midline synchronously turned to forming longitudinal projections, indicating that the rostrocaudal guidance cue gradients were preserved (Fig 2.2B). However, only 37.49% ± 14.23% of the sites revealed axons reaching the ventral midline when electroporations were performed on E13.5 tissue (Fig 2.2E).

This difference in the frequency of the fibers reaching the midline is not likely to be due to the various widths of the spinal explants in these two stages. The length of the growth front (defined as the distance from the center of the electroporated area to the longest axon) is significantly increased in E12.5 explants (Fig 2.2F, E12.5=876.00 μm ±75.99 μm, E13.5= 661.90 μm ± 61.53. μm). When the width of the hemicords is taken in consideration, this difference is even more pronounced (Fig 2.2G, E12.5= 1.09 ± 0.09 growth front length/ hemicord width ratio, E13.5= 0.649 ± 0.09), suggesting that E12.5 cells grow faster than older neurons, possibly due to more sensitivity to the guidance cues secreted by the floorplate.

2.4.2 – Math-1- GFP expression can be used for live imaging of SCN axon guidance

Based on the efficient expression of Math-1-GFP by SCN axons we asked whether such technique would enable the observation of axon projections *ex vivo*. Explants were electroporated within 2 hours from being plated to the culture inserts and left to recover for approximately 12 hours before live imaging session. Spinal cord preparations were imaged using a spinning disk confocal microscope with environment control (37 ºC, 5% CO_2, saturated humidity). 12 hours after electroporation, GFP signal was visible in the electroporated population (Fig 2.3). From this point up to approximately 20h, a few short processes were observed. Axonal extension accelerated after 24 hours, when many cells extended their axons directly to the ventral midline. At approximately 36 hours, the growth front of the electroporated site reaches the region of ventral midline.

A detailed observation of the cells that do not project their axons straight to the ventral midline in the beginning of the movies shows that some of them have the capacity to correct their paths (Fig 2.4). Each electroporated site had at least a few cells that initially projected parallelly to the dorsal edge and changed the direction of growth afterwards. Future studies on the properties of these cells and the mechanisms by which they find their paths afterwards can be performed using this *ex vivo* electroporation technique and live imaging.

2.4.3 – *Ex vivo* electroporation of the spinal cord can be used in different regions of the developing spinal cord

In order to better understand the growth of the Math-1-GFP positive SCNs, we stopped the growth of the explants at 30 hours after electroporation. In addition, we divided the spinal cord in three segments: brachial (defined as the segment that ends at forelimb level), medial (the intermediate segment) and caudal (the segment situated from the hindlimb level to the tip of the tail) (Fig 2.5A). This division is necessary since the differentiation of the spinal cord follows an anterio-posterior wave, in which the commissural cells differentiate earlier as they get closer to the cervical region (Roberts et al., 1988). To avoid contamination by the hindbrain cells, which project in a distinct manner, electroporation on the brachial region was restricted to the narrower, posterior portion.

All the three segments showed very similar electroporation patterns (Fig 2.5B, C). In the three regions, the vast majority of the cells projected fibers that were perpendicular

to the ventral midline, indicating they were directly attracted by it (Fig 2.5C, D). Most of the cells that projected at lower angles were born closer to the edge of the explant, suggesting that the position of the cells can influence the guidance of its axons. This phenotype is particularly obvious in the medial and caudal portions of the spinal cord. The brachial portion of the spinal cord yielded more variable results. When the axons are divided in 10-degree bins, the trend of perpendicularity of the fibers become more evident (Fig 2.5D), where 64.8% of the brachial axons, 75.3% of the medial axons and 76.4% of the caudal fibers project within 71 – 90 degrees to the midline. Chi-squared analysis with 18 degrees of freedom confirms that there is no significant difference in the distribution of the projection angles of the three groups. Therefore, the Math-1 positive E12.5 SCNs have similar properties along the spinal, and the different degrees of SCN maturation in the rostrocaudal axis do not affect their guidance.

2.4.4 – General promoters are suitable for guidance cue manipulations

While the utilization of a general eukaryote promoter, such as CMV, was not an efficient method for the labelling of SCNs at this developmental stage, we attempted to use it for ectopic expression of guidance cues (Fig 2.6). In this system, we ectopically expressed Netrin-1, an important attractant endogenously secreted in the floorplate and the ventricular zone of the spinal cord (Kennedy et al., 1994; Kennedy et al., 2006). We observed that while the GFP electroporated cells kept the stereotypical pattern of Tag-1 expression in bundles that are approximately perpendicular to the ventral midline, the

Tag-1 bundles became more disorganized when exogenous Netrin-1 was expressed in the dorsal portion of the spinal cord (Fig 2.6).

Thus, although general promoters do not seem suitable for the analysis of SCN development, they can still be a valuable tool for the observation of extrinsic factors to SCN development.

Altogether we can conclude Math-1-GFP *ex vivo* electroporation is a suitable model for observation of commissural guidance, applicable to different regions of the spinal cord.

2.5 – Discussion

The electroporation-based transfection method described here accurately reproduces the *in vivo* pattern of development. Math-1-GFP electroporated cells can be easily traced and the trajectory of the axons can be easily assessed by confocal microscopy. The cells clearly reproduced the circumferential growth seen in pre-crossing SCNs and synchrounously turned longitudinally. Following these cells for up to 70 hours in culture the commisural neurons projected in a stereotypical and expected manner. Thus, we believe that the guidance cues expressed at the spinal cord followed their physiological pattern and this *ex utero* system can be used for studies on both pre-crossing and post-crossing SCN development.

It has been recently suggested that the current knowledge on guidance receptors and chemoattractants is sufficient for the field, and the demand for studies that focus on regulatory mechanisms and intrinsic properties of the developing SCNs is increasing

(Stoeckli, 2017). In this context, a system that reproduces the embryonic environment but allows genetic manipulations and time lapse imaging is necessary.

2.5.1 – Importance of the utilization of mammalian SCNs

Dynamic genetic manipulation of spinal cord tissue has been studied by *in ovo* electroporation of chicken embryos (Andermatt et al., 2014; Domanitskaya et al., 2010; Itasaki et al., 1999). This type of study is not completely suitable for the field due to genetic differences between avian and mammalian genetics. The chicken genome is much more compact than the mammalian (1.28 Gb for *Gallus gallus*, compared to 3.55 Gb in *Homo sapiens* and 3.48 Gb in *Mus musculus*) (Ensembl database,www.ensembl.org). In this context, some avian genes may take over the role of multiple mammalian proteins, changing regulatory mechanism. One example is Netrin-1 signaling, in which mammalians have two independent receptors (Neogenin and DCC), while chickens count only with Neogenin. Whereas DCC is the most important receptor for pre-crossing SCN attraction in mammalians, Neogenin takes over this role in chicken embryos (Fazeli et al., 1997; Keino-Masu et al., 1996; Phan et al., 2011). It is unclear whether the regulatory mechanisms for mammalian DCC possess any orthologue process in chicken. Thus, *ex utero* approaches are a more straightforward method for understanding the regulation of guidance responses, compared to *in ovo.*

2.5.2 – Comparisons to the *in vivo* SCN development

Although the commissural neurons in this system projected in an expected direction their growth rate was slightly slower than what is observed *in vivo* (Phan et al., 2010). Similar results were obtained in other organotypic preparations, such as the oblique thalamocortical slices studied by Mire and colleagues (2012). Still, the authors were able to observe the growth rate of the thalamocortical axons, as they developed. Therefore, we can assume that the growth rate in *ex utero* preparations is regulated by the same factors as *in vivo*. In addition, we cannot rule out that the previous studies have overestimated the growth rate *in vivo*, since such studies consisted of the comparison of histological sections at different stages. Our system is an alternative that could supply the lack of dynamic studies, in which the mammalian SCN axons are imaged over time.

Also, future studies can unveil what are the main differences between the two developmental stages analyzed here (E12.5 and E13.5). Although both seemed to project towards the same regions, E13.5 cells grew significantly slower. It is unclear whether there are different subpopulations of Math-1 positive cells in the spinal cord. Future work could focus on the identification of specific promoters for different SCN populations. Also, the use of different SCN specific promoters such as Ngn-1 and Mash-1 can be applied to extend the analysis of the SCN interneuron populations that are traceable using this method (Bermingham et al., 2001; Casarosa et al., 1999; Kidd et al., 1998a).

2.5.3 – Simplicity and versatility of this technique

The current work focus on the usage of Math-1-GFP as a proof of principle to understand SCN development. Math-1 promoter–driven overexpression or loss of

function of genes of interest represents a versatile method to genetically manipulate commissural neurons and to essess affects on axon guidance. Since we have a fine control of the electroporated area it is possible to electroporate each hemicord with a different plasmid of interest to design elegant experiments with internal controls of perfectly matching the age and spinal cord level.

Our *ex utero* system is very simple and cost effective. The electroporation procedure, simplified from Uesaka and colleagues (2007), utilizes common electrophysiology equipment that can be easily found. Another advantage of using SCN specific promoters is that the dissection procedure is much faster and gentler to the tissue. When compared to the traditional dissection method (Moore and Kennedy, 2001), we can achieve clearly traceable SCN axons from various developmental stages without the necessity of enzyme digestion. Also, the removal of the meninges and dorsal root ganglia can be a meticulous, laborious task, in which damage to the tissue might occur. Tissue damage can disrupt the guidance of the axons, as we have often seen fibers deviating from tissue scars in our system (data not shown).

In our experience, the non-neural tissue tolerates the culture protocol well, without any signal of tissue death over time. We could even observe the preparations twitching and contracting after a few days in culture, suggesting that muscle function is still intact. Further studies on the influences of the surrounding tissue on SCN development can be performed with this protocol. This protocol can be also easily adapted to study dorsal root ganglion neurons and peripheral tissue innervation, which can be achieved by microinjecting the appropriate area of the spinal cord preparations.

2.6 – Acknowledgements

We would like to thank Stephanie Harris for assistance with the E11.5 dissections and plasmid production. We would like to also express our gratitude to Elena Kutsarova and Dr. Edward Ruthazer for their assistance with the electroporation set up. Finally, we thank Dr. Frederic Charron for the donation of the Math-1-GFP plasmid.

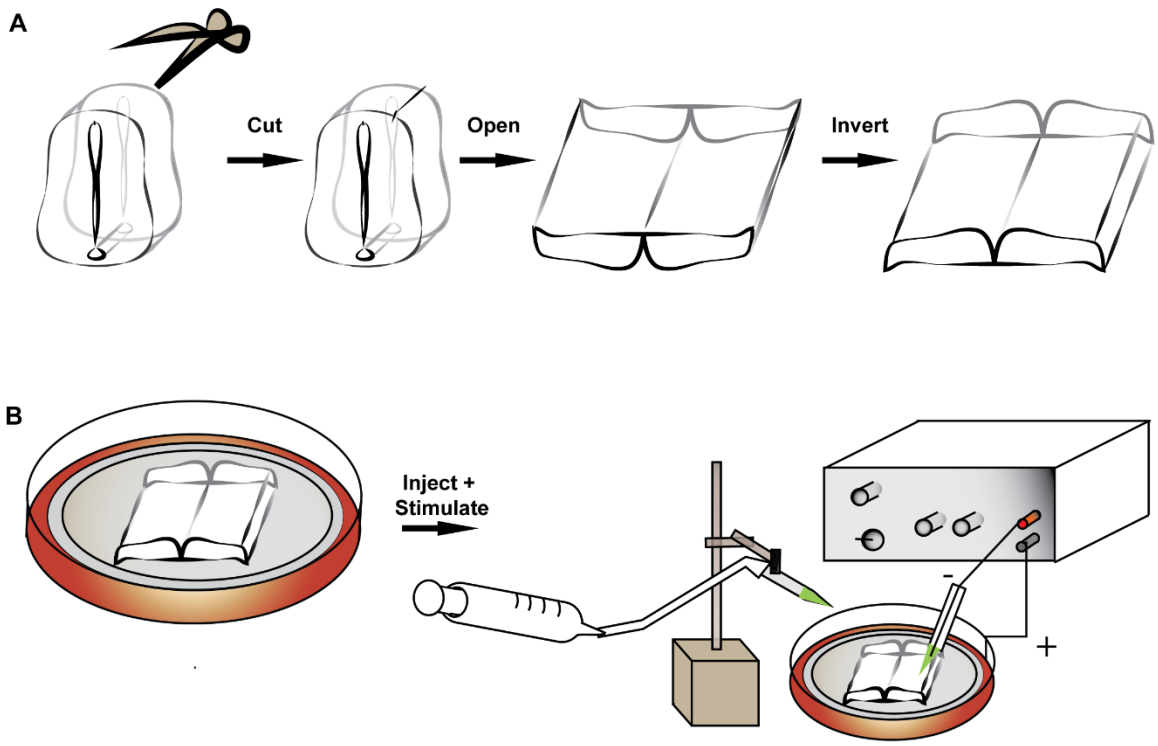

Figure 2.1: Schematic of the electroporation protocol. A. Spinal cords are cut open at the roofplate and plated with the former central canal of the neural facing down. B. Openbook preparations are subjected to the local microinjection of the DNA solution into their dorsal portion, and electrical current is applied to the same region immediately after. The micromanipulator that holds the electrode pipette has been removed from the schematic for simplicity.

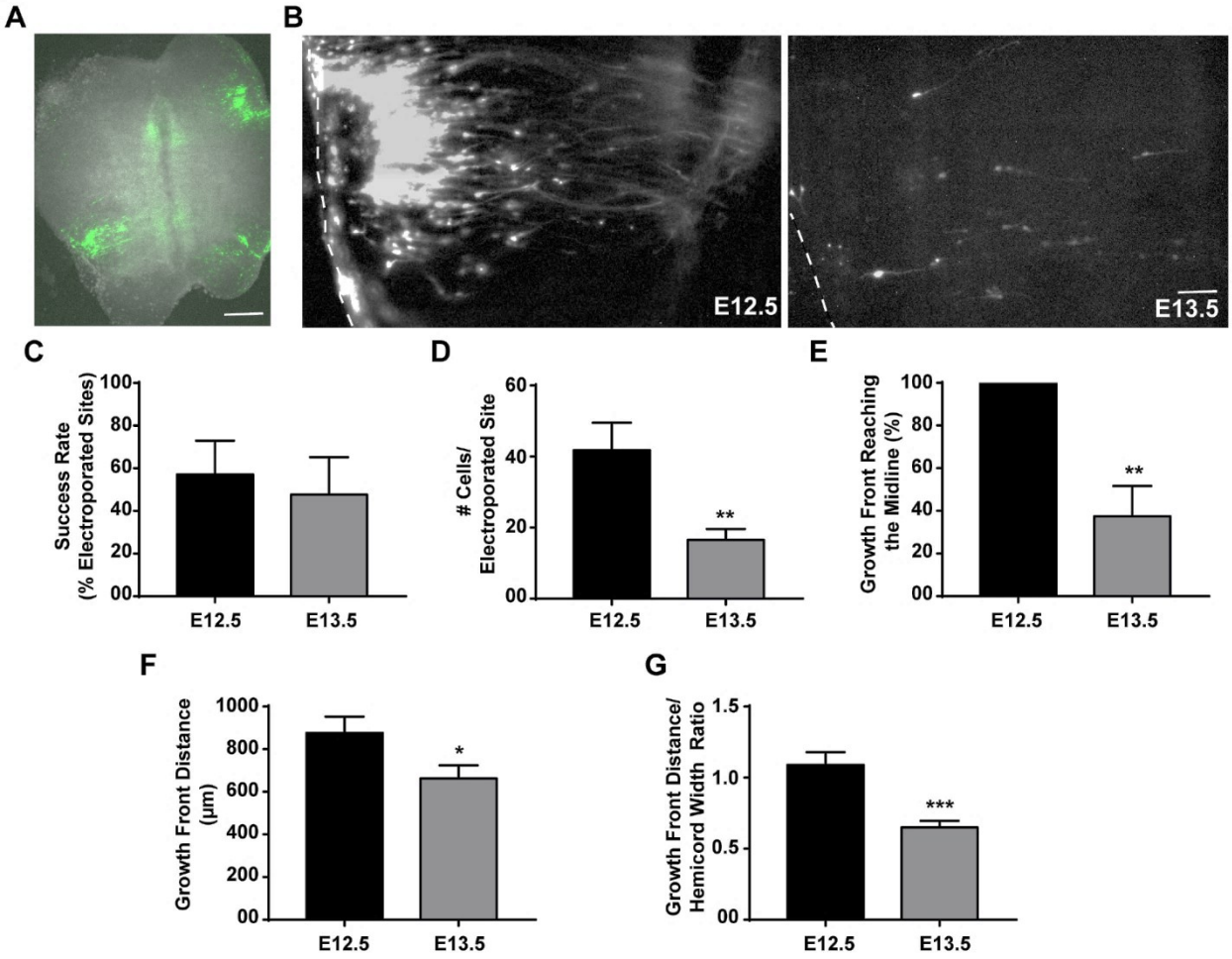

Figure 2.2: SCNs at E12.5 robustly express fluorescent constructs under a Math-1 promoter. A. E12.5 openbook preparation showing the sites that were electroporated with a Math-1 GFP plasmid. Scale bar: 150 µm. B. Representative electroporated sites of E12.5 and E13.5 openbook preparations. While E12.5 cells express the fluorescent construct at high levels, E13.5 cells weakly express it. In addition, the E12.5 SCNs seem to grow faster than E13.5 cells. Dashed line: dorsal edge of the explant. Scale bar: 35 µm. C. Quantification of the success rate of the electroporation protocol (expressed as percentage of electroporated sites that showed at least one electroporated cell). D. Average number of cells per successfully electroporated site. E. Percentage of electroporated sites in which the longest growing axon reached the midline approximately

48h after electroporation. F. Growth front distance from the center of the electroporated site. G. Growth front distance, normalized to the electroporated hemicord. N= 7 spinal cords per condition. Analysis done by Student's t-test. *: $p < 0.05$; **: $p < 0.01$; ***: $p < 0.001$.

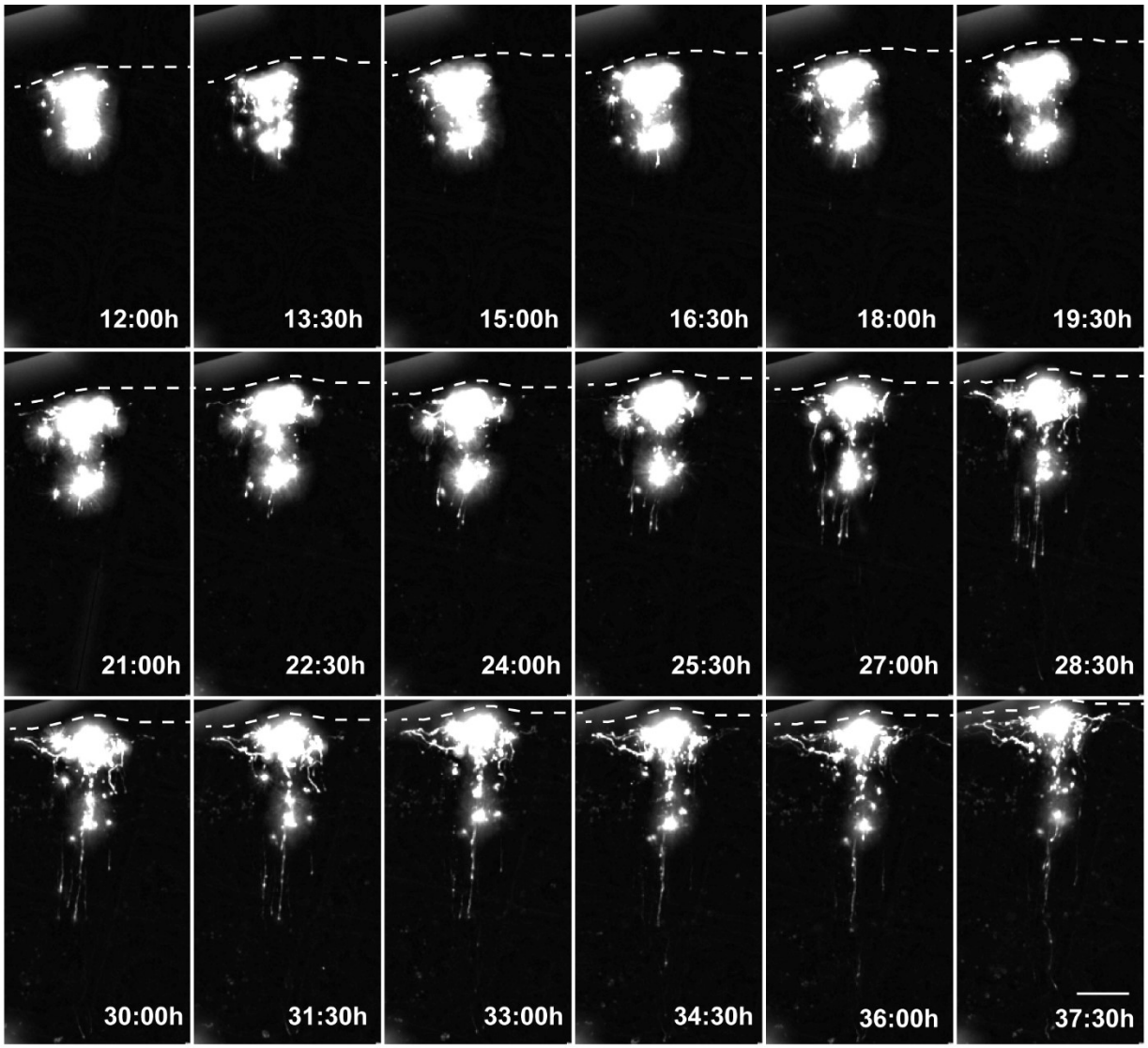

Figure 2.3: Math-1 GFP expression allows live imaging observation of SCN axons. The projection pattern of the cells was followed for over 1 day, starting at 12h after electroporation. Most of the axonal growth was observable starting at 24h and at approximately 36h the first axons reach the ventral midline. Dashed line: dorsal edge of the explant. The ventral midline is located in the lower edge of the field of view. Representative image series of 9 electroporated sites, 3 explants. Scale bar: 50 μm.

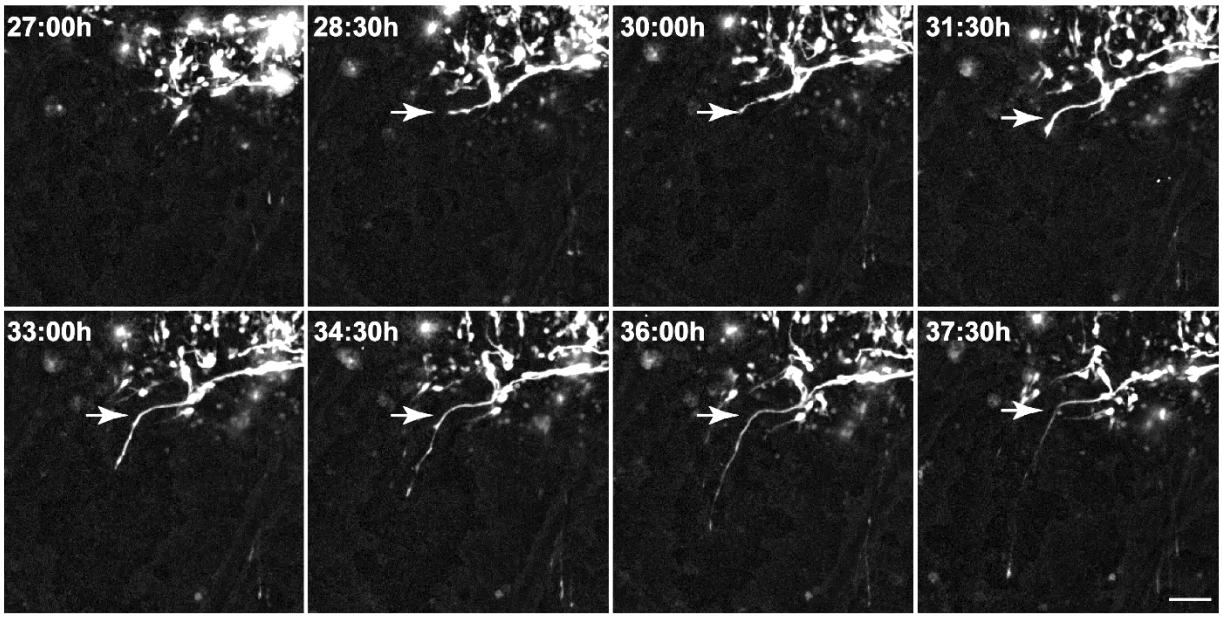

Figure 2.4: Live imaging shows that cells growing parallel to the ventral midline correct their paths. The arrows indicate the tip of a representative axon in the first frame it was visible. The ventral midline is situated parallel to the lower edge of the image. Scale bar: 20 μm.

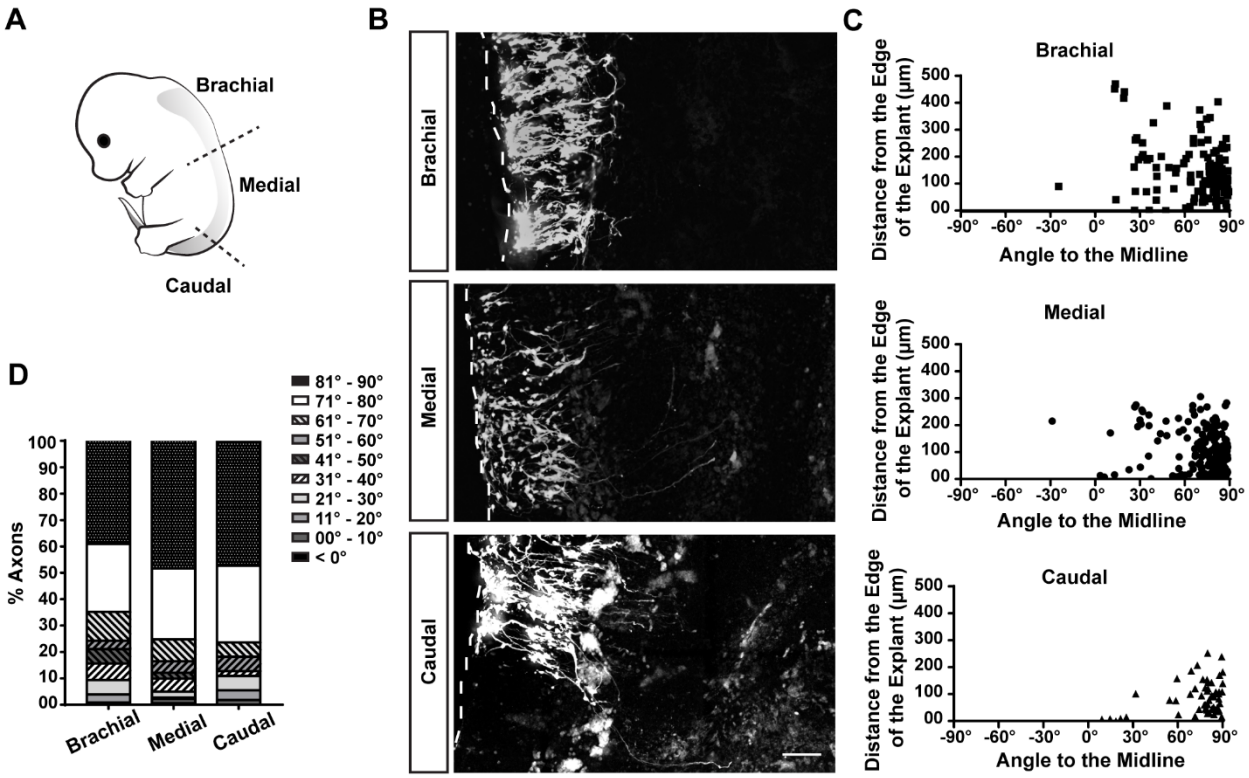

Figure 2.5: Math1-GFP electroporated cells have similar growth properties in different regions of the spinal cord. A. Schematic of a rat embryo showing the three regions of the spinal cord described here. B. Representative images of different electroporated from each section of the spinal cord at approximately 30 hours after electroporation. Scale bar: 35 µm. C. Dispersion graph showing the angle formed between the axon and the ventral midline and the dorsal edge of the explant. In all sections, the majority of the cells project axons perpendicularly to the floorplate, with most of the exceptions located close in the proximity of the dorsal edge of the explant. D. Bar graph showing the frequency of axons projecting in each angle range.

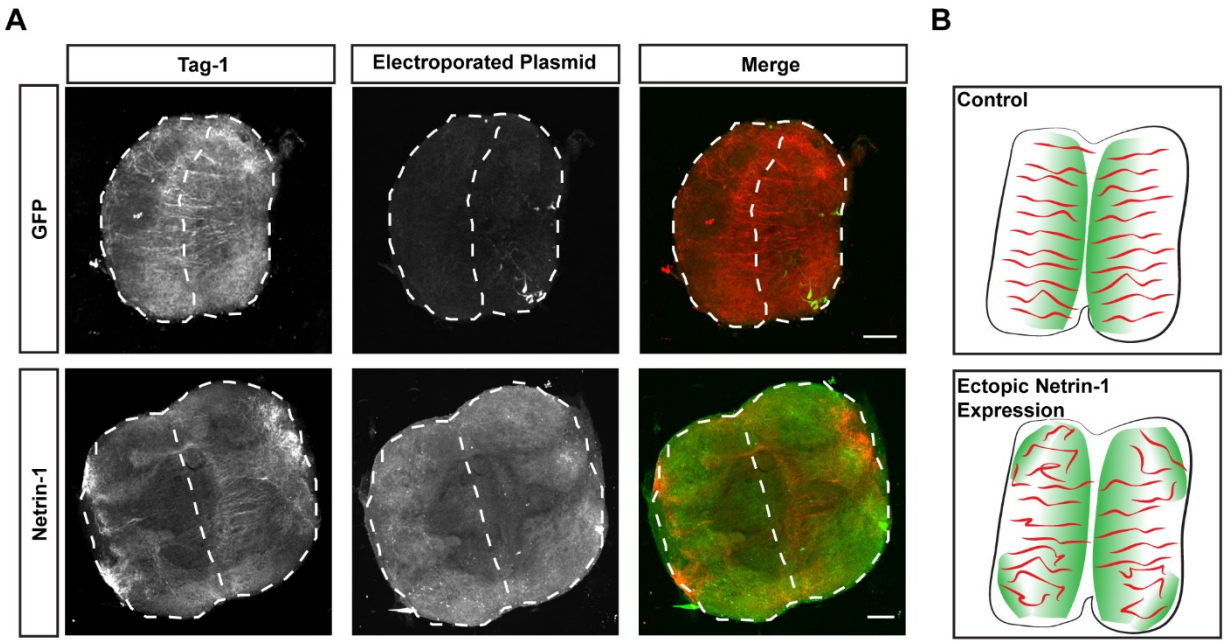

Figure 2.6: General promoters can be used to study extrinsic cues. A. Tag-1 and GFP (or Netrin-1) staining in the spinal cord explants. Scale bar: 100 μm. n= 4 GFP control explants, 7 Netrin-1 electroporated explants. B. Schematic showing the observed phenotype. In control explants, the physiologically relevant gradients of attractants are expressed solely by the floorplate, and the commissural Tag-1 fibers project straight to the ventral midline. After ectopic expression of Netrin-1 to the dorsal edges of the openbook preparation, the Tag-1 positive fibers become disorganized.

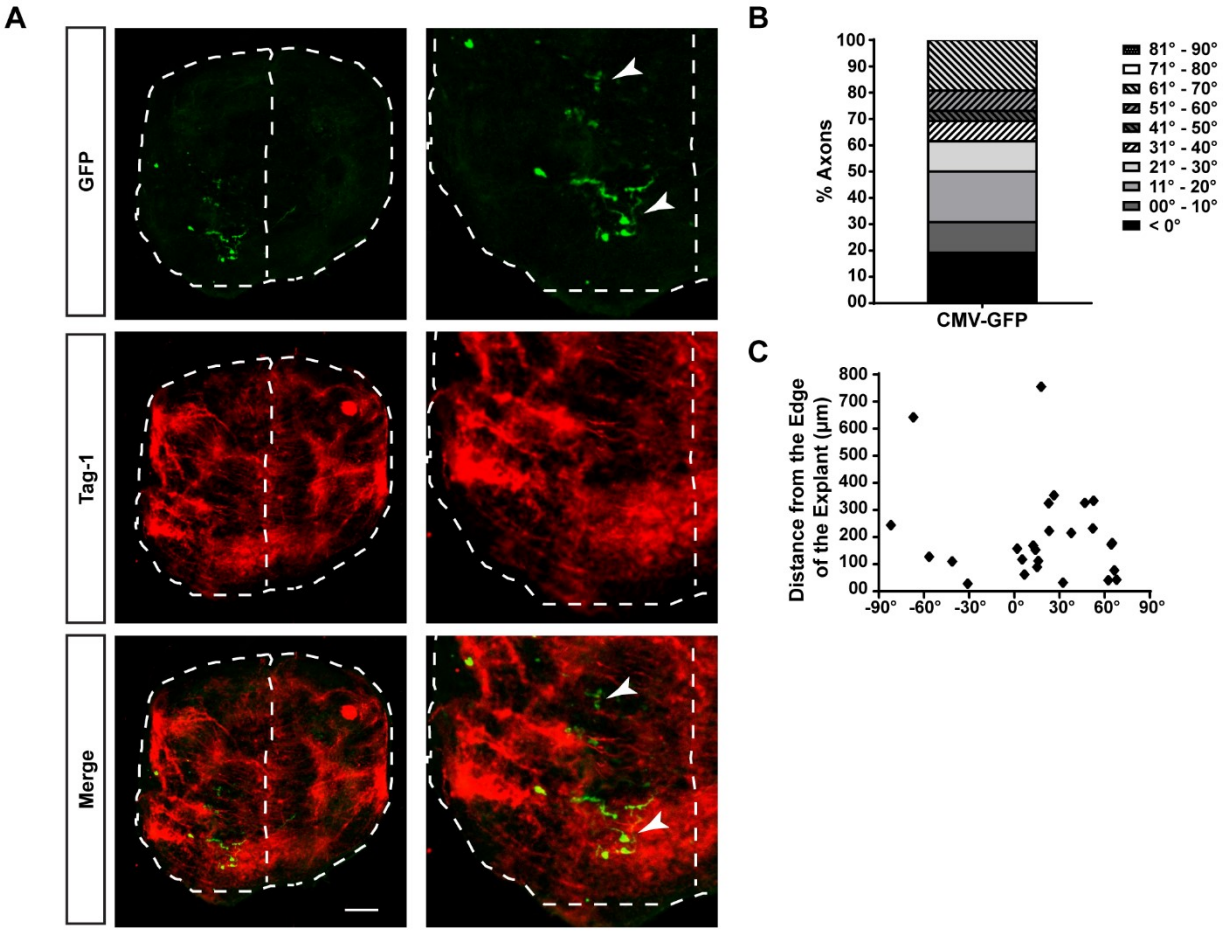

Supplementary figure 1: GFP electroporated spinal cells do not follow the pattern of projection characteristic to commissural neurons. A. GFP signals and Tag-1 staining on E10.5 spinal cord explants. Left panels show the whole view of the openbook explant. Scale bar: 100 µm. Right panels are blowups of the left panels, showing details of the electroporated cells. Arrowheads: GFP signal parallel to the midline. B. Quantifications of the orientations of the fibers (angles relative to the midline). N=4 explants. C. Dispersion plot of the turning angles of the cells possessing neurites, showing that the GFP positive cells project in diverse angles, independently of where they are born.

Chapter 3 – Preface

In this chapter, we analyze the effects of 14-3-3s during pre-crossing spinal cord commissural axon development. 14-3-3s, a family of adaptor proteins that is abundant in the growth cones of axons, has been previously shown to play a role in later, post-crossing spinal cord commissural neuron development.

Here we investigate the effects of this family of proteins in early axon guidance, and we search to identify its molecular mechanism.

Chapter 3 – 14-3-3ζ regulates pre-crossing spinal cord commissural projections via regulation of Rac1 signaling

Ricardo Alchini[1], Simon Hua[1], Christopher Kent[1], Andrew Kaplan[1], Isabel Rambaldi[1], Jonathan Degeer[2], Timothy Kennedy[1], Nathalie Lamarche-Vane[2], Quenten Schwarz[3] and Alyson E. Fournier[1].

1- Montreal Neurological Institute, McGill University, Montreal Canada.

2- Department of Anatomy and Cell Biology, McGill University, Montreal, Canada.

3- Cancer Research Centre, University of South Australia, Adelaide, Australia.

3.1 – Abstract

During development, axons must navigate through complex paths, while being guided by numerous guidance cues. We have previously shown that the 14-3-3 family of adaptor proteins modulates the polarization of axonal responses. Spinal commissural neurons that are attracted to sonic hedgehog (Shh) at the midline during development are repelled by Shh after crossing the midline and this is mediated by an upregulation of 14-3-3 proteins that suppress PKA activation. Intriguingly some 14-3-3 isoforms that do not bind to PKA are also expressed in pre-crossing spinal cord commissural neurons leading us to investigate their role in early stages of commissural neuron development. Here we showed that global 14-3-3 loss of function disrupts the trajectory of commissural neurons projecting to the floorplate and that this is phenocopied by loss of the 14-3-3ζ isoform. Global inhibition of 14-3-3s and loss of 14-3-3ζ reduces the sensitivity of the

spinal cord commissural axons to the midline attractant Netrin-1. 14-3-3 loss of function results in global activation of the small GTPase Rac1 resulting in the failure of commissural neurons to locally coordinate cytoskeletal rearrangements in response to Netrin-1.

3.2 – Introduction

Axons of spinal cord commissural neurons (SCNs) navigate a complex path in response to multiple guidance cues in the developing spinal cord. SCN axons initially extend ventrally towards the floorplate in response to repulsive cues at the roof plate including BMPs and Draxin and attractive cues at the floorplate including Netrin-1, Sonic Hedgehog (Shh) ad VEGF (Augsburger et al., 1999; Charron et al., 2003; Islam et al., 2009; Kennedy et al., 1994; Ruiz de Almodovar et al., 2011). SCN axons then cross the midline and undergo a series of molecular changes to avoid recrossing the floorplate and to migrate anteriorly towards the brain (Andermatt et al., 2014; Bourikas et al., 2005; Brose et al., 1999; Kidd et al., 1999; Lyuksyutova et al., 2003).

Guidance molecules signal through their cognate receptors initiating intracellular signaling pathways that converge to regulate the growth cone cytoskeleton and the direction of outgrowth (Ridley, 2006). The actin cytoskeleton present in the periphery of growth cone is critical for directed axon guidance and is regulated by Rho GTPases, small G proteins that function as molecular switches cycling between GDP-bound inactive forms to GTP-active forms. GTP-Rac binds to effector proteins to asymmetrically modify

the growth cone cytoskeleton controlling the direction of the outgrowth (Li et al., 2002a; Moore et al., 2008; Quinn et al., 2008; Shekarabi et al., 2005).

14-3-3 adaptor proteins have also been shown to function as molecular switches in axon guidance. 14-3-3 proteins are a seven isoform family that bind to target substrates and enhance or inhibit their function through various mechanisms including altering protein conformation, modifying subcellular localization or promoting proteosomal degradation (Xiao et al., 1995). Multiple 14-3-3 isoforms are expressed in the axonal growth cone. 14-3-3β and 14-3-3γ stabilize the PKA holoenzyme mediating sensitivity to several repulsive guidance molecules in postnatal neurons (Kent et al., 2010). *In vivo*, upregulation of 14-3-3β and 14-3-3γ in post crossing SCNs converts the neuronal response to Sonic Hedgehog from attraction to repulsion directing SCNs anteriorly in response to a caudal-rostral Sonic Hedgehog gradient (Yam et al., 2012).

The presence of distinct 14-3-3 isoforms in pre-crossing SCNs led us to ask if these proteins play a role in early guidance decisions. Here we show that 14-3-3 expression by pre-crossing SCNs mediates cell sensitivity to Netrin-1 and the formation of organized commissures. 14-3-3ζ plays an important role in regulating localized activation of Rac1 by controlling the activation of the Rac guanine nucleotide exchange factor (GEF), β-Pix.

3.3 – Materials and methods

3.3.1 – Reagents

Commercial antibodies were acquired for full length deleted in colorectal cancer (DCC) from BD Biosciences (San Jose, CA), pan-14-3-3 from Santa Cruz Biotechnologies (Santa Cruz, CA). The pCEP4 plasmid expressing full-length rat DCC and pHSVPrPUC plasmids expressing GFP and GFP-R18 were previously described (Kent et al., 2010; Li et al., 2002a).

Recombinant Herpes Simplex viruses (HSVs) were produced by transfecting pHSVPrPUC plasmids into 2-2 Vero cells, following a previously detailed protocol (Neve et al., 1997). VI-V fragment Netrin-1 was purified from constitutively expressing cell lines (Riou et al., 2013). TAT fusion peptide constructs were provided by Dr. Jing Cheng (Emory University) and protein was purified from competent bacteria as previously described (Dong et al., 2008). Glutathione s-transferase (GST), GST-CRIB and RacG15A (a generous gift from Dr. Jean-François Coté, Institut de Recherches Cliniques de Montréal) proteins were purified from IPTG-induced bacteria as previously described (Cote and Vuori, 2006).

3.3.2 – SCN cultures

E13.5 staged pregnant Sprague Dawley rats were purchased from Charles River Laboratories (St. Constant, Canada). All animal care and use was in accordance with the McGill University guidelines and approved by the Montreal Neurological Institute Animal Care Committee. Rat embryos (Witschi stage 27- 28) were dissected, and the neural tubes were isolated and cultured following a previously described protocol (Moore and Kennedy, 2001).

For dissociated cultures, cells were plated on 20 µg/ml poly-L-lysine coated dishes, and left to recover overnight in Neurobasal 10% FBS, after which the medium was exchanged to Neurobasal B27. SCN cultures were used at 2 DIV (45-55 h after plating). For the phenotypical assays, low-density cultures were obtained by plating cells at approximately 20 000 cells/ cm^2. Biochemical assays were performed on cells plated at 500 000 cells/ cm^2.

For organotypic cultures, E12.5 embryonic spinal cords were dorsally open and placed lumen down on Type I rat tail collagen (BD Biosciences) coated Millicell (Millipore, Bedford, MA) culture inserts. The cords were left recovering in Neurobasal medium (Invitrogen, Carlsbad, Ca) supplemented with 10% heat-inactivated fetal bovine serum (Sigma, St-Louis, MO), after which the medium was exchanged to Neurobasal supplemented with 2% B27 standard supplement (Sigma, St-Louis, MO). In order to analyze whether 14-3-3s play a role in axon guidance, cords were exposed to 5 µM BV02 (Sigma, St-Louis, MO) or dimethyl sulfoxide (DMSO, Sigma, St-Louis, MO) as a vehicle control. Openbooks were used at 2 DIV (45-55 h after plating), when fixed using 4 % paraformaldehyde (Electron Microscopy Sciences, Hatfield, PA) in PBS, and immersed in 50% formamide/ 20 % poly ethylene glycol, following the ClearT2 protocol (Kuwajima et al., 2013). Tissue samples were stained for Tag1 (Goat IgG, R&D Systems) following a standard protocol, and fluorescence signals were acquired using a spinning disk system (Quorum Wave FX-X1, on a Leica DMI6000B inverted microscope) equipped with 10x objective lens and the appropriate filters. Z-series of 10-30 optical sections were sampled at 5 µm step size, covering the whole surface of the cord. Z-projections of the commissural axons were analyzed using AngleJ (Gunther

et al., 2015), a plugin for ImageJ. Average angle and angle distribution in 10º bins were plotted and statistical analysis was performed using Prism 7.0 (GraphPad)

3.3.3 – Spinal cord *ex vivo* gene transduction

E12.5 rat spinal cords (Witschi stage 25-26) were dissected and segments corresponding to somites 5 to 20 were plated as openbooks, with the lumen facing down on collagen coated Millicell culture inserts. Math1-GFP or Math1-R18 plasmid solutions (2.0 µg/µl) were injected on the dorsal region of the openbooks with a glass microsyringe (approximately 20 µm tip diameter). Electrical pulses (7-10 trains of 1 ms pulses at 200 Hz, 50 V) were delivered across a silver wire placed inside a glass micropipette (approximately 20 µm tip diameter), where a silver wire ground electrode was placed in the culture medium (Neurobasal 10% FBS). The procedure was repeated to 2 to 3 sites in each hemicord. Cords were fixed with 4 % PFA in PBS, cleared using the ClearT2 protocol (Kuwajima et al., 2013). GFP signals were acquired using the same spinning disk system, in Z-series of 5-20 optical sections with 5 µm step size, covering the whole electroporated site.

The angle formed by the cell body, the axonal tip and the midline was measured for individual cells and their average and distribution were plotted and statistical analysis (Student t-test or Two way ANOVA with Sidak correction) was performed using Prism 7.0 (GraphPad).

3.3.4 – Dunn chamber turning assays

Dunn chamber axon guidance assay was performed as previously described (Yam et al., 2009). In brief, SCNs were dissociated and grown on square #3D coverslips (Fischer Scientific, Waltham, MA), and then assembled in a Dunn chamber at the desired stage. For the 14-3-3ζ knockdown experiments, the plasmid constructs containing previously validated shRNA sequences were electroporated into SCNs using Amaxa Nucleofector I kit (Lonza , Switzerland) (Yam et al., 2012). For each electroporation, 5 x 10^6 cells were placed in the supplied cuvette with 1 µg of DNA. The program O-003 was used following the manufacturer's instructions. Experiments that required Lipofectamine 2000 (Invitrogen, Waltham, MA) transfection or HSV transduction, had these agents being added at 30 h in culture. Gradients were generated in the Dunn chamber with 0.2 µg/ml recombinant VI,V fragment of Netrin-1 in the outer well (Yam et al., 2012). After Dunn chamber assembly, time-lapse phase contrast images were acquired for 2 h. The turning angle was defined as the angle between the original direction of the axon and a straight line connecting the base of the growth cone from the first to the last time point of the assay. Analysis of the films was performed using ImageJ. Growth cone displacement rate and turning angles were plotted using Prism 7.0, were statistical analysis (One way ANOVA with Tukey post-test) was performed.

3.3.5 – Immunoprecipitation

HEK293T cells were transfected overnight with the plasmids of interest using Lipofectamine 2000 following the protocol recommended by the supplier. When indicated, cells were treated with 200 ng/ml Netrin-1 for 5 min and then lysed in Buffer D (20 mM Hepes pH 7.4, 0.5% Triton-X, 50 mM NaCl for the experiments aiming 14-3-3s and DCC interaction or 150 NaCl for the others, 10% glycerol, 5 mM NaF, 1 mM Na_3VO_4 and protease inhibitor cocktail). Lysates were incubated with anti-pan 14-3-3 (Santa Cruz), anti-HA (Sigma), anti-V5 (Sigma) or anti-myc (Sigma) antibody conjugated agarose beads. Precipitates were extensively washed with the same buffer and eluted in Laemmli buffer.

Protein samples were separated by SDS-PAGE and transferred to PVDF membranes (Pierce Biotechnology Rockford, IL). Horseradish peroxidase conjugated secondary antibodies and ECL were used so that the proteins of interest could be observed with chemiluminescence.

3.3.6 – Whole mount staining and clearing

SV129 mouse embryos imaged in this study were raised according to the guidelines of University of Adelaide. E11.5 embryos were fixed in ice cold 4% PFA in PBS, and then processed as described in the iDISCO protocol (Erturk et al., 2012; Renier et al., 2014). Samples were blocked at room temperature for 12 h in 6% donkey serum (Sigma, St. Louis, Missouri), and 0.1% Triton X - 100 (Sigma, St. Louis, Missouri) in PBS. For visualization of the spinal cord commissural projections, embryos were stained for Tag-1, 1:200 in wash solution (0.6% donkey serum, 0.1% Triton X-100 PBS)

for 48 h at 37°C. Samples were vigorously washed for 12 h and subsequently incubated in Alexa 568 conjugated donkey anti-goat IgG (Invitrogen, Eugene, Oregon) (1:250 in wash solution) for 36 h at 37°C. Finally, samples were washed for 12 h with PBS and kept at 4°C until imaging. Tissue was dehydrated using a tetrahydrofuran gradient (50%, 75%, and 100% THF) (Sigma, St. Louis, Missouri) at room temperature, for 1 h per solution. Samples were then immersed in dibenzyl ether (DBE, Sigma, St. Louis, Missouri) for at least 30 min prior to imaging. The cleared samples were imaged on a light sheet microscope (Ultramicroscope II; LaVision Biotec) equipped with a sCMOS camera (Andor Neo) and a 6.3×/0.5 NA objective lens equipped with a 6-mm working distance dipping cap. Images were blinded and SCN axons were traced using Neurolucida 360 (MBF, Williston, Vermont), with assistance of the user-guided semi-automatic tracing tool. Tortuosity and growth angle related to the midline were plotted and analyzed using Prism 7.0 (GraphPad).

3.3.7 – CRIB and Rac G15A pulldowns

Rac activity was assessed by GST-CRIB pulldowns (Royal et al., 2000). In brief, HEK293Ts cells transiently expressing myc-tagged Rac were stimulated with 200 ng/ml Netrin-1 (Enzo Life Sciences, Farmingdale, NY) 16–20 h after transfection. Cells were lysed in 25 mM HEPES, pH 7.5, 1% NP-40, 10 mM $MgCl_2$, 100 mM NaCl, 5% glycerol, 5 mM sodium fluoride, 1 mM sodium vanadate, 1 mM PMSF, 10 µg/ml aprotinin, 10 µg/ml leupeptin. Protein levels and solution volumes were equalized and lysates were incubated for 30 min at 4°C with purified GST-PAK purified in a twofold volume of binding buffer (25

mM HEPES, pH 7.5, 30 mM $MgCl_2$, 40 mM NaCl, 0.5% NP-40, 1 mM DTT). Beads were washed two times in binding buffer containing 1% NP-40.

For the analysis of GEF activity, HEK293Ts expressing the GEF of interest were lysed on GEF buffer (20 mM HEPES (pH 7.5), 150 mM NaCl, 5 mM $MgCl_2$, 1% (vol/vol) Triton X-100, 1 mM DTT and protease inhibitor cocktail) (Guilluy et al., 2011). Protein levels and solution volumes were equalized and lysates were incubated for 45 min at 4°C with 30 µg of purified GST-Rac G15A (or GST control). Beads were washed 3 times with GEF buffer and resuspended in Laemmli buffer. Levels of the proteins were evaluated by Western blotting.

3.4 – Results

3.4.1 – 14-3-3 proteins affect pre-crossing SCN guidance

Based on our previous report of 14-3-3 expression in pre-crossing SCNs we asked if 14-3-3 proteins have a role in pre-crossing SCN development. We bath applied BV02, a cell permeable 14-3-3 inhibitor, to openbook preparations of rat embryonic spinal cords and evaluated the trajectory of Tag-1-positive SCN axons. The Tag-1 positive cells elongated radially towards the ventral midline (Fig 3.1A).

In control treated cords, Tag-1 positive cells projected towards the midline in an organized fashion. In openbook preparations exposed to BV02, SCNs also reached the ventral midline but the trajectory of the fibers appeared disorganized (Fig 3.1B). To quantify the trajectory of pre-crossing SCNs, we performed semi-automated analysis

using the ImageJ plugin AngleJ (Gunther et al., 2015). Blinded images of the spinal cord were divided into segments of 200 μm in length and aligned so that the ventral midline would be localized vertical to the field of view. The automated quantification skeletonized the fibers and determined the angles in which each string of two pixels had grown such that a value of 0 degree represents growth parallel to the midline and 90 degrees perpendicular to the midline (Fig 3.1C). In order to avoid the influence of the longitudinal (post-crossing) projections, a region of about 50 μm adjacent to the midline was excluded from the analysis. BV02 treated axons projected with an average angle of 54.00 ± 0.64 degrees from the midline, while control axons grew at an average angle of 68.62 ± 1.80 degrees(Fig 3.1D). We also observed a reduction in the frequency of the outgrowth happening in the range of 70 to 90 degrees to the midline, the predominant bins for the control axons (Fig 3.1E).

To determine if the function of 14-3-3 proteins in pre crossing SCN guidance was intrinsic to SCN neurons, we *ex utero* electroporated SCNs with GFP-R18, a competitive inhibitor of 14-3-3-substrate binding. GFP-R18 was selectively electroporated into dorsal spinal cord neurons using a Math1 promoter, and the GFP signal from the fusion protein was used to visualize the axons. Sparse electroporation allowed for the visualization of individual axons such that the the angle formed between each individual axon and the midline could be calculated (Fig 3.1F). R18 transfection had a similar effect to BV02 treatment. The average angle to the midline was 72.79 ± 1.16 degrees for the control, and 44.55° ± 11.62 degrees for the R18 transfected cells (Fig 3.1G). The percentage of cells projecting from 80 – 90 degrees was strongly affected in the R18 condition (Fig 3.1H). We also observed that the frequency of cells

that grew away from the midline in R18 transfected cells increased to 10.55% ± 0.07%, from 2.15% ± 0.02 in the control. Together these results suggest that 14-3-3 proteins function in a cell autonomous manner to regulate the appropriate guidance of pre crossing SCNs (Fig 3.1I).

3.4.2 – 14-3-3s affect growth cone responses to Netrin-1

To evaluate potential molecular mechanisms that could explain this phenotype we performed Dunn chamber turning assays to examine if pre-crossing SCNs had an altered sensitivity to physiologic axon guidance cues. SCNs responses to Netrin-1, the most prominent attractant released by the ventral midline were evaluated in the presence and absence of R18 (Fig 3.2). Control non-infected or GFP-transduced SCNs were attracted to a Netrin-1 gradient (NI: 17.35 ± 3.98 degrees; GFP: 12.65 ± 4.66 degrees), while R18 transduced cells were insensitive to the Netrin-1 grandient and exhibited random turning angles in the presence of Netrin-1 (Fig. 3.2A-B, 0.94 ± 4.66 degrees). This effect of 14-3-3 loss of function was specific to the guidance of the axons, and not to their outgrowth, as no significant difference was observed in the displacement of axons during the imaging sessions (Fig 3.2C, NI: 24.40 ± 0.66 μm; GFP: 20.21 ± 0.59 μm; R18: 22.50 ± 0.75 μm, Fig 3.2C).

3.4.3 – 14-3-3ζ interacts with the Netrin-1 receptor DCC and is responsible for GC phenotypes

These results suggested that 14-3-3s might play a role in the immediately early phase of Netrin-1 signaling in the cell. We thus analyzed if individual 14-3-3 isoforms interact with DCC, the predominant receptor for Netrin-1 in pre-crossing SCNs. We first demonstrated that a small pool of the total 14-3-3 protein in the cell co-precipitates with DCC in brain lysates (Fig 3.3A). We then investigated which 14-3-3 isoforms interact with this receptor by performing co-immunoprecipitations with myc-tagged 14-3-3 isoforms and HA-tagged DCC in transfected HEK293T cells. We found that 14-3-3β, γ and ζ co-immunoprecipitated DCC whereas 14-3-3ε, η and θ failed to interact (Fig 3.3B). Performing the immunoprecipitation in the opposite direction revealed that 14-3-3ζ but not β or γ co-immunoprecipitated with DCC (Fig 3.3C). We therefore followed up on the function of the 14-3-3ζ isoform, which is a robustly expressed isoform in pre crossing commisural neurons (Yam et al., 2012).

We first tested if 14-3-3ζ antagonism would phenocopy the results of 14-3-3 loss of function. 14-3-3ζ levels were supressed by transducing a previously validated shRNA sequence targeting 14-3-3ζ (Kent et al., 2010; Yam et al., 2012). Similarly to R18, cells transduced with a 14-3-3ζ shRNA plasmid were insensitive to Netrin-1 in the Dunn chamber turning assay (Fig 3.4A, B). Reintroduction of a shRNA resistant form of 14-3-3ζ restored the attractive response to Netrin-1 in the Dunn chamber turning assay supporting the specificity of the shRNA (Fig 3.4A, B). 14-3-3ζ shRNA had not impact on mean displacement of cells in the Dunn chamber turning assay (Fig 3.4C). Further, cells transduced with 14-3-3ζ shRNA were resistant to netrin-dependent growth cone expansion in response to acute netrin-1 treatment, suggesting that 14-3-3ζ is capable of modulating fast growth cone responses to Netrin-1 and phenocopying

the effects of R18 (experiment contained in Dr. Christopher Kent's doctoral thesis) (Fig 3.4E). Together this data supports a role for 14-3-3ζ in regulating neuronal responses to Netrin-1.

3.4.4 – 14-3-3ζ affects SCN development *in vivo*

To test if 14-3-3ζ regulates the formation of SCN projections we analyzed SCN projection in 14-3-3ζ knockout mice. We performed whole mount staining and clearing of E11.5 mouse embryos to observe the spinal cord commissures in 3 dimensions without deconstructing the tissue in histological slices (Fig 3.5A). (Erturk et al., 2012; Renier et al., 2014). When compared to control (wild type) embryos, 14-3-3ζ null mice form less well defined commissures (Fig 3.5B). 14-3-3ζ deficient axons are still capable of reaching the floorplate, suggesting that 14-3-3s are not required for target recognition of these axons. Semi-automated tracings of the commissural fibers were performed and the angles formed between these axons and the midline were assessed (Fig 3.5C-E). The average angle formed between the fibers and the midline was not significantly affected by the loss of 14-3-3ζ (wild type= 74.87 ± 1.08 degrees, heterozygous = 76.26 ± 1.37 degrees, knockout = 66.46 ± 3.04 degrees, $p= 0.514$ when comparing wild type and knockout animals by one way ANOVA with Dunnett's post-test). However, when plotting the data in 10 degree bins similarly to the analysis done with the openbooks, there was a significant decrease in the frequency of outgrowth perpendicular to the midline (80 – 90 degrees, $p<0.001$ by two way ANOVA with Dunnett's post-test). Interestingly, the analysis of the tortuosity index of these axons

showed the most dramatic phenotype. Defined as the ratio between the actual length of an axon segment and the shortest possible line between its origin and its ending, tortuosity is expressed in a scale that starts from 1.0 (straight axons). A fan-in projection of commissural axons shows that control axons project in very smooth lines, with a narrow range of projecting angles, while the 14-3-3ζ null axons project in a much broader range of values, and seem to change directions continuously during their growth (Fig 3.5F). Control axons deviate very little from this theoretical shortest path when they project towards the ventral midline (1.12 ± 0.01) while 14-3-3ζ deficient axons are significantly more tortuous (1.19 ± 0.01) (Fig 3.5G).

We then performed traditional histological sections as an alternative approach to understand the phenotype of the 14-3-3ζ knockout embryos. Through these axial sections, we confirmed that the formation of the commissures is overal intact (Fig 3.5H, J). Consistent with the tortuosity measurements seen in the 3D projections, we could observe that the Tag-1 staining occupied a larger area in the knockouts (20.15% ± 1.33% of the neural tube area in the control animals, 25.92% ± 1.33% of the neural tube area in the knockout mice, Fig 3.5H). This is a result of the fibers taking a more irregular path, as the initial thickness of the bundles is unaffected (control= 17.14% ± 1.51 % of the hemicord thickness, 14-3-3ζ knockout mice: 19.36% ± 0.98%, Fig 3.5I) but the bundles become wider in the ventral region (control= 15.17 % ± 1.13% of the hemicord thickness, 14-3-3ζ knockout mice= 28.40% ± 1.09%, Fig 3.5J). This phenotype is reminiscent of the TRIO knockout mice, indicating that 14-3-3s may play a role in the regulation of some GEFs involved in Netrin-1/ DCC signaling (Briancon-Marjollet et al., 2008).

3.4.5 – 14-3-3 loss of function enhances Rac activation

Based on the similar phenotypes exhibited by 14-3-3ζ and TRIO knockout mice, we investigated how 14-3-3s affect signaling downstream of Netrin-1/DCC. We treated DCC-transfected HEK293T cells with netrin-1 in the presence of R18 or WLKL control peptide. R18 had a variable effect on netrin-1-dependent stimulation of ERK, Src or ERM phosphorylation (data not shown). However, we did find that R18 treatment led to a marked upregulation in Rac-GTP levels and that netrin-1 failed to further activate Rac-GTP in HEK293T cells (Fig 3.6A). A similar affect on Rac-GTP levels was found in cells subjected to 14-3-3ζ knockdown (Fig 3.6B).

We then evaluated what Rac guaninine nucleotide exchange factors (GEFs) may be activated by R18. Lysates from HEK293T cells treated with R18 were subjected to pull downs with nucleotide free RacG15A which has a high affinity for active GEFs. Binding to DOCK180, TRIO and β-Pix were evaluated because of their ability to interact with DCC (Briancon-Marjollet et al., 2008; Nishino et al., 2008). HEK293Ts cells were transduced with vectors for Rac1 GEFs, after which the cells were treated with membrane permeable forms of R18, or the control peptide WLKL, and the Rac G15A pulldown was performed (Fig 3.6C). β-Pix, but not DOCK-180 or TRIO exhibited an increased affinity for RacG15A in response to R18 treatment (Fig 3.6C). We further analyzed whether 14-3-3s played a role in the formation of a DCC/β-Pix complex (Fig 3.7D). R18 disrupted the interaction between DCC and β-Pix indicating that 14-3-3 proteins stabilize the binding of β-Pix to DCC.

Finally, we investigated whether the abnormal activation of Rac1 could be the mechanism by which 14-3-3s impact on Netrin-1 attraction. Exogenous wild type Rac1 was transduced into SCNs, as well as two constitutively active mutants of Rac1: Rac V12 and Rac Q61L (Fig 3.7A-C). Wild type Rac1 did not impair the axonal ability of the axons to turn towards the Netrin-1 gradient (average= 20.78 ± 4.12 degrees), while both constitutively active mutants failed to turn towards the Netrin-1 source (V12= -7.18 ± 6.23 degrees, Q61L= 1.839 ± 4.56 degrees, Fig 3.7B). Thus, the disorganized activation of Rac1, such as that caused by 14-3-3 loss of function, is a possible mechanism by which 14-3-3s mediate the attraction to Netrin-1 and subsequently the development of spinal cord commissures (Fig 3.8).

3.5 – Discussion

Our findings demonstrate that 14-3-3 proteins play an important role in appropriate guidance of pre-crossing SCNs. This effect is mediated in part through 14-3-3ζ-dependent regulation of Rac1 levels through the Rac GEF β-Pix. We suggest a model wherein 14-3-3ζ regulates the local activation of β -Pix to confer localized responsiveness to Netrin-1. Depletion of 14-3-3 reduces the sensitivity of the SCN axons to Netrin-1, and results in tortuous, disorganized projections *ex vivo.* Such effect is phenocopied by loss of 14-3-3ζ, which itself seems to be responsible for the role of 14-3-3 in mediating Netrin-1 attraction and is also required for the straightness of the commissural fibers *in vivo.*

In our model, 14-3-3ζ is bound to DCC in a Netrin-1-independent manner, localizing it in a complex with the GEF β-Pix. Thus, 14-3-3s localize a Rac GEF in the vicinity of

DCC, spatially regulating its signaling. The interaction between DCC and β-Pix has been shown to be required for Netrin-1 attraction, and it is not modulated by Netrin-1 (Lai Wing Sun, 2015). We speculate that 14-3-3s may play a role in local release of β-Pix from a DCC complex to mediate local Rac activation in the vicinity of Netrin engagement. 14-3-3s have been previously shown to interact with β-Pix (Chahdi and Sorokin, 2008; Kim et al., 2001). 14-3-3β, -γ and -ζ bind to β-Pix in a phospho-dependent (14-3-3β and 14-3-3-γ) and independent (14-3-3ζ) manner (Chahdi and Sorokin, 2008). 14-3-3 proteins were shown to stabilize β-Pix, inactivating it. Our results corroborate this by showing that 14-3-3 loss of function increases the levels of active β-Pix and, consequently, Rac1. Moreover, the ability of β and γ to also bind β-Pix might result in some compensation *in vivo* explaining why the phenotype of the 14-3-3ζ null mice was milder than what was expected based on the R18 / BV02 treatments. When in excess (see Fig 3.3), β and γ are also able to interact with DCC, therefore they could take over 14-3-3ζ role in this single knockout mouse line, despite their relatively low expression in this stage.

Analysis of a triple knockout for the three 14-3-3 isoforms could potentially reveal more robust effects of 14-3-3s in pre-crossing SCN development. Analysis of the spinal cord phenotypes of the neuronal specific 14-3-3 knockout mouse line could be an alternative approach (Foote et al., 2015; Qiao et al., 2014). These mice, as well as 14-3-3ζ null mice, have locomotor defects that might be partially due to problems in their commissures (Cheah et al., 2012; Ramshaw et al., 2013; Xu et al., 2015). However, they have not been reported to reproduce the hopping behavior that has been observed in other transgenic mice that have a SCN ventral midline broadening phenotypes.

The relative contribution of individual Rac GEFs downstream to DCC to proper SCN axon guidance is also an open question. Trio, DOCK180 and β-Pix all affect Netrin-1 signaling and responsiveness to Netrin-1 *in vitro*. Trio null embryos have a spinal cord phenotype that is identical to the14-3-3ζ knockout phenotype reported here while DOCK180 knockout mice do not have a severe neural phenotype and β-Pix mice have not been analyzed due to embryonic lethality before the stage of midline crossing (Briancon-Marjollet et al., 2008; Laurin et al., 2008; Omelchenko et al., 2014).

Altogether, our data suggest that 14-3-3s, especially 14-3-3ζ, play an important role in regulating growth cone attraction to Netrin-1, via the spatial regulation of GEF activation and consequently Rac1.

3.6 – Acknowledgements

We would like to thank Erika Tse-Wen Lee and Elke Kuster-Schock from the Advanced BioImaging Facility, McGill University, for the assistance with microscopy and the Montreal Neurological Institute Microscopy Facility for the support with the analysis of the lightsheet images. We thank Dr. Julien Ferrent and Dr. Frederic Charron for the assistance with the histology experiments. We would also like to thank Nathalie Marçal for the contribution with reagent production.

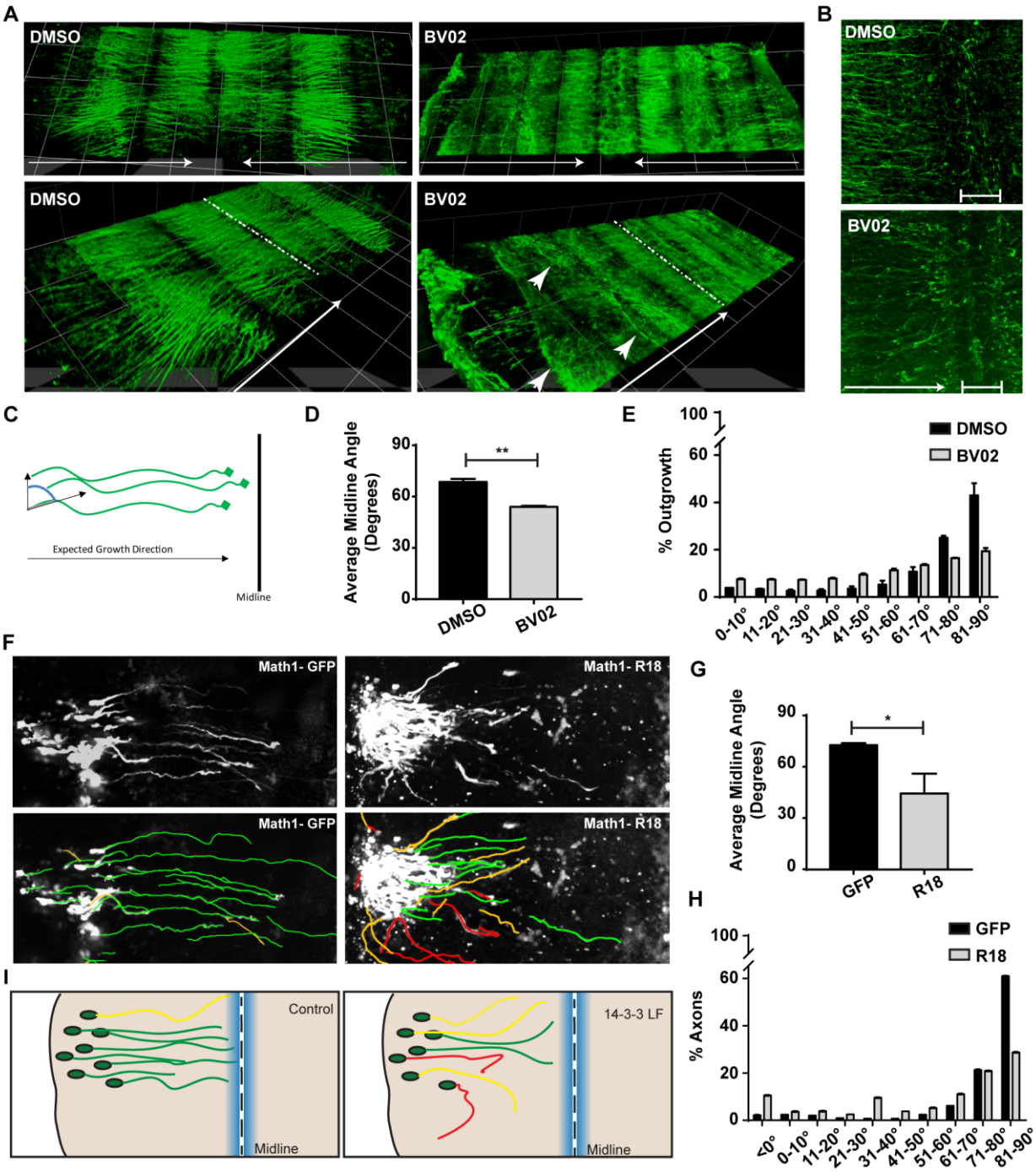

Figure 3.1: 14-3-3 loss of function results in disorganized pre-crossing projections from SCNs. A. Representative images of Tag-1 stained openbooks that have been treated with BV02 or vehicle controls. Maximum intensity projection of the openbooks (upper panels) and 45 degrees tilted 3D images of the same openbooks (lower panels).

Grid size: 100 μm. Dotted line: ventral midline. Arrows indicate the expected direction of growth (perpendicular to the midline). Arrow heads indicate some of the axon bundles that deviated from the expected direction. B. Single optical slice confocal image of the midline region of the openbooks. C. Schematic of the measurements made. Every sequence of 2 adjacent pixels was analyzed by the ImageJ plugin AngleJ. The angle between these pixels and the midline was calculated. D. Average angle formed between the Tag-1 outgrowth and the midline of the DMSO and BV02 treated openbooks. Results are expressed as the mean angle per spinal cord ± SEM (n=5 per condition). E. Distribution of the outgrowth angles in each spinal cord, in 10 degree bins. F. Representative images of Math1-GFP and Math1-R18 electroporated SCNs, in openbook preparations. Images are paired with trancing overlays. Green tracings represent axons growing within 70 to 90 degrees related the midline. Yellow tracings highlight axons that project towards the midline between 0 to 70 degrees. Axons in red are deflecting from the midline. G. Average angle formed between the electroporated cells and tip of their axons. H. Distribution of the axons growing in different angles, relative to the midline. I. Schematic showing the phenotype observed by the 14-3-3 loss of function paradigms. Results are expressed as mean ± SEM (n= 11 openbooks for GFP, n=5 openbooks for R18).

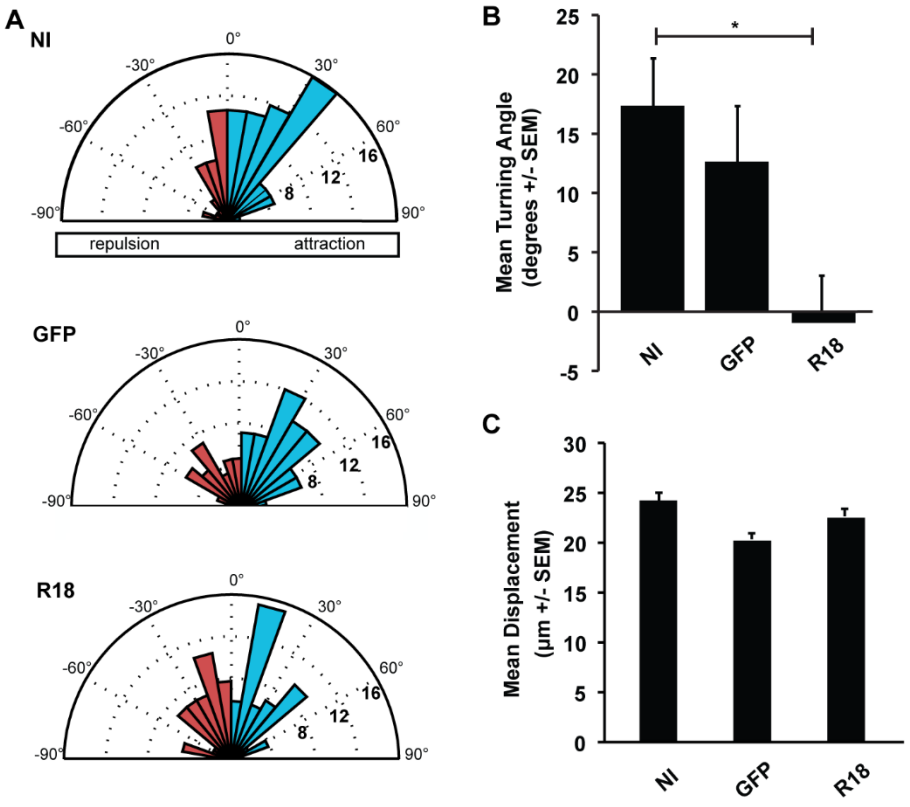

Figure 3.2: 14-3-3 loss of function impairs Netrin-1 attraction. A. Rose histograms of the distribution of turned angles of SCNs at 2 DIV in a gradient of the Netrin VI-V fragment. Responses of individual neurons were clustered in 10° bins and the percentage of total neurons per bin is represented by the radius of each segment. SCNs were infected with HSV-GFP or HSV-R18-GFP. Inhibition of 14-3-3 proteins with R18 randomizes turning responses in response to the Netrin-1 gradient. n= 84 axons (not induced - NI), n= 82 (GFP), n= 106 (R18). B. Average turning angle. (+/- SEM). *$p<0.05$, after analysis by One way ANOVA with Dunnett's post-test**.** C. Mean displacement of axons during the 2 hour imaging. period (+/- SEM).

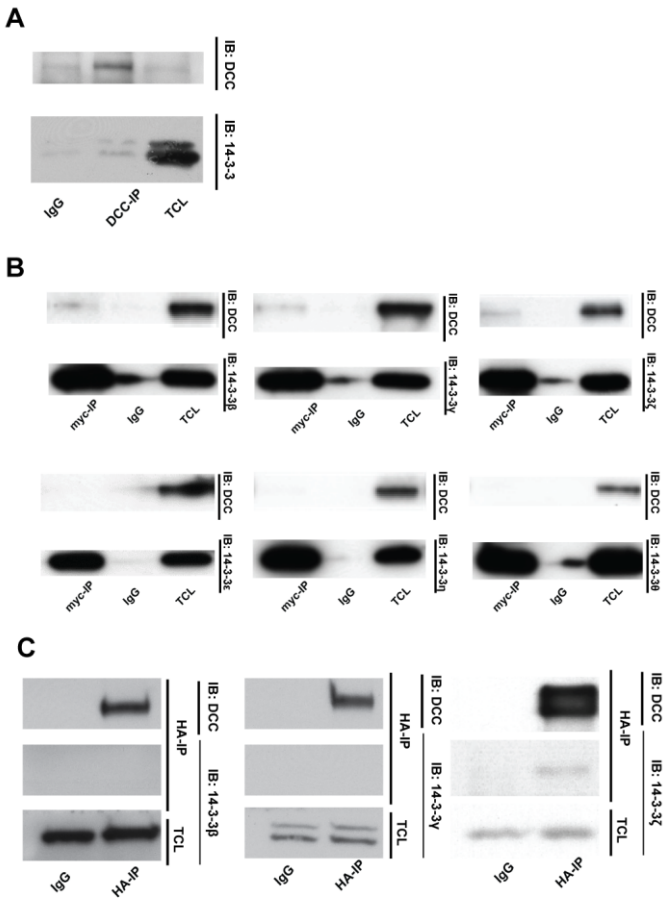

Figure 3.3: 14-3-3s interact with DCC. A. 14-3-3s co-precipitate with DCC from rat brain lysates. TCL: Total cell lysate. B. Exogenous 14-3-3β, γ and ζ have the ability to precipitate DCC from HEK293T cells. Myc-tagged isoforms were expressed one at a time and antibodies against myc were used for co-immunoprecipitation. C. DCC precipitates endogenous 14-3-3ζ from HEK293Ts. HA-DCC was overexpressed into HEK293Ts and co-immunoprecipitation for HA was performed. Levels of endogenous 14-3-3 were assessed using specific antibodies. Images are representative blots from 3 to 4 independent experiments each.

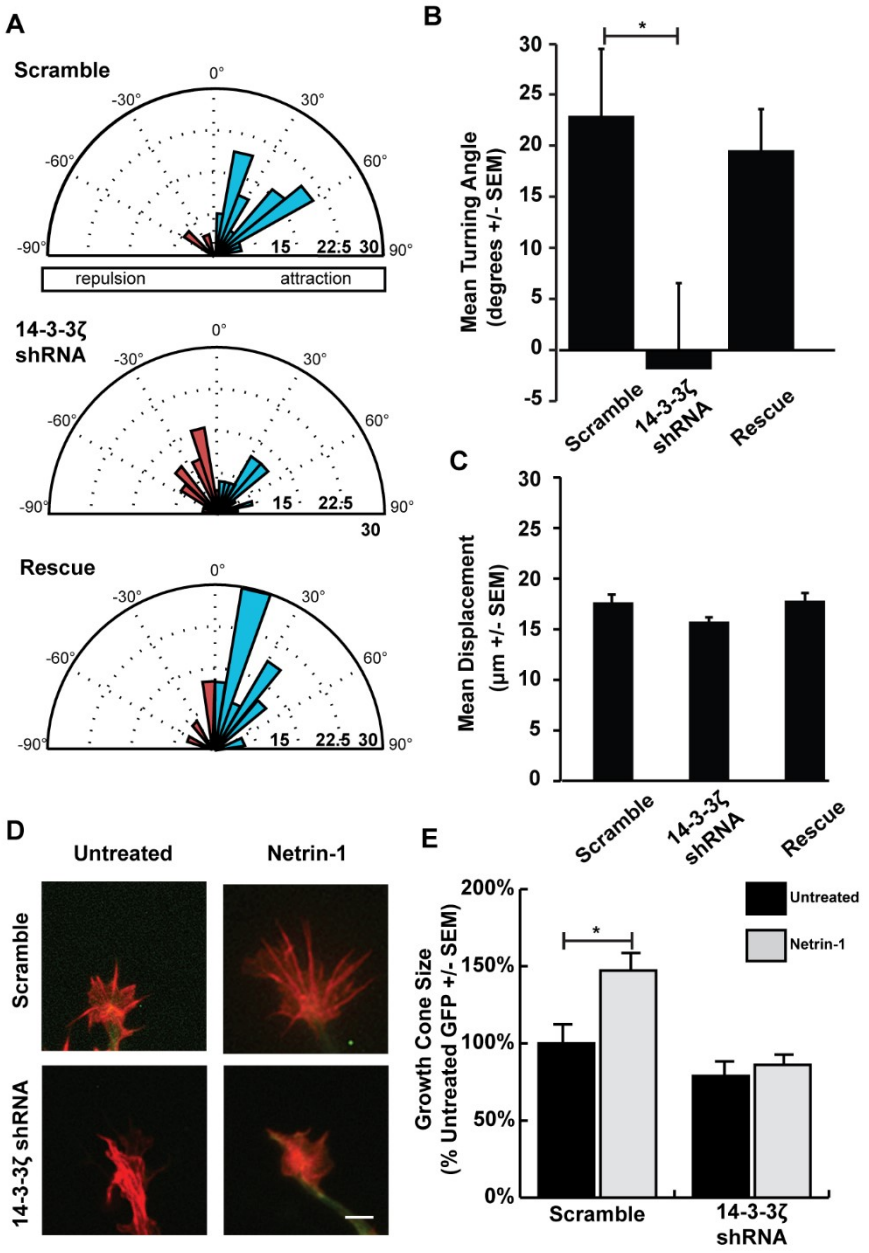

Figure 3.4: 14-3-3ζ knockdown phenocopies 14-3-3 loss of function. A. Rose histograms of the distribution of turned angles of SCNs at 2 DIV in a Netrin gradient. Responses of individual neurons were clustered in 10° bins and the percentage of total neurons per bin is represented by the radius of each segment. SCNs were transfected with a control (scramble) shRNA plasmid vector, a vector containing shRNA targeting rat

14-3-3ζ or doubled transfected with shRNA for rat 14-3-3ζ and the mouse gene. Knockdown of 14-3-3ζ with R18 randomizes turning responses in response to the Netrin-1 gradient. n= 25 axons (scramble shRNA), n= 39 (14-3-3ζ knockdown), n= 34 (rescue). B. Average turning angle. (+/- SEM). *p<0.05, One way ANOVA with Dunnett's post-test**.** C. Mean displacement of axons during the 2 hour imaging. period (+/- SEM). D. Representative images from transfected growth cones. Actin cytoskeleton was visualized with rhodamine-tagged phalloidin. transfection was confirmed by observation of GFP fluorescence from the viral constructs. E. Quantification of the growth cone area, normalized to the average area of untreated control cells in each experiment (mean ± SEM, n=3 experiments). *: p< 0.05, by Two way ANOVA with Buonferoni's post-test. Scale bar: 10 μm.

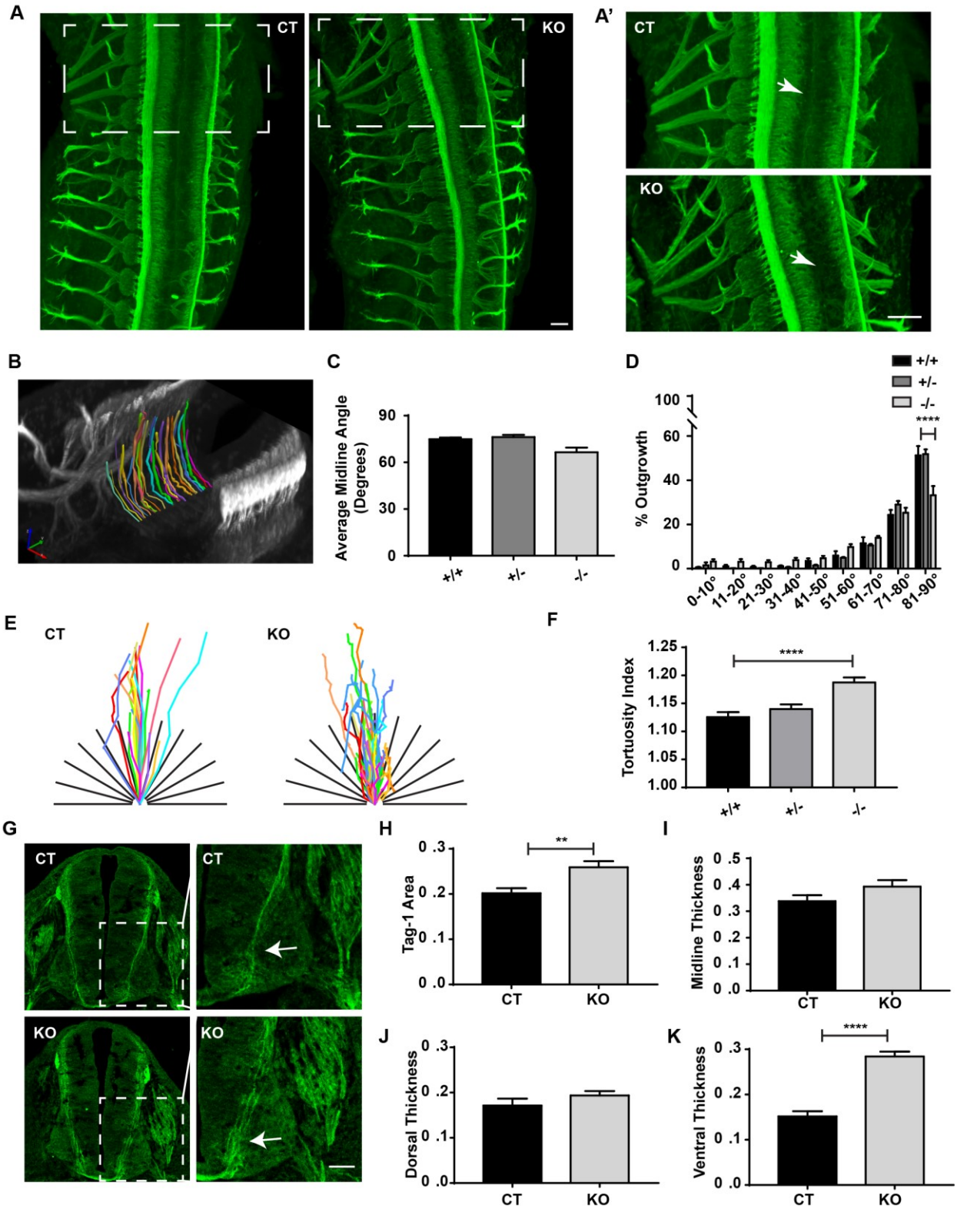
A
CT
KO
A'
CT
KO
B
C
Average Midline Angle (Degrees)
90
60
30
0
+/+
+/-
-/-
D
+/+
+/-
-/-
100
60
40
20
0
% Outgrowth
****
0-10°
11-20°
21-30°
31-40°
41-50°
51-60°
61-70°
71-80°
81-90°
E
CT
KO
F
Tortuosity Index
1.25
1.20
1.15
1.10
1.05
1.00
****
+/+
+/-
-/-
G
CT
CT
KO
KO
H
Tag-1 Area
0.3
0.2
0.1
0.0
**
CT
KO
I
Midline Thickness
0.5
0.4
0.3
0.2
0.1
0.0
CT
KO
J
Dorsal Thickness
0.3
0.2
0.1
0.0
CT
KO
K
Ventral Thickness
0.3
0.2
0.1
0.0
****
CT
KO

Figure 3.5: 14-3-3ζ affects SCN projections *in vivo*. A. Dorsal view, maximum intensity projection images of the lightsheet microscopy on control (CT) and 14-3-3ζ knockout (KO) E11.5 embryos, showing Tag-1 positive fibers in the spinal cord and adjacent dorsal root ganglia. A'. Blow up of the commissural projections at the brachial level. Control spinal cords have clearly identifiable midlines, while knockout embryos show a less defined structure. Arrow heads show the ventral midlines seen from the top of the neural tube, in which the controls have a very well-defined line and the knockout mice show a less organized structure. B. Optical cross-section of the brachial spinal cord of a control animal showing the traced axons in one hemicord. C. Average angle formed between the midline and the axonal outgrowth. n=4 wild type (+/+), n=3 heterozigous (+/-) embryos, n= 5 14-3-3ζ knockout (-/-) embryos). Results are expressed as mean ± SEM. D. Distribution of the outgrowth angles in each spinal cord, in 10 degree bins. ****: $p < 0.0001$ by One way ANOVA, with Tukey post-test. E. Representative fan-in projection of one segment of the spinal cord of a control and a knockout embryo, showing the tortuosity of the knockout fibers. F. Average tortuosity of the fibers in the different genotype. (Mean ± SEM). ****: $p < 0.0001$ by One way ANOVA with Dunnett's post-test. G. Representative images of E11.5 spinal cord histological sections. Left frames show the entire axial sections of the neural tubes, right frames are enlargements of the corresponding ventral area of the hemicord. Arrows point at the ventral portion of the commissure, which was measured in the ventral thickness analysis. Scale bar: 50 μm. H. Quantification of the total area covered by Tag-1 in the slices, normalized to the total area of each slice. I. Thickness of the ventral commissure normalized to the ventral thickness. J. Thickness of the dorsal portion of the commissural bundles, normalized to the thickness

of the hemicord in that region. K. Thickness of the ventral portion of the commissural bundles, normalized to the thickness of the hemicord in that region. H-K: Results are expressed as means ± SEM** n= 5 embryos per genotype. **: $p < 0.01$. ****: $p<0.0001$. Analysis done by Student t-test with Welch correction.

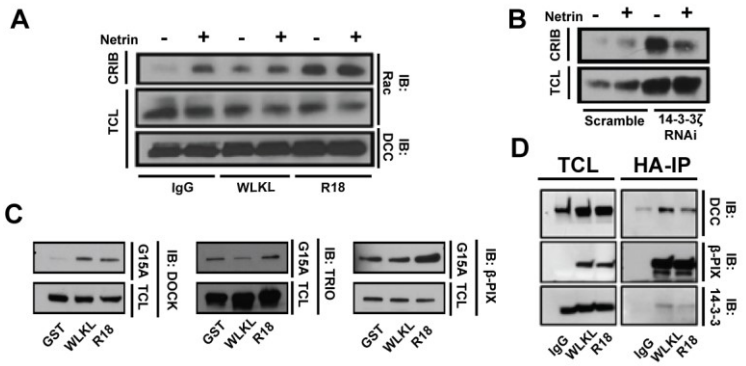

Figure 3.6: 14-3-3ζ disrupts small Rac-1 signaling. A. 14-3-3 loss of function increases basal levels of Rac1 activation, so that Netrin activation does not further act on it. CRIB pulldowns were performed to identify levels of Rac1-GTP in HEK293T cells, which were assessed by probing to the myc-tag of the transfected protein. Cells were treated with TAT-WLKL or TAT-R18 for 6 hours prior to Netrin-1 stimulation for 5 minutes. B. 14-3-3ζ impairs Netrin -1 activation of Rac1 in HEK293T cells. Endogenous 14-3-3ζ was knocked down by transfection with RNAi targeting it during 5 days prior to Netrin-1 stimulation for 5 minutes. Cells were lysed and levels of CRIB bound Rac1-GTP were assessed by probing for the tag of the exogenously expressed protein. C. Nucleotide independent Rac (G15A) – GST fusion proteins were used as bait for active GTPases. WLKL and R18 treated HEK293T cells were transfected with Flag-tagged DOCK180, TRIO-GFP or HA-β-Pix, and antibodies against the respective tags were used to assess GEF levels. GST protein was used as a stickiness control. D. HA-β-Pix co-precipitates with DCC and 14-3-3s in HEK293T cells. Co-immunoprecipitation was performed using anti-HA beads. Myc-DCC and V5-14-3-3ζ levels were assessed by probing for the respective tags. Cells that were not transfected with the bait HA-β-Pix were used as stickiness control to the antibody (IgG).

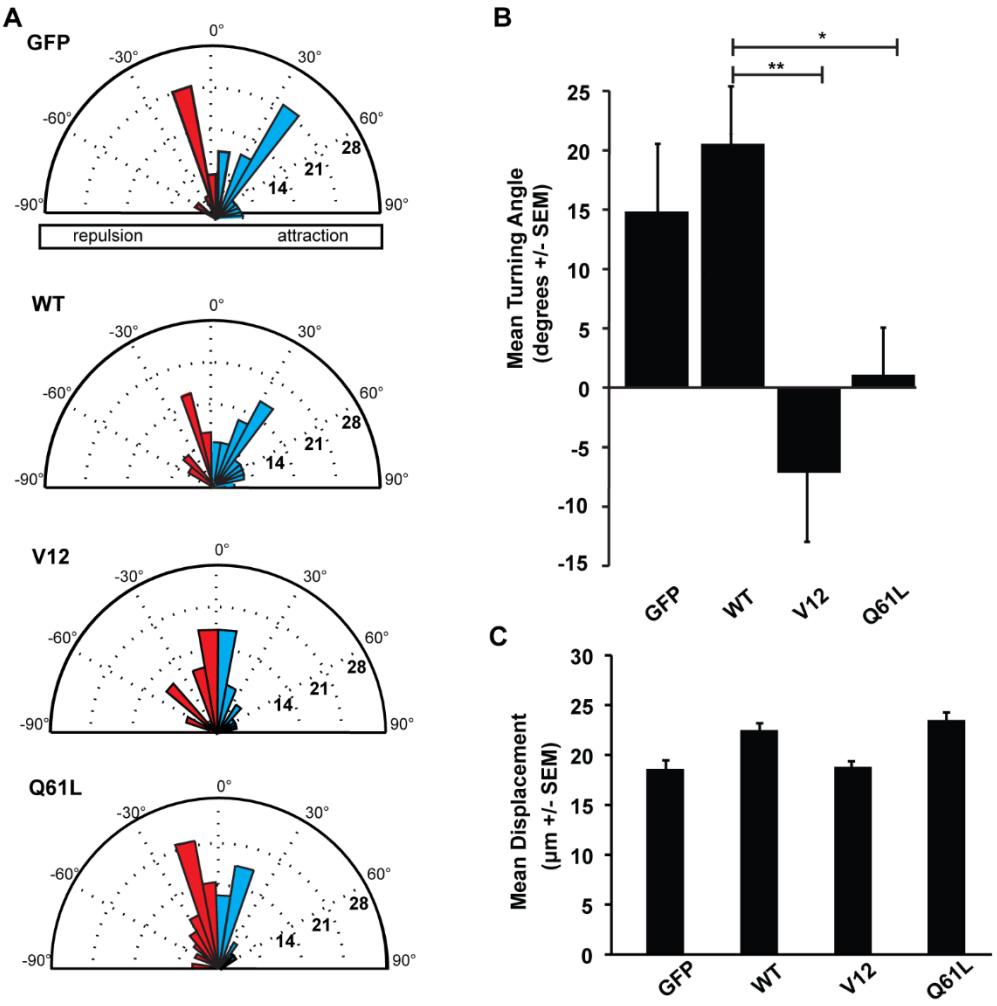

Figure 3.7: Overexpression of constitutively active Rac1 impairs turning responses to Netrin-1. A. Rose histograms of the distribution of turned angles of SCNs at 2 DIV exposed to a Netrin gradient. Responses of individual neurons were clustered in 10° bins and the percentage of total neurons per bin is represented by the radius of each segment. SCNs were transfected with a control (GFP) plasmid vector, or vectors containing wild-type Rac1 sequences, the constitutively active Rac1 mutant V12 or the constitutively active mutant Q61L. Compared to the overexpression of the wild type protein, constitutively active forms of Rac1 are considerably less sensitive to the Rac1 gradient. n= 28 (GFP), n= 37 (WT Rac1), n= 36 (V12), n=41 axons (Q61L). B. Average turning

angle. (+/- SEM). *p<0.05, ** p< 0.01 by One way ANOVA with Dunnett's post-test**.** C. Mean displacement of axons during the 2 hour imaging. period (+/- SEM).

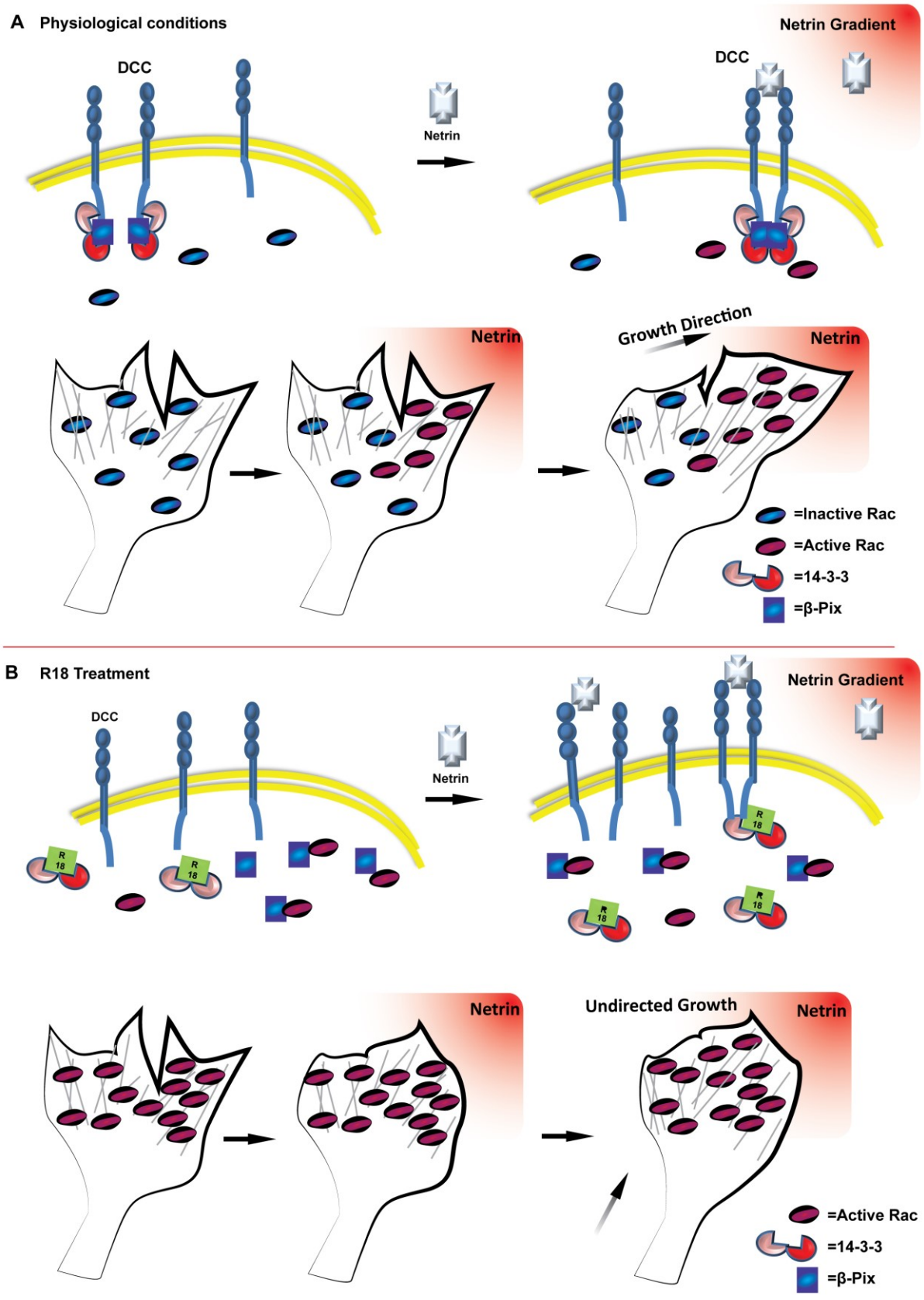
A Physiological conditions
Netrin Gradient
DCC
Netrin
DCC
Netrin
Growth Direction
Netrin
=Inactive Rac
=Active Rac
=14-3-3
=β-Pix
B R18 Treatment
Netrin Gradient
DCC
Netrin
R 18
Netrin
Undirected Growth
Netrin
=Active Rac
=14-3-3
=β-Pix

Figure 3.8: Working model. A. Under physiological conditions,14-3-3 recruits the GEF β-Pix to the vicinity of DCC, where it localizes Rac1 activation so that it follows the Netrin-1 gradient and leads to directed growth cone responses. B. After R18 treatment (i.e. in the absence of 14-3-3's function), β-Pix is delocalized, in the growth cone, which leads to abnormal activation of Rac1 and undirected movements of the growth cone.

Chapter 4 – Preface

In this last result chapter, we analyze the role of 14-3-3s, the same family of proteins as chapter 3, in the development of oligodendrocytes.

This project started as a collaboration with Dr.Mark Kotter, at Cambridge University, who is studying the effects of the nucleocytoplasmic translocation of a FoxO transcription factor in oligodendrocyte differentiation. Based on the known regulatory effect of 14-3-3s on FoxO, we hypothesized that manipulation of 14-3-3s could constitute a mechanism to manipulate FoxO. Contrary to our expectation, 14-3-3s did not affect the subcellular localization of FoxO in oligodendrocytes (data not shown), suggesting that distinct signaling cascades regulate FoxO in these cells.

Still, we present here a description of 14-3-3 expression by differentiating oligodendrocytes, and the effects of 14-3-3 loss of function and stabilization. These experiments implicated 14-3-3s in the differentiation of oligodendrocyte progenitor cells, opening new venues for the research of novel remyelination therapies. Biochemical studies will follow the findings presented here.

Chapter 4 – 14-3-3s inhibit the expansion of myelin basic protein (MBP) rich membranes in differentiating oligodendrocytes

Ricardo Alchini[1], Ana Amaral[2], Mark Kotter[2], Alyson Fournier[1]

1-Montreal Neurological Institute, McGill University, Montreal, Canada.

2- Department of Clinical Neurosciences, Cambridge University, Cambridge, United Kingdom.

4.1 – Abstract

Oligodendrocytes are the cells responsible for producing myelin and consequently for efficient saltatory conduction. Oligodendrocyte function is disrupted in several neurodegenerative diseases such as multiple sclerosis, neuromyelitis optica and leukodystrophic disorders. Finding pharmacological treatments that can improve oligodendrocyte differentiation and myelination efficiency could therefore be useful for the treatment of several illnesses. Some 14-3-3 client proteins affect oligodendrocyte differentiation thus we sought to investigate the role of 14-3-3 proteins in oligodendrocyte development. Here we demonstrate that 14-3-3β,-γ,-ε,-ζ,-η and -θ are expressed by oligodendrocytes. We find that inhibition of 14-3-3 protein function increases the production of myelin basic protein (MBP) whereas a drug that stabilizes 14-3-3 binding to its target proteins has the opposite effect. Our findings suggest that 14-3-3 proteins inhibit myelin formation and that suppression of 14-3-3 function represents an approach to remyelinating therapies. Further studies could unveil new molecular mechanisms involved in the regulation of myelin producing cells.

4.2 – Introduction

Oligodendrocytes are the cells responsible for producing myelin in the central nervous system (CNS), which is the substance that insulates axons, allowing for efficient nerve pulse transmission (Sherman and Brophy, 2005). Their function is disrupted in several neurodegenerative diseases such as multiple sclerosis, neuromyelitis optica and leukodystrophic disorders (Peschl et al., 2017). Thus, pharmacological treatments that can improve oligodendrocyte differentiation and myelination have a potential usage for the treatment of several illnesses.

Oligodendrocytes differentiate from migrating polysialylated neuronal cell adhesion molecule (PSA-NCAM)/ Nestin/ Vimentin positive pre-progenitor cells, into neural/ glial antigen 2 (NG2)/ A2B5/ Nestin bipolar oligodendrocyte progenitors (Biname et al., 2013; Grinspan and Franceschini, 1995; Schnitzer and Schachner, 1982). These cells give rise to O4 positive multipolar pre-oligodendrocytes, which later mature into O4/MBP positive myelinating oligodendrocytes (Colman et al., 1982; Sommer and Schachner, 1981). This stereotypical process can be reproduced *in vitro* (Barateiro and Fernandes, 2014), and is finely regulated by different molecular pathways including PKA, PI3K, Rho GTPase and transcriptional signaling (Baer et al., 2009; Emery and Lu, 2015; Pfeiffer et al., 1993). 14-3-3 adaptor proteins are known to modulate these signaling pathways in other contexts, such as axon guidance and tumorigenesis (Kent et al., 2010; Nagata et al., 1998; Tzivion et al., 2011). In adult tissue, 14-3-3s can be found in the myelin-rich white matter, and their expression and subcellular localization is modulated in disease models, suggesting

that 14-3-3 proteins may have a physiological function in oligodendrocytes (Lee et al., 2015; Saia-Cereda et al., 2015; Umahara et al., 2007).

In addition, 14-3-3s are known to regulate the subcellular localization of class IIa histone deacetylases (HDACs) and Forkhead box (FoxO) transcription factors, antagonizing their role in transcription regulation (Bardai and D'Mello, 2011; Dobson et al., 2011; Wei et al., 2015). Recent studies placing FoxO family members as key regulators of myelination (direct communication from Dr. Mark Kotter) and reports of broad spectrum HDAC inhibitors to promote the differentiation of oligodendrocytes suggest that 14-3-3s may be used to modulate these pathways (Lyssiotis et al., 2007; Ye et al., 2009).

Here, we provide immunocytochemical and Western blotting evidence for 14-3-3 expression in oligodendrocytes. 14-3-3 inhibition by the drug BV02 leads to an increase in the production of MBP, while fusicoccin, a drug which stabilizes 14-3-3-client protein interactions, has the opposite effect. These data suggest that 14-3-3 proteins inhibit myelin formation, and that inhibiting 14-3-3 proteins may represent a therapeutic approach for enhancing remyelination.

4.3 – Materials and methods

4.3.1 – Mixed glial cultures

Mixed glial cultures were prepared as previously described (McCarthy and de Vellis, 1978). Postnatal 0 - 3 (P0 – P3) day Sprague Dawley rat pups were purchased from

Charles River (St. Constant, Canada) and utilized following the ethical guidelines of the Animal Care Facility at the Montreal Neurological Hospital. Brains were removed from the skull and the cortex was isolated from the surrounding structures. Chemical dissociation of the isolated cortices was performed by adding 1mL of 0.25% trypsin-ethylenediaminetetraacetic acid (EDTA) (Gibco, Grand Island, NY) at 37°C for 30 min. Mechanical dissociation was performed by pipetting the pre-digested tissue using a 1mL pipette tip. Cells were plated in growth medium consisting of Dulbecco's Modified Eagle Media (DMEM – Gibco, Grand Island, NY)-10% fetal bovine serum (FBS)-1% antibiotics (penicillin and streptomycin, Gibco, Grand Island, NY) on 0.001% poly-L-lysine (PLL, Sigma, St-Louis, MO) pre-coated T-75 flasks (Greiner, Frickenhausen, Germany). Cultures were incubated at 37°C with 5% CO_2, and the growth medium was changed every 2 to 3 days for 10 to 14 days.

4.3.2 – OPC isolation and differentiation

Isolation of OPCs was performed following a standard protocol (Baer et al., 2009; McCarthy and de Vellis, 1980). Loosely adhering microglia was removed by shaking the flasks at 37°C for 1 h at 250 rpm. The supernatants were discarded, fresh growth medium was added to the flasks. Vigorous manual agitation separated the OPCs from strongly adhering astrocytes. OPC supernatants were collected and transferred to PLL pre-coated culture dishes at the appropriated density. Cells were incubated at 37°C with 5% CO_2 for recovery.

Sato medium (Bottenstein and Sato, 1979) was used to differentiate OPCs into oligodendrocytes. The growth medium was removed and replaced by Sato differentiation medium for the time indicated in the experiments (2 to 5 days), which were allowed to differentiate at 37°C in 5% CO_2 and humidified air. When specified, either 1 μM BV02 (Sigma, St-Louis, MO), a 14-3-3 competitive inhibitor, or the equivalent amount of dimethyl sulfoxide (DMSO - the vehicle control, Sigma, St-Louis, MO) were added to the solution. For the experiments using fusicoccin (FC, Sigma, St-Louis, MO), the drug was added in the indicated concentration (50 or 100 μM) and the equivalent volume of methanol was utilized as vehicle control.

4.3.3 – Protein expression analysis

Cells were lysed on ice, using ice cold RIPA buffer (10 mM Tris-Cl (pH 8.0), 0.5 mM EGTA, 1% Triton X-100, 0.1% sodium deoxycholate, 0.1% SDS, 140 mM NaCl) supplemented with a protein inhibitor cocktail – EDTA (Gibco,Grand Island, NY). Protein levels were equalized among samples, and resuspended in Laemmli buffer (Laemmli, 1970).

Protein samples were separated by SDS-PAGE and transferred to PVDF membranes (Pierce Biotechnology Rockford, IL). 14-3-3 isoform specific antibodies (anti-14-3-3β,-γ,-ε,-ζ,-θ rabbit IgG and anti-14-3-3η, -σ goat IgG, Santa Cruz, all used at 1:1000 dilution), HRP conjugated mouse anti-pan14-3-3 IgG (Santa Cruz, 1:10000 dilution) and mouse anti-glyceraldehyde 3-phosphate dehydrogenase (GAPDH) IgG (Santa Cruz, 1:10000) antibodies were used for overnight incubation at 4ºC where

indicated. After intensively washing, horseradish peroxidase conjugated secondary antibodies were incubated for 1 h at room temperature and ECL was used so that the proteins of interest could be observed with chemiluminescence.

4.3.4 – Immunostaining of oligodendrocyte precursor cells and oligodendrocytes

14-3-3 immunostaining followed a previously described protocol (Kent et al., 2010). Cells were fixed with modified Davidson solution (Moore and Barr, 1954), depleted of eosin and supplemented with 20% sucrose (Fischer, Fair Lawn, NJ). Permeabilization was performed with 0.02% saponin (Calbiochem, Darmstad, Germany) for 5 min, and samples were blocked with 5% bovine serum albumin for 30 min at room temperature.

The same 14-3-3 isoform specific antibodies were used for immunocytochemistry at 1:100 dilution in PBS, while anti-MBP (chicken IgY, Aves), anti-O4 (mouse IgG, RD Sciences, Minneapolis, MN), at 4ºC overnight. Samples were extensively washed, and incubated with the appropriate species-specific Alexa conjugated secondary anti-serum (Invitrogen, Eugene, OR). Nuclear staining was achieved by Hoescht (Sigma, St-Louis, MO). Samples were mounted with Fluoromount-G (Southern Biotech, Birminham, AL) and imaged using a SP8 confocal microscope (Leica), equipped with the appropriate filters and objectives. For 14-3-3 expression analysis, matching controls lacking the primary antibodies were used to determine the imaging settings, in order to avoid autofluorescence signal.

Immunofluorescence analysis was performed as follows: 10 fields with 20 to 40 cells each were randomly acquired for each condition. A different subject blinded the images for every experiment using a macro for ImageJ, which automatically saves the images with random names and performed the quantifications. For the analysis of "%O4 or %MBP positive cells", the average percentage of cells positive to the mentioned marker were calculated for each field, and fields from 3 different experiments were combined. For the "O4 or MBP Area/ Cell" analysis, the images were thresholded, and total area covered by each marker was calculated using ImageJ's "Create Selection" function. This value was divided by the total number of positive cells in the respective field. After unblinding and combining the fields from the same condition together, results were normalized to the respective vehicle control of that experiment. Statistical analysis (Student's t-test with Welch correction for the experiments in which 2 conditions were compared, One way ANOVA with Dunnett's post hoc for the experiments with more than 2 groups) was performed using Prism 7 (GraphPad). Results are represented as mean ± standard error of the mean (SEM) unless indicated otherwise.

4.4 – Results

4.4.1 – 14-3-3 proteins are expressed developing OPCs

To explore the role of 14-3-3 proteins in oligodendrocyte differentiation we first investigated the expression of 14-3-3 isoforms in cultured oligodendrocytes (Fig 4.1). Using previously validated antibodies that are selective for individual 14-3-3 isoforms

(Kent et al., 2010), we assessed 14-3-3 expression at 2 DIV and 5 DIV. 2 DIV is the earliest timepoint when cell debris is cleared and O4 positive cells can be clearly visualized in culture whereas 5 DIV corresponds to a timepoint when mature OPCs populate the culture (Barateiro and Fernandes, 2014; Syed et al., 2017). O4 and MBP antibodies were used to confirm cell commitment to the oligodendrocyte lineage. Samples that were stained with goat anti-14-3-3η antibodies were only co-stained for O4, due to the lack of the appropriate secondary antibody for chicken anti-MBP staining.

At both 2 DIV and 5 DIV, 14-3-3β,-γ,-ε,-ζ,-η and -θ expression was observed in the majority of the cells. 14-3-3σ signal was not detected at 2 DIV or 5 DIV. Most of the signal was located in the cytoplasm, spreading to the processes, although in variable degrees. Most cells also showed a clear perinuclear staining of the 14-3-3 isoforms, suggesting that immunostaining might not be the adequate technique to observe nuclear 14-3-3 due to their relative abundance in the cytoplasm.

There was no obvious change in the expression of 14-3-3 proteins between 2 and 5 DIV as detected by immunofluorescence. In order to confirm the stable expression level of 14-3-3s over the course of OPC differentiation we performed Western blotting from cell lysates at these two stages in culture (Fig 4.2). Using a pan-14-3-3 antibody or antibodies recognizing 14-3-3β,-γ,-ζ and –ε we confirmed that 14-3-3 proteins were expressed at similar levels at 2 DIV and 5 DIV.

4.4.2 – 14-3-3s impair the spreading of MBP rich membranes

We next analyzed if 14-3-3 proteins regulate oligodendrocyte development in culture. Since 2 DIV is the stage in which OPCs are still differentiating in culture and there is a mixed pool between pre-oligodendrocytes and mature oligodendrocytes, we performed pharmacological treatments to inhibit or enhance the function of 14-3-3 proteins during the first 2 days of OPC differentiation. We assessed effects on the number of cells committed to the oligodendrocyte lineage and on the maturation of oligodendrocytes. Treatment with the 14-3-3 competitive inhibitor BV02 positively impacted on the expression of MBP (Fig 4.3A, E). 14-3-3 inhibition did not affect the percentage of cells becoming O4-positive oligodendrocytes (CT=82.51% ± 2.93%, BV02 = 89.58% ± 3.17%, n= 3 experiments, p= 0.1128 by Student's t -test, Fig 4.3B). The O4 positive cells did not show any obvious morphological alterations and the total area covered by their processes and cell bodies was not significantly affected by 14-3-3 inhibition (CT= 1.00 ± 0.10, BV02= 1.05 ± 0.08 of the control area, n=3 experiments, p=0.69). 14-3-3 loss of function did not affect the number of cells maturing into MBP-positive oligodendrocytes (CT= 39.82% ± 3.95%, n= 3 experiments, p=0.35, Fig 4.3D) but BVO2-treated cells did exhibit a significant increase in the MBP-positive area per cell (CT= 1.00 ± 0.08, BV02= 1.342 ± 0.14 of the control area, n=3 experiments, p=0.019. Fig 4.3A, E). This indicates that 14-3-3- proteins suppress the morphological differentiation of oligodendrocytes in culture.

We next treated cells with fusicoccin, a drug that enhances binding between 14-3-3 proteins and their clients (Fig 4.4). As with BVO2 cell commitment to O4-positive oligodendrocytes (CT= 75.34% ± 16.34%, 50 μM FC = 75.62% ± 19.95%, 100 μM FC = 75.62% ± 19.95% O4 positive cells, n= 3 experiments, Fig. 4A, B) and the average area

of O4 positive cells was unaffected (CT= 1.00 ± 0.21, 50 μM FC = 0.65 ± 0.19, 100 μM FC = 1.06 ± 0.22 of the control area, n= 3 experiments, Fig 4.4A,C). The percentage of cells differentiating into MBP-positive oligodendrocytes was also unaffected (CT= 26.91% ± 2.27%, 50 μM FC = 23.97% ± 2.20%, 100 μM FC = 26.23% ± 3.13% of the MBP positive cells, n= 3 experiments, Fig 4.4A,D). However, fusicoccin treatment did result in a significant decrease in the area occupied by the MBP positive cells (CT= 1.00 ± 0.11, 50 μM FC = 0.66 ± 0.03, 100 μM FC = 0.52 ± 0.04 of the area of the control cells, n= 3 experiments, CT vs 50 μM FC p= 0.0014, CT vs 100 μM FC p= 0.0001 by One-way ANOVA with Dunnett's post hoc comparison, Fig 4.4A,E). Together these findings support a role for 14-3-3 proteins in suppressing the morphological expansion of oligodendrocytes differentiation in culture.

4.5 – Discussion

In the current work, we describe the expression profile of 14-3-3 proteins in oligodendrocytes and determine how the gain of loss of 14-3-3 function affects oligodendrocyte differentiation in culture.

As relatively ubiquitously expressed proteins (Fu et al., 2000), it is not surprising that 14-3-3 proteins are expressed in oligodendrocytes, but we do show here that individual isoforms are expressed with varying abundance since all antibodies robustly detect their target antigen (Kent et al). Global loss of function of 14-3-3s enhanced the amount of MBP-positive membrane produced by the differentiating oligodendrocytes. An open question is the relative contribution that individual 14-3-3s isoforms play in this process.

For instance, 14-3-3γ modulates demyelination in autoimmune mouse models, being a strong candidate for playing a role in oligodendrocyte physiological function (Lee et al., 2015). Ongoing experiments with loss of function and overexpression of single isoforms can be used to address this question in the future.

Interestingly, the expression levels of 14-3-3 isoforms did not change markedly over the course of oligodendrocyte differentiation. It is therefore likely that 14-3-3 function is regulated by its subcellular localization, its level of phosphorylation or by regulation of phosphorylation of client proteins (Aitken et al., 1995a; Aitken et al., 1995b; Martin et al., 1994; Woodcock et al., 2003). Phosphorylation of 14-3-3 proteins on a specific residue induces the formation of 14-3-3 monomers leading to trapping of inactive 14-3-3 in the nucleus and this phosphorylation could be monitored in future experiments using a commercially available phospho-specific 14-3-3 antibody (Woodcock et al., 2003). A report of 14-3-3 trapping in the cell nucleus of white matter cells after brain infarction suggests the existence of mechanisms to regulate their subcellular localization in oligodendrocytes (Umahara et al., 2007). Additional fluorescence analysis and subcellular fractionation experiments could be performed to help determine whether there is shuttling of 14-3-3 proteins in the system (Alchini et al., 2017; Martin et al., 1994; Vokes and Carpenter, 2008). Studies on 14-3-3 subcellular localization would help unveil more information about their function during OPC differentiation.

Several transcription factors and transcriptional regulators are involved in the differentiation of OPCs and could be regulated by 14-3-3 proteins (Emery and Lu, 2015). One example is the histone deacetylases (HDACs). 14-3-3s bind to class II HDACs, mediating their nucleocytoplasmic translocation, sequestering them from the nucleus and

preventing their transcriptional regulation activity (Grozinger and Schreiber, 2000). While HDAC6, a class II HDAC, is required for the morphological stability of OPCs, broad range HDAC inhibition promotes OPC differentiation (Lyssiotis et al., 2007; Noack et al., 2014). Therefore, understanding whether 14-3-3s regulates HDAC activity during oligodendrocyte differentiation and the full slate of proteins that are regulated by 14-3-3 in oligodendrocytes may provide insights on the molecular mechanisms underlying differentiation of OPCs. In addition, proteins such as YY1, Tcf4 and Id2/4, all of which playing a crucial function in the development of OPCs, bear 14-3-3 binding motifs and are candidates to mediate 14-3-3 function in OPC development as predicted by the 14-3-3 interaction database ANIA (ania-1433.lifesci.dundee.ac.uk) (Chen et al., 2009; He et al., 2007b; Tinti et al., 2014; Weng et al., 2017).

Another tentative pathway to be affected by 14-3-3s is Rac signaling. Rac1 is activated during the elongation of the processes of Schwann cells, the myelin producing cells of the peripheral nervous system, and Rac1 inhibition blocks membrane expansion of myelinating cells (Nodari et al., 2007; Tep et al., 2012). Rac1 has also been associated with myelination of the CNS, although its function has not been extensively studied in the differentiation of oligodendrocytes, being described especially during the migration of the OPCs (Wang et al., 2009; Xiao et al., 2013). 14-3-3s regulate several guanine exchange factors (GEFs), proteins that activate Rac1 (Chahdi and Sorokin, 2008; Zhu et al., 2015). In our experience, 14-3-3 loss of function results in a marked increase in Rac1 activation, which could explain the phenotype of expansion of MBP positive membranes in developing oligodendrocytes. Current work in our group will study if 14-3-3 loss of function also leads to an increase in Rac1 activation in OPCs to promote myelination *in vitro*.

Altogether, we have seen that 14-3-3s inhibit the expansion of the processes and membranes of maturing oligodendrocytes. Further work will confirm whether they can be used in remyelination therapies, and the signaling mechanisms involved in the process

4.6 – Acknowledgement

We would like to thank Luyang (Simon) Hua for his assistance in the experiments related to the downstream regulation of 14-3-3 in oligodendrocytes, which have not been included in this manuscript but have contributed to the rationale here presented.

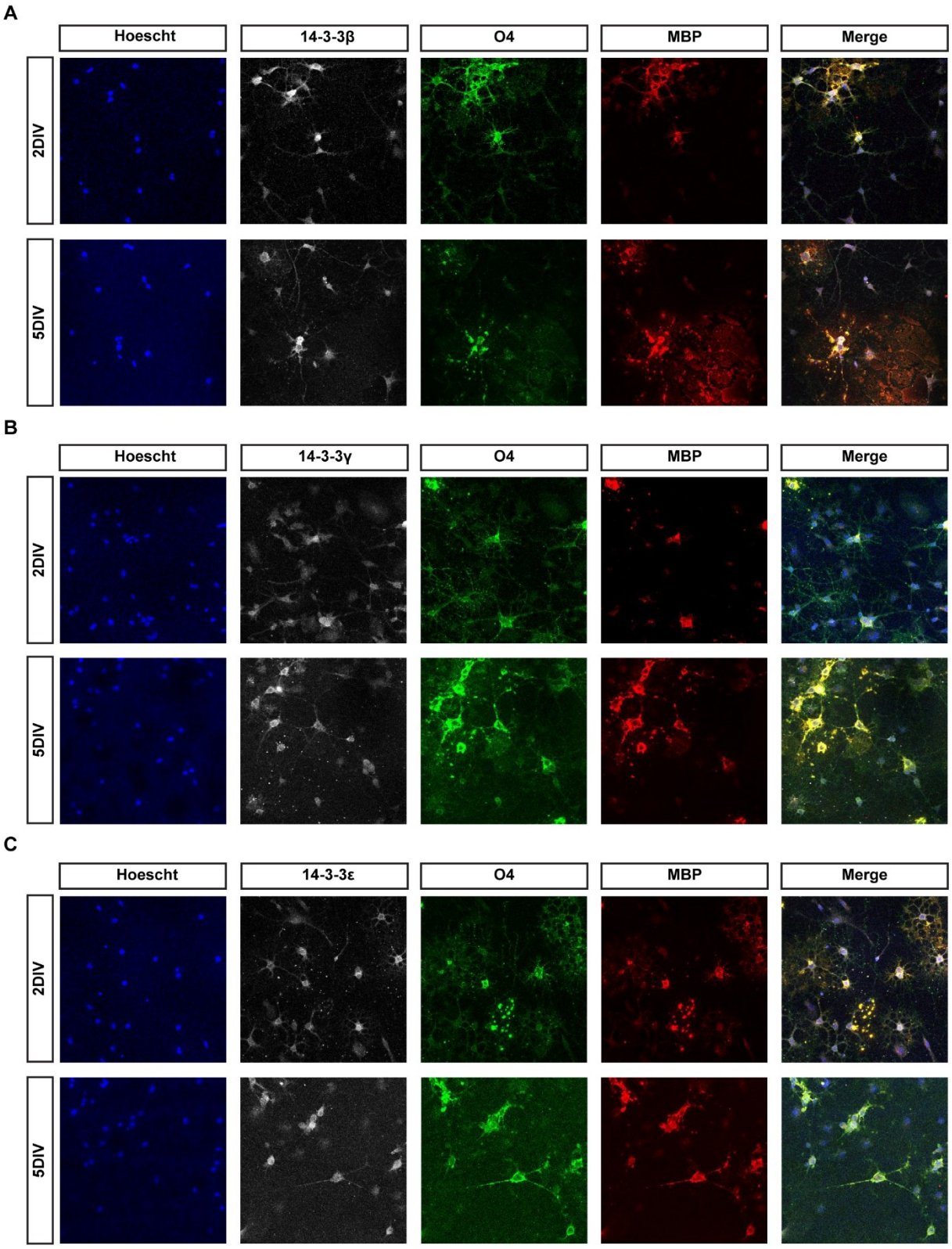
A
Hoescht
14-3-3β
O4
MBP
Merge
2DIV
5DIV
B
Hoescht
14-3-3γ
O4
MBP
Merge
2DIV
5DIV
C
Hoescht
14-3-3ε
O4
MBP
Merge
2DIV
5DIV

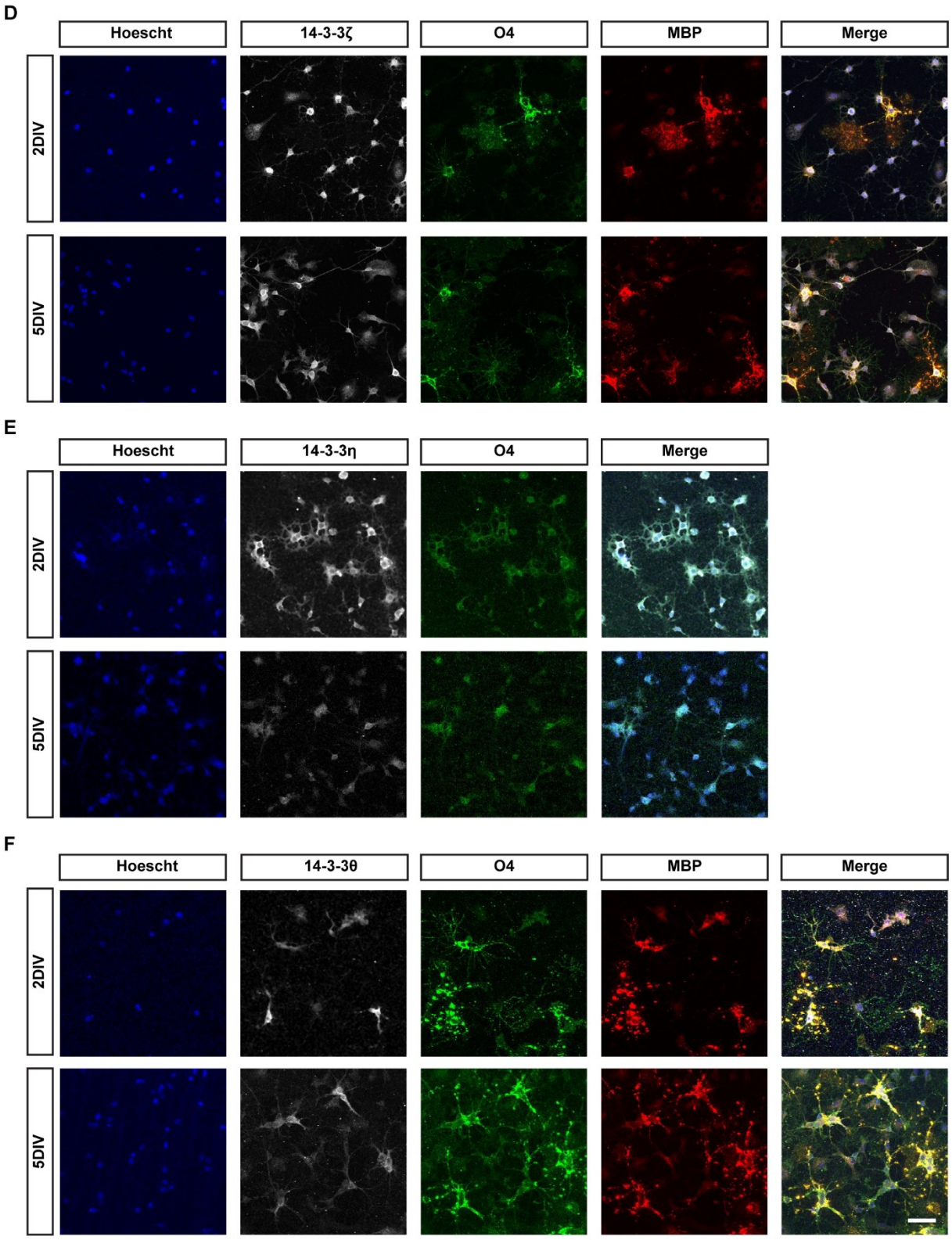
D
Hoescht
14-3-3ζ
O4
MBP
Merge
2DIV
5DIV
E
Hoescht
14-3-3η
O4
Merge
2DIV
5DIV
F
Hoescht
14-3-3θ
O4
MBP
Merge
2DIV
5DIV

Figure 4.1: Different 14-3-3 isoforms are expressed throughout the cells in differentiating OPC. A-F. Representative images for 14-3-3β,-γ,-ε,-ζ,-η and -θ, respectively, at 2 and 5 DIV. n=3 independent experiments. Scale bar: 30 μm.

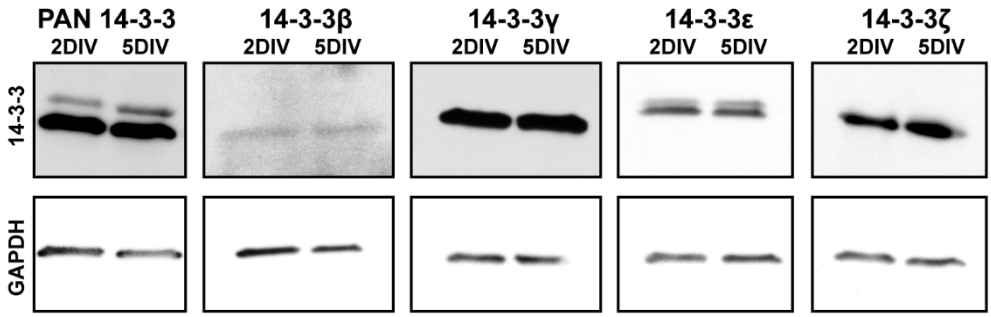

Figure 4.2: 14-3-3s are constantly expressed during the differentiation of OPCs *in vitro*. Representative blots of 3 independent experiments. GAPDH is used as a loading control. Antibodies for the specific isoforms are indicated above the respective panels.

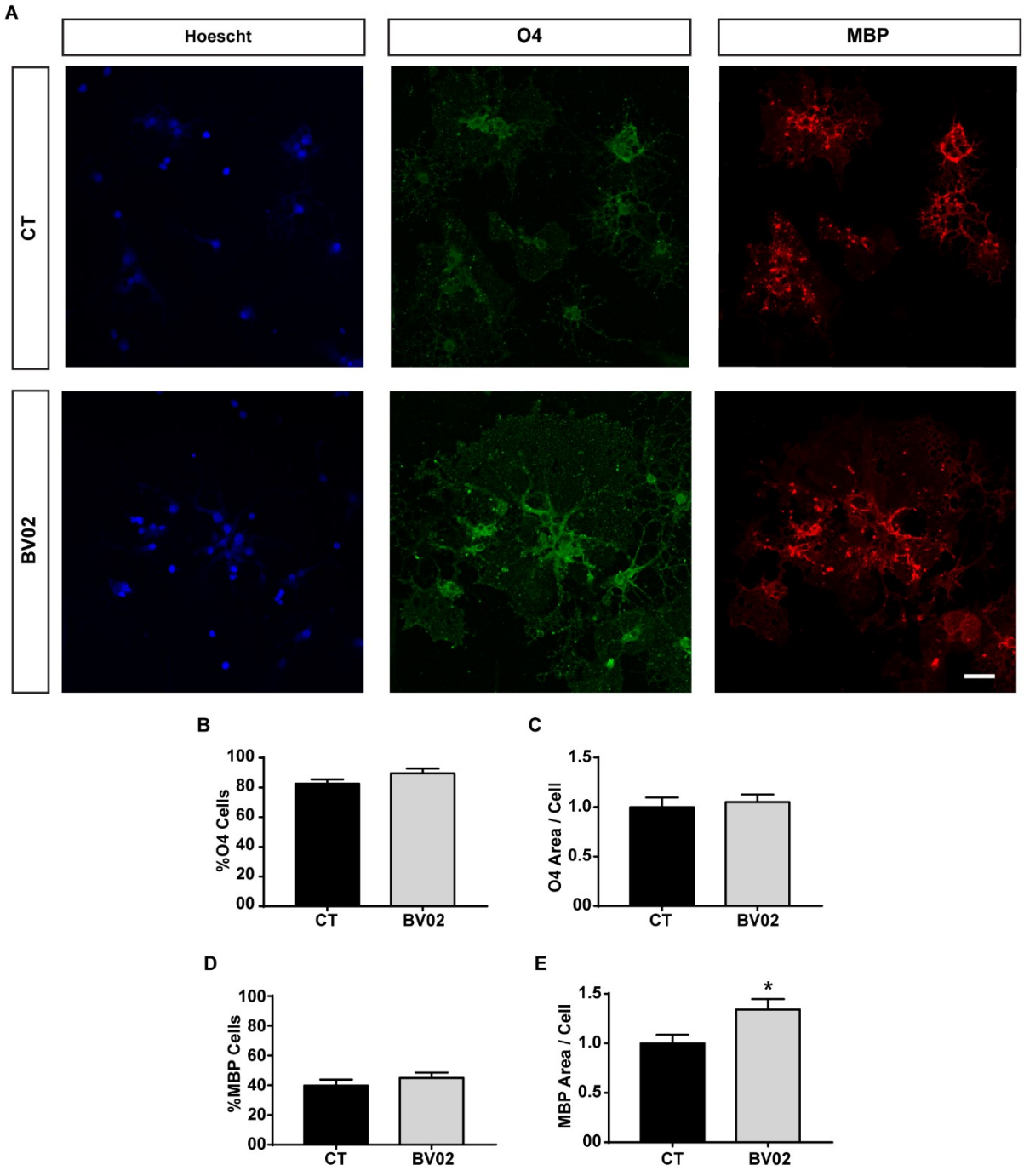

Figure 4.3: 14-3-3 loss of function impacts on the area covered by MBP in differentiating OPCs. A. Representative images of cells treated with BV02 and vehicle controls. Cells were fixed at 2 DIV and staining was performed for the early

oligodendrocyte marker O4 and the mature marker MBP. B. 14-3-3 loss of function does not impact on the commitment of the cells to the oligodendrocyte lineage. Results are expressed as the percentage of O4 positive cells per field. Scale bar: 30 μm. C. 14-3-3 loss of function does not affect the area covered by O4 in differentiating OPCs. Results are shown as the average area occupied by the O4 staining normalized by the number of cells per field and the average area of each experiment. D. 14-3-3 loss of function does not affect the maturation of OPCs into oligodendrocytes. Results are expressed as the average percentage of MBP positive cells per field, per experiment. E. 14-3-3 loss of function leads to a significant increase in the area covered by MBP rich membranes. Results are expressed as the average area covered by MBP signal, normalized by the number of cells per field and the average area of the control cells in the respective experiments. n=3 independent experiments. *: $p<0.05$ by Student's t-test with Welch correction.

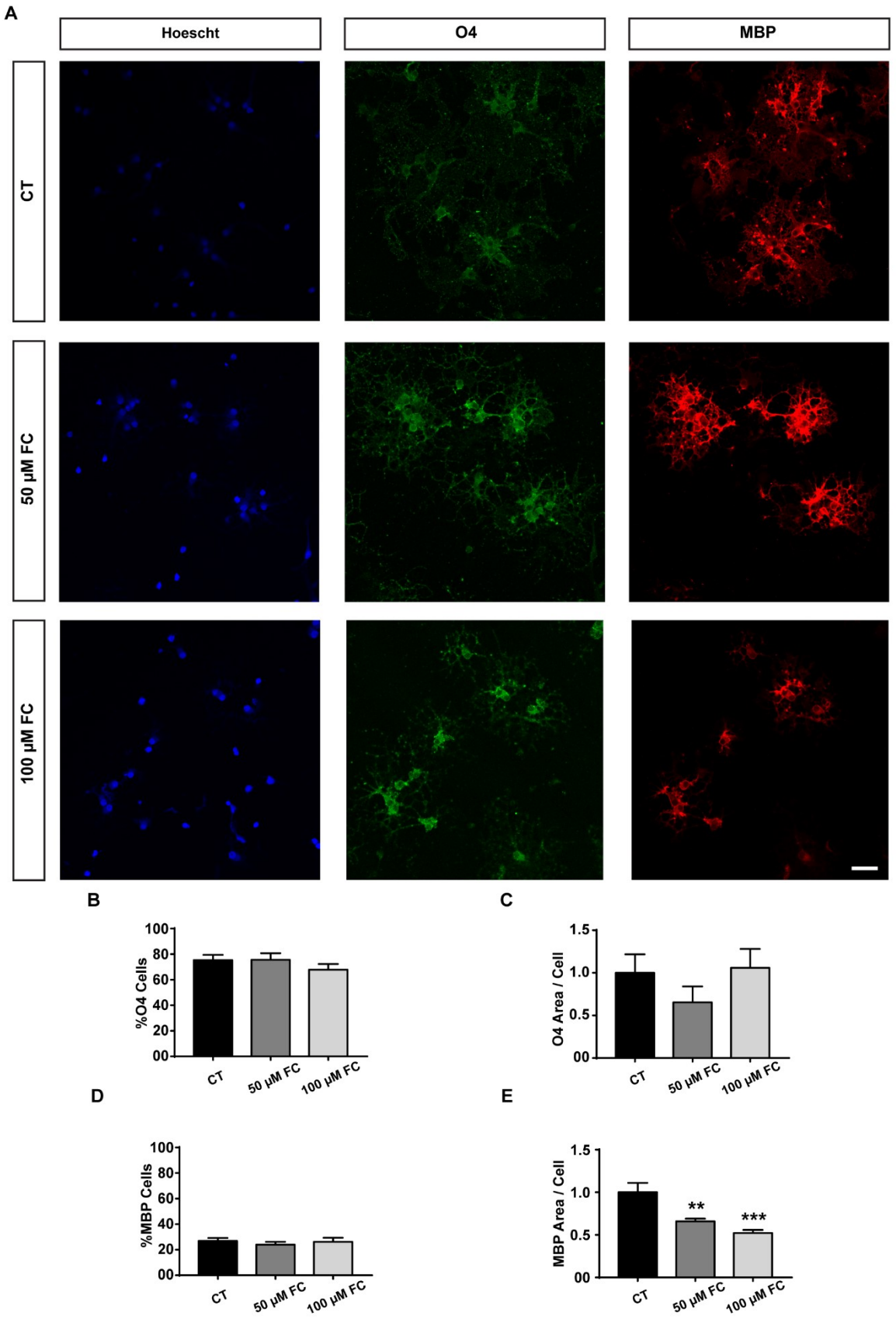
A
Hoescht
O4
MBP
CT
50 µM FC
100 µM FC
B
%O4 Cells
100
80
60
40
20
00
CT
50 µM FC
100 µM FC
C
O4 Area / Cell
1.5
1.0
0.5
00
CT
50 µM FC
100 µM FC
D
%MBP Cells
100
80
60
40
20
00
CT
50 µM FC
100 µM FC
E
MBP Area / Cell
1.5
1.0
0.5
00
**
***
CT
50 µM FC
100 µM FC

Figure 4.4: Stabilization of 14-3-3 interactions antagonizes the formation of MBP rich membranes in OPCs. A. Representative images of O4 and MBP signals in cells treated with 50 or 100 μM FC and vehicle controls at 2 DIV. Scale bar: 30 μm. B. FC treatment does not impact on the commitment of the cells to the oligodendrocyte lineage. Results are expressed as the percentage of O4 positive cells per field. C. FC treatment does not affect the area covered by O4 in differentiating OPCs. Results are shown as the average area occupied by the O4 staining normalized by the number of cells per field and the average area of each experiment. D. FC treatment does not affect the maturation of OPCs into oligodendrocytes. Results are expressed as the average percentage of MBP positive cells per field, per experiment. E. Stabilization of 14-3-3 function reduces the area covered by MBP rich membranes. Results are expressed as the average area covered by MBP signal, normalized by the number of cells per field and the average area of the control cells in the respective experiments. n=3 independent experiments. **: $p<0.01$, ***: $p<0.001$ by One way ANOVA with Dunnett's post test.

Conclusions

5.0 – General discussion

5.1 – Summary

The principal goal of this thesis was to understand the role of 14-3-3s in the guidance of spinal cord commissural neurons. We started from the development of a protocol for *ex utero* electroporation, which can be used in a variety of different contexts. We used this system to characterize the growth of Math-1 spinal cord commissural neurons (SCNs) *ex vivo*. In addition, we showed that ectopic expression of Netrin-1 can disrupt the guidance of SCN axons. Next, we sought to investigate the role of 14-3-3s in the pre-crossing stage of spinal cord commissural neuron development. We showed a novel, role for 14-3-3s in axon guidance and demonstrated that 14-3-3s play a role in the maintenance of Rac1-GTP levels (Kent et al., 2010; Yam et al., 2012). Also, we investigated the expression of 14-3-3s by differentiating oligodendrocytes and the effects of its manipulation on the differentiation of oligodendrocyte progenitor cells (OPCs), which was unexplored to date.

5.2 – 14-3-3s in axon guidance

The field of axon guidance keeps evolving since its first seminal work. Whereas many of the initial studies focused on the identification of axon tracts, the last two decades saw it switching to a more molecular emphasis (Evans and Bashaw, 2010; Kennedy et al., 2006; Stoeckli, 2017). The first works in this “molecular phase” identified guidance

cues and their receptors, and the next studies focused on the genetic specification of the cells. Recently, the regulatory mechanisms of cell signaling have taken a leading role in this process (Stoeckli, 2017). With an interactome of thousands of targets, 14-3-3s are perfect candidates to integrate so many signaling pathways evoked during the development of the nervous system (Tinti et al., 2014; Xiao et al., 1995). In different systems, they have been shown to execute functions as diverse as the regulation of cell cycle and transcription, phosphorylation of proteins in the cytosol, transport of proteins, regulation of Rho-GTPases and cell morphology among other functions (Fu et al., 2000; Michelsen et al., 2005; Morrison, 1995; Tzivion et al., 2011; Xiao et al., 1995).

In our work, 14-3-3s have been proposed to act as a clock whereby some of the isoforms increase their expression levels with time leading to a switch in responses to Sonic Hedgehog, or other chemoattractants that depend on PKA levels (Kent et al., 2010; Yam et al., 2012). In the case of SCNs, we see that there is a segregation between the isoforms expressed in the cell: levels of 14-3-3ζ and θ remain constant as commissural neurons are guided to their final targets whereas 14-3-3β, γ and ε gradually increase their expression (which coincides with the crossing point) (Yam et al., 2012). Interestingly, PKA plays a very mild role in Netrin-1 signaling (Moore and Kennedy, 2006). It makes sense that while one of the isoforms is constitutively regulating GEF activation by DCC, different isoforms will be controlling PKA activity. However, whether the differential expression of 14-3-3 isoforms is the only method of regulation between these two functions remains unknown.

In plants, 14-3-3 activity is crucial and is considered a major metabolic regulator (Cotelle and Leonhardt, 2015; Wilson et al., 2016). Hence the need of thirteen to twenty

five distinct isoforms, each capable of mediating isolated functions. Mammalians 14-3-3 proteins consist of seven isoforms, five of which are derived from genetic duplication of 14-3-3ζ (Fu et al., 2000; Xiao et al., 1995). This gives rise to some degree of redundancy between isoforms (Yaffe et al., 1997), which could be observed for instance in our 14-3-3 co-immunoprecipitations with DCC, in which three of the isoforms showed to be able to bind to this receptor *in vitro.* Part of the specificity of these proteins can be explained by the availability of their clients, since all of them compete to bind to the same 14-3-3 units. Whether 14-3-3β, γ and ζ compete to bind to DCC has not been explored, but it is unlikely to play an important physiological role, since 14-3-3β and γ peak in a stage that no longer requires DCC signaling. Yet, it seems fundamental that strategies to regulate 14-3-3 activity have evolved with time. The factors that regulate 14-3-3 transcription, phosphorylation and dimerization are mostly unexplained. Thus, future work on the regulation of 14-3-3s can provide many insights on the regulation of the signaling pathways evoked by them, and be used as screening method for new players in the same phenomena.

5.3 – Netrin-1 role in axon guidance

The characterization of netrin-1 as a *diffusible* guidance cue has also been recently contested as a series of mutants for Netrin-1, with deletions in different portions of the neural tube, showed that ventricular zone deletion of Netrin-1 causes more severe phenotypes than its floorplate deletion (Dominici et al., 2017; Varadarajan et al., 2017). These works claim that Netrin-1 is a haptotactic factor, acting by promoting the adhesion

of axons on their way to the floorplate. According to a more recent report, the haptotactic Netrin-1 forms hederal boundaries in the developing neural tube, where axons develop (Varadarajan and Butler, 2017).

Both the ectopic expression of netrin-1 in chapter 2 and turning assay experiments in chapter 3 support the classical, chemotactic model for Netrin-1 function. According to the classical model, in the presence of multiple sources of Netrin-1 the axons might deflect from their original endogenous target attracted by the numerous gradients, consistent to our results. In the case of the haptotactic model, the interpretation becomes more complicated. One hypothesis is that flooding the system with a haptotactic cue would cause the axons to stall, since they would be strongly adhering to the protein, differently from what we have observed. In our experiments, axons reached the midline, they just took a longer path. Another hypothesis is that Netrin-1 forms hederal boundaries that serve as substrate, guiding the axons (Varadarajan and Butler, 2017). In this case, flooding the system with exogenous Netrin-1, would only cause disruptions in guidance if the exogenous protein is capable of overcome such boundaries. Additional stainings using antibodies against Netrin-1, could confirm the pattern of expression of Netrin-1 in our system, and the pattern of these hederal boundaries. Due to the flat, homogenous pattern of exogenous Netrin-1 that was observed in the openbooks it is very unlikely that Netrin-1 boundaries were intact, or just slightly smudged. In addition, the *in vitro* experiments performed in chapter 3 were performed based on the chemotactic model. Netrin is not expected to leave a haptotactic boundary in the Dunn chambers during our turning assays or in the growth cone expansion assays.

This haptotactic model for Netrin-1 does not explain how the classical experiments with axons deflecting from the floorplate in the presence of adjacent explants of cells expressing Netrin-1, thus suggesting that these two models might work complementary to each other (Kennedy et al., 1994; Kennedy et al., 2006; Moore and Kennedy, 2006; Morales, 2017). Based on the strong phenotypes observed in the haptotatic null mice, we might infer that the haptotactic function plays a predominant role *in vivo* (Dominici et al., 2017; Varadarajan et al., 2017). We cannot discard that these two functions (haptotactic and chemotactic) signal through different pathways. Differences in multimerization patterns of the netrin receptor 'deleted in colorectal cancer` (DCC) can explain how these two functions might signal through different pathways (Finci et al., 2014; Xu et al., 2014). Netrin-1 leads to the multimerization of DCC, which is regulated by different domains of DCC (Finci et al., 2014; Mille et al., 2009). Differences in the availability of Netrin-1 and the density of the receptors that form the DCC/Netrin-1 complexes could account for distinct signaling in the haptotatic model, compared to chemotactic. This would also explain why the *in vitro* phenotypes of our 14-3-3 loss of function experiments had much stronger phenotypes than the *in vivo*. Whereas the *in vitro* experiments were predominantly chemotactic, both functions of Netrin-1 might be required *in vivo.* Therefore, further elucidation on the biochemical distinctions of these two models might be required before we evaluate whether 14-3-3s participate in only one of them.

5.4 – 14-3-3 molecular interactions and mechanisms for regulation of 14-3-3 action in axon guidance and OPC differentiation

In our current work, we focused on the role of 14-3-3s as regulators of Rac1, a Rho GTPase, and its implications in netrin signaling. This section aims at discussing alternative molecular pathways that can be explored for 14-3-3 function in axon guidance, as well as some tentative pathways for OPC differentiation.

5.4.1 – PKA regulation by 14-3-3s

One of the pathways regulated by 14-3-3 is PKA activity (Kent et al., 2010). During axonal development, spatial distribution of PKA is precisely controlled through the coordination of cyclic adenosine monophosphate (cAMP) levels at microdomains, mainly due to the activity of protein kinase A anchoring proteins (AKAPs) (Logue and Scott, 2010). Several cytoskeletal associated proteins have been shown to function as AKAPs, such as WASP family Verprolin-homologous protein 1 (WAVE1), microtubule associated protein 2 (MAP2) and ezrin (Dransfield et al., 1997; Theurkauf and Vallee, 1982; Westphal et al., 2000). Hence, these cytoskeletal associated proteins can regulate actin remodelling in the leading at the same time as they localize PKA in the active remodelling regions of the growth cone. 14-3-3s antagonize PKA activity by stabilizing the two regulatory subunits of the holoenzyme, rendering the enzyme inactive (Kent et al., 2010). In addition, active PKA autophosphorylates, generating 14-3-3 binding motifs and regulating interactions to AKAP (Budillon et al., 1995; Manni et al., 2008). Another method of regulation of PKA by 14-3-3s is through AKAP-Lbc, which can also function as a guanine exchange factor (GEF) and positively regulate Rho GTPase activity (Jin et al., 2004). Depending on the state of oligomerization of AKAP-Lbc, 14-3-3s can dock them in an

GEF inactive conformation (Diviani et al., 2006). 14-3-3s can, thus, modulate PKA activity and regulate its interactions with other proteins in different ways.

In our axon guidance model, we focused on a stage of prominent PKA activity, which is thought to regulate the sensitivity of the SCNs to Netrin-1 through the recruitment of DCC to the membrane, instead of the switches in the polarity (Bouchard et al., 2008; Moore and Kennedy, 2006). The contribution of PKA to our guidance phenotype was mostly unexplored. It is possible that the overactivation of the GEF β-Pix and Rac1 are partially due to an increase in membrane DCC. This question can be easily assessed by the addition of a PKA inhibitor, such as PKI, to the cell cultures and analysis of the basal activation of Rac1.

However, it is in OPC differentiation that 14-3-3 regulation of PKA can be of more interest to us. PKA activity is inhibited by proteins such as the G protein-coupled receptor GPR17, which acts as an inhibitor of oligodendrocyte maturation, where GPR17 activation also reduce expansion of myelin basic protein (MBP) positive membranes (Chen et al., 2009; Simon et al., 2016). GPR17 is highly expressed in demyelinating diseases such as multiple sclerosis (MS), making therapies that enhance PKA an attractive way to counteract GPR17 activity. Confirmation of whether the MBP membrane expansion that we observed is due to an increase of PKA activity provoked by BV02 treatment can be valuable to understand the mechanisms by which 14-3-3s act in the development of OPCs. If proven true, inhibition of 14-3-3s can be a potential therapy to increase PKA activity in demyelinating disease.

5.4.2 – Rho GTPase regulation

In Chapter 3, we hypothesized that 14-3-3s act in DCC signaling by localizing β-Pix in the vicinity of the DCC receptor. However, 14-3-3s can play additional roles in GEF and Rho GTPase signaling.

For instance, Rho GEFs are often regulated by phosphorylation. In many examples, phosphorylation results in increases in the GDP-GTP exchange rate and Rho GTPase activation, although there are exceptions where the presence of phospho-residues negatively impacts its activity, by changing the conformation of its catalytic domain or promoting its binding to scaffold proteins that sequester them (Hodge and Ridley, 2016). This phosphorylation of Rho GEFs can create binding sites for 14-3-3s. As in the case of GEF-H1, 14-3-3s sequester the GEF to the vicinity of the microtubules, away from their region of activity, therefore repressing their function (Zenke et al., 2004). Total internal reflection fluorescence (TIRF) experiments are being performed by us, in order to observe the existence of a similar mechanism related to β-Pix localization in DCC signaling, and whether 14-3-3s also play a role in the sequestering of β-Pix.

In relation to the spatial regulation of Rac activation by 14-3-3, fluorescence life-time imaging microscopy combined to fluorescence resonance energy transfer (FLIM-FRET) experiments using a Rac1- Raichu probe are currently being performed to analyze whether 14-3-3 impacts in the local activation of Rac1 in the cell (Navarro-Lerida et al., 2015; Rappaz et al., 2016).

Despite many examples of 14-3-3s inhibiting GEF activity, 14-3-3s can also stimulate GEF activity. 14-3-3ζ binding to TIAM1 recruits it to adhesion complexes that contain β1-integrin (O'Toole et al., 2011). There, TIAM1 is able to interact with Rac1,

whose activation promotes cell motility. This interaction between 14-3-3 and TIAM1 has been shown to require phosphorylation in three residues (S60, S172 and S231), and is thought to promote the stabilization of the GEF (Woodcock et al., 2009). It is unclear whether TIAM is phosphorylated at these residues during DCC signaling and that would be an additional manner 14-3-3s modulate Rac activation in our system, although its physiological relevance would be very limited, as we see an increase in overall Rac1 activation in the absence of 14-3-3ζ.

As discussed in the introduction, the role of GEFs and Rho GTPases during the development of OPCs has been very scarcely studied. Based on Schwann cell studies, it is possible that these proteins can execute similar functions in the expansion of developing oligodendrocytes, but this hypothesis has been mostly unexplored (Nodari et al., 2007). We are currently working on the biochemical analysis of Rac1 activation during OPC differentiation, to confirm whether 14-3-3 loss of function causes an increase of Rac1 activation similar to the observed in the chapter 3 of this thesis. Preliminary FLIM-FRET experiments with Rac-Raichu did not show any clear activation of Rac to specific domains of the developing oligodendrocytes (data not shown), but since these cells are radially expanding, it is likely that Rac1 activation happens through the whole processes. If proven true, we will focus on the biochemical screening of the proteins that regulate Rac1 in oligodendrocytes, as the literature on oligodendrocytic GEFs is very restricted.

5.4.3 – Calcium signaling, MAPK and DCC activity in oligodendrocyte development

Another signaling pathway that might be affected by 14-3-3 is calcium signaling, through the activity of calcium/ calmodulin-dependent protein kinase (CaMK) and calcium dependent kinase (PKC). 14-3-3s modulate calcium signaling through different mechanisms. One of which is the regulation of intracellular calcium levels. Calcium influx is regulated by transmembrane channels, one of which being the voltage channel CaV2.2. In neurons, binding of 14-3-3s to CaV2.2 slows their inactivation, leading to sustained calcium influx (Li et al., 2006). 14-3-3s also stabilize Ca levels by inhibition of sodium/calcium exchangers (Pulina et al., 2006). The regulation of calcium channels by 14-3-3s in oligodendrocytes has not been explored.

Calcium dependent kinase (PKC) is inhibited by 14-3-3 binding, and its activation leads to an increase in myelin production (Aitken et al., 1995a; Baer et al., 2009). Similarly, 14-3-3s inhibit CamKK, a CaMK activator and CaMK IIβ requirement for oligodendrocyte development has been suggest by animal models, but the signaling involved in this process is mostly unknown (Davare et al., 2004; Waggener et al., 2013). Therefore, promoting myelination by 14-3-3 inhibition might be achieved by suppressing mechanisms that antagonize PKC and CaMK activities.

Both kinases converge on class IIa histone deacetylase (HDAC) activity (Liu and Schneider, 2013; Wei et al., 2015). As discussed in the introduction, class IIa HDACs have been shown to regulate axonal morphology, and are candidate proteins to regulate OPC differentiation. However, their role in both these processes are still an unexplored domain.

14-3-3s are also well-known regulators of the mitogen activated protein kinase (MAPK) pathway, in which 14-3-3s regulate Raf relatively upstream in the cascade,

serving as a scaffold protein and promoting Raf activity (Freed et al., 1994; Qiu et al., 2000; Roy et al., 1998). MAPK has been shown to be extremely important for oligodendrocyte health and maintenance of myelin structure, therefore inhibition of 14-3-3 proteins might have some detrimental side effect, which can be minimized by the choice of isoform specific inhibitors (Ishii et al., 2013; Ishii et al., 2014; Ishii et al., 2012).

Finally, as chapter 2 was devoted to explaining the role of 14-3-3s in DCC signaling, it would be interesting to analyze whether 14-3-3s affect DCC signaling in oligodendrocytes. DCC is especially important at two very distinct phases of oligodendrocyte development: the migration of the progenitor cells, and the maintenance of the myelin structure in mature circuits (Jarjour et al., 2008; Jarjour et al., 2003; Rajasekharan et al., 2009). These two stages are very unlikely to be regulated by the same molecular mechanisms. However, as 14-3-3s can bind to DCC and dock it to other proteins, they might execute different functions in either or both these stages. To date, there is no report of β-Pix activity in oligodendrocytes, leading us to think that if 14-3-3s play a role in oligodendroglial DCC signaling, this might not be through the same mechanisms as in pre-crossing SCNs. Thus, further biochemical studies would be necessary to investigate the role of 14-3-3/ DCC signaling in oligodendrocytes.

5.5 – Concluding remarks

Here, we described the function of 14-3-3s in the development of pre-crossing SCNs. In addition, we contributed to knowledge about netrin signaling and its effects on SCN development. Finally, we described the pattern of expression of 14-3-3 by OPCs *in*

vitro. The functions of 14-3-3s in axon guidance can be further explored by more detailed studies on its interactions with DCC, small GTPases and GEFs, as well as further studies on 14-3-3 regulation during development. In addition, our data with OPCs suggests that 14-3-3s can play important roles in oligodendrocyte differentiation, which will be explored in the future, especially regarding its biochemical mechanisms.

6.0 – Appendix: PhD publication list

ALCHINI, R; HUA, L; KENT, C; KAPLAN, A; RAMBALDI, I; DEGEER, J; KENNEDY, T; LAMARCHE-VANE, N; SCHWARZ, Q; FOURNIER, A. 14-3-3ζ regulates pre-crossing spinal cord commissural projections via regulation of Rac1 signaling. (*In preparation*)

ALCHINI, R; KENNEDY, TE; FOURNIER, AE. *Ex utero* electroporation of rodent spinal cords as a method to study commissural axon guidance. (*In preparation*)

ROUGER, V; **ALCHINI, R;** KAZARINE, A; GOPAL, AA; GIROUARD, MP; FOURNIER, A; WISEMAN, PW. Low cost multi-modal light-sheet implementation for optically cleared tissues and living specimens. Journal of Biomedical Optics 1;21(12):126008.

GIROUARD, MP; POOL, M; RAMBALDI, I.; **ALCHINI, R**; FOURNIER, AE. RhoA proteolysis regulates the actin cytoskeleton in response to oxidative stress. Plos One, 11(12):e0168641, 2016.

ANTOINE-BERTRAND, J; DUQUETTE, PM; **ALCHINI, R**; KENNEDY, TE; FOURNIER, AE; LAMARCHE-VANE, N. p120RasGAP mediates netrin-1-induced cortical axon outgrowth and guidance. Journal of Biological Chemistry, 291 (9):4589-602, 2016.

KHAZAEI, M; GIROUARD, MP; **ALCHINI, R**; ONG TONE, S; SHIMADA, T; BECHSTEDT, S; COWAN, M; GUILLET, D; WISEMAN, P; BROUHARD, G; CLOUTIER, JF; FOURNIER, AE. Collapsin Response Mediator Protein 4 regulates growth cone dynamics through coordinated regulation of the actin and microtubule cytoskeleton. Journal of Biochemistry; 289(43):30133-43, 2014.

KAPLAN, A*; SANZ, R*; FERRARO, GB*; **ALCHINI, R***; FOURNIER, AE. Neurite outgrowth and growth cone collapse assays to assess neuronal responses to extracellular cues. Methods Mol Biol. 1162:43-56, 2014. *Equally contributing authors.

YAM, PT; KENT, CB; MORIN, S; FARMER, WT; **ALCHINI, R**; LEPELLETIER, L; COLMAN, DR; TESSIER-LAVIGNE, M; FOURNIER, AE; CHARRON, F. 14-3-3 proteins regulate a cell-intrinsic switch from Sonic hedgehog-mediated attraction to repulsion of commissural axons after midline crossing. Neuron, 76: 735-749, 2012

7.0 – References

Aggarwal, S., Yurlova, L., Snaidero, N., Reetz, C., Frey, S., Zimmermann, J., Pahler, G., Janshoff, A., Friedrichs, J., Muller, D.J., *et al.* (2011). A size barrier limits protein diffusion at the cell surface to generate lipid-rich myelin-membrane sheets. Developmental cell *21*, 445-456.

Aitken, A., Howell, S., Jones, D., Madrazo, J., Martin, H., Patel, Y., and Robinson, K. (1995a). Post-translationally modified 14-3-3 isoforms and inhibition of protein kinase C. Molecular and cellular biochemistry *149-150*, 41-49.

Aitken, A., Howell, S., Jones, D., Madrazo, J., and Patel, Y. (1995b). 14-3-3 alpha and delta are the phosphorylated forms of raf-activating 14-3-3 beta and zeta. In vivo stoichiometric phosphorylation in brain at a Ser-Pro-Glu-Lys MOTIF. The Journal of biological chemistry *270*, 5706-5709.

Alchini, R., Sato, H., Matsumoto, N., Shimogori, T., Sugo, N., and Yamamoto, N. (2017). Nucleocytoplasmic Shuttling of Histone Deacetylase 9 Controls Activity-Dependent Thalamocortical Axon Branching. Scientific Reports *7*, 6024.

Almeida, R.G., Czopka, T., Ffrench-Constant, C., and Lyons, D.A. (2011). Individual axons regulate the myelinating potential of single oligodendrocytes in vivo. Development *138*, 4443-4450.

Altman, P.L., and Katz, D.D. (1962). Growth including reproduction and morphological development (Washington: Federation of American Societies for Experimental Biology).

Andermatt, I., Wilson, N.H., Bergmann, T., Mauti, O., Gesemann, M., Sockanathan, S., and Stoeckli, E.T. (2014). Semaphorin 6B acts as a receptor in post-crossing commissural axon guidance. Development *141*, 3709-3720.

Antoine-Bertrand, J., Duquette, P.M., Alchini, R., Kennedy, T.E., Fournier, A.E., and Lamarche-Vane, N. (2016). p120RasGAP Protein Mediates Netrin-1 Protein-induced Cortical Axon Outgrowth and Guidance. The Journal of biological chemistry *291*, 4589-4602.

Armstrong, R.C., Harvath, L., and Dubois-Dalcq, M.E. (1990). Type 1 astrocytes and oligodendrocyte-type 2 astrocyte glial progenitors migrate toward distinct molecules. Journal of neuroscience research *27*, 400-407.

Augsburger, A., Schuchardt, A., Hoskins, S., Dodd, J., and Butler, S. (1999). BMPs as mediators of roof plate repulsion of commissural neurons. Neuron *24*, 127-141.

Baer, A.S., Syed, Y.A., Kang, S.U., Mitteregger, D., Vig, R., ffrench-Constant, C., Franklin, R.J.M., Altmann, F., Lubec, G., and Kotter, M.R. (2009). Myelin-mediated inhibition of oligodendrocyte precursor differentiation can be overcome by pharmacological modulation of Fyn-RhoA and protein kinase C signalling. Brain *132*, 465-481.

Barateiro, A., and Fernandes, A. (2014). Temporal oligodendrocyte lineage progression: in vitro models of proliferation, differentiation and myelination. Biochimica et biophysica acta *1843*, 1917-1929.

Bardai, F.H., and D'Mello, S.R. (2011). Selective toxicity by HDAC3 in neurons: regulation by Akt and GSK3beta. The Journal of neuroscience : the official journal of the Society for Neuroscience *31*, 1746-1751.

Barres, B.A., Hart, I.K., Coles, H.S., Burne, J.F., Voyvodic, J.T., Richardson, W.D., and Raff, M.C. (1992). Cell death and control of cell survival in the oligodendrocyte lineage. Cell *70*, 31-46.

Barres, B.A., Lazar, M.A., and Raff, M.C. (1994). A novel role for thyroid hormone, glucocorticoids and retinoic acid in timing oligodendrocyte development. Development *120*, 1097-1108.

Bellardita, C., and Kiehn, O. (2015). Phenotypic characterization of speed-associated gait changes in mice reveals modular organization of locomotor networks. Current biology : CB *25*, 1426-1436.

Bermingham, N.A., Hassan, B.A., Wang, V.Y., Fernandez, M., Banfi, S., Bellen, H.J., Fritzsch, B., and Zoghbi, H.Y. (2001). Proprioceptor pathway development is dependent on Math1. Neuron *30*, 411-422.

Biname, F., Sakry, D., Dimou, L., Jolivel, V., and Trotter, J. (2013). NG2 regulates directional migration of oligodendrocyte precursor cells via Rho GTPases and polarity complex proteins. The Journal of neuroscience : the official journal of the Society for Neuroscience *33*, 10858-10874.

Black, D.L., and Zipursky, S.L. (2008). To cross or not to cross: alternatively spliced forms of the Robo3 receptor regulate discrete steps in axonal midline crossing. Neuron *58*, 297-298.

Boston, P.F., Jackson, P., and Thompson, R.J. (1982). Human 14-3-3 protein: radioimmunoassay, tissue distribution, and cerebrospinal fluid levels in patients with neurological disorders. Journal of neurochemistry *38*, 1475-1482.

Bottenstein, J.E., and Sato, G.H. (1979). Growth of a rat neuroblastoma cell line in serum-free supplemented medium. Proceedings of the National Academy of Sciences of the United States of America *76*, 514-517.

Bouchard, J.F., Horn, K.E., Stroh, T., and Kennedy, T.E. (2008). Depolarization recruits DCC to the plasma membrane of embryonic cortical neurons and enhances axon extension in response to netrin-1. Journal of neurochemistry *107*, 398-417.

Bourikas, D., Pekarik, V., Baeriswyl, T., Grunditz, A., Sadhu, R., Nardo, M., and Stoeckli, E.T. (2005). Sonic hedgehog guides commissural axons along the longitudinal axis of the spinal cord. Nature neuroscience *8*, 297-304.

Briançon-Marjollet, A., Ghogha, A., Nawabi, H., Triki, I., Auziol, C., Fromont, S., Piché, C., Enslen, H., Chebli, K., Cloutier, J.-F.*, et al.* (2008). Trio Mediates Netrin-1-Induced Rac1 Activation in Axon Outgrowth and Guidance. Molecular and cellular biology *28*, 2314-2323.

Briancon-Marjollet, A., Ghogha, A., Nawabi, H., Triki, I., Auziol, C., Fromont, S., Piche, C., Enslen, H., Chebli, K., Cloutier, J.F.*, et al.* (2008). Trio mediates netrin-1-induced Rac1 activation in axon outgrowth and guidance. Molecular and cellular biology *28*, 2314-2323.

Bribian, A., Esteban, P.F., Clemente, D., Soussi-Yanicostas, N., Thomas, J.L., Zalc, B., and de Castro, F. (2008). A novel role for anosmin-1 in the adhesion and migration of oligodendrocyte precursors. Dev Neurobiol *68*, 1503-1516.

Briggs, L.E., Burns, T.A., Lockhart, M.M., Phelps, A.L., Van den Hoff, M.J., and Wessels, A. (2016). Wnt/beta-catenin and sonic hedgehog pathways interact in the regulation of the development of the dorsal mesenchymal protrusion. Developmental

dynamics : an official publication of the American Association of Anatomists *245*, 103-113.

Brinkmann, B.G., Agarwal, A., Sereda, M.W., Garratt, A.N., Muller, T., Wende, H., Stassart, R.M., Nawaz, S., Humml, C., Velanac, V.*, et al.* (2008). Neuregulin-1/ErbB signaling serves distinct functions in myelination of the peripheral and central nervous system. Neuron *59*, 581-595.

Brose, K., Bland, K.S., Wang, K.H., Arnott, D., Henzel, W., Goodman, C.S., Tessier-Lavigne, M., and Kidd, T. (1999). Slit Proteins Bind Robo Receptors and Have an Evolutionarily Conserved Role in Repulsive Axon Guidance. Cell *96*, 795-806.

Brunet, A., Bonni, A., Zigmond, M.J., Lin, M.Z., Juo, P., Hu, L.S., Anderson, M.J., Arden, K.C., Blenis, J., and Greenberg, M.E. (1999). Akt promotes cell survival by phosphorylating and inhibiting a Forkhead transcription factor. Cell *96*, 857-868.

Budillon, A., Cereseto, A., Kondrashin, A., Nesterova, M., Merlo, G., Clair, T., and Cho-Chung, Y.S. (1995). Point mutation of the autophosphorylation site or in the nuclear location signal causes protein kinase A RII beta regulatory subunit to lose its ability to revert transformed fibroblasts. Proceedings of the National Academy of Sciences of the United States of America *92*, 10634-10638.

Buttermore, E.D., Thaxton, C.L., and Bhat, M.A. (2013). Organization and maintenance of molecular domains in myelinated axons. Journal of neuroscience research *91*, 603-622.

Cai, J., Qi, Y., Hu, X., Tan, M., Liu, Z., Zhang, J., Li, Q., Sander, M., and Qiu, M. (2005). Generation of oligodendrocyte precursor cells from mouse dorsal spinal cord independent of Nkx6 regulation and Shh signaling. Neuron *45*, 41-53.

Cajal, S.R.y. (1889). Conexíon general de los elementos nerviosos. La Medicina Práctica *2*, 341-346.

Cajal, S.R.y. (1890). A quelle époque apparaissent les expansions des cellules nerveuses de la moëlle épiniere du poulet? Anatomischer Anzeiger *5*, 631-639.

Cajal, S.R.y. (1892). La rétine des vertèbres. Cellule *9*, 121-255.

Cajal, S.R.y. (1899). Textura del sistema nervioso del hombre y de los vertebrados: estudios sobre el plan estructural y composición histológica de los centros nerviosos adicionados de consideraciones fisiológicas fundadas en los nuevos descubrimientos (Madrid: Moya).

Campa, C.C., Ciraolo, E., Ghigo, A., Germena, G., and Hirsch, E. (2015). Crossroads of PI3K and Rac pathways. Small GTPases *6*, 71-80.

Campbell, J.K., Gurung, R., Romero, S., Speed, C.J., Andrews, R.K., Berndt, M.C., and Mitchell, C.A. (1997). Activation of the 43 kDa inositol polyphosphate 5-phosphatase by 14-3-3zeta. Biochemistry *36*, 15363-15370.

Carson, M.J., Behringer, R.R., Brinster, R.L., and McMorris, F.A. (1993). Insulin-like growth factor I increases brain growth and central nervous system myelination in transgenic mice. Neuron *10*, 729-740.

Casarosa, S., Fode, C., and Guillemot, F. (1999). Mash1 regulates neurogenesis in the ventral telencephalon. Development *126*, 525-534.

Celis, J.E., Gesser, B., Rasmussen, H.H., Madsen, P., Leffers, H., Dejgaard, K., Honore, B., Olsen, E., Ratz, G., Lauridsen, J.B.*, et al.* (1990). Comprehensive two-dimensional gel protein databases offer a global approach to the analysis of human cells:

the transformed amnion cells (AMA) master database and its link to genome DNA sequence data. Electrophoresis *11*, 989-1071.

Chahdi, A., and Sorokin, A. (2008). Protein kinase A-dependent phosphorylation modulates beta1Pix guanine nucleotide exchange factor activity through 14-3-3beta binding. Molecular and cellular biology *28*, 1679-1687.

Chang, C., Adler, C.E., Krause, M., Clark, S.G., Gertler, F.B., Tessier-Lavigne, M., and Bargmann, C.I. (2006). MIG-10/Lamellipodin and AGE-1/PI3K Promote Axon Guidance and Outgrowth in Response to Slit and Netrin. Current Biology *16*, 854-862.

Chardin, P. (2006). Function and regulation of Rnd proteins. Nature reviews Molecular cell biology *7*, 54-62.

Charron, F., Stein, E., Jeong, J., McMahon, A.P., and Tessier-Lavigne, M. (2003). The morphogen sonic hedgehog is an axonal chemoattractant that collaborates with netrin-1 in midline axon guidance. Cell *113*, 11-23.

Cheah, P.S., Ramshaw, H.S., Thomas, P.Q., Toyo-oka, K., Xu, X., Martin, S., Coyle, P., Guthridge, M.A., Stomski, F., van den Buuse, M.*, et al.* (2012). Neurodevelopmental and neuropsychiatric behaviour defects arise from 14-3-3[zeta] deficiency. Molecular psychiatry *17*, 451-466.

Chédotal, A. (2011). Further tales of the midline. Current Opinion in Neurobiology *21*, 68-75.

Chen, Y., Wu, H., Wang, S., Koito, H., Li, J., Ye, F., Hoang, J., Escobar, S.S., Gow, A., Arnett, H.A.*, et al.* (2009). The oligodendrocyte-specific G protein-coupled receptor GPR17 is a cell-intrinsic timer of myelination. Nature neuroscience *12*, 1398-1406.

Cherfils, J., and Zeghouf, M. (2013). Regulation of small GTPases by GEFs, GAPs, and GDIs. Physiological reviews *93*, 269-309.

Chizhikov, V.V., and Millen, K.J. (2005). Roof plate-dependent patterning of the vertebrate dorsal central nervous system. Developmental biology *277*, 287-295.

Cho, Y., and Cavalli, V. (2012). HDAC5 is a novel injury-regulated tubulin deacetylase controlling axon regeneration. The EMBO journal *31*, 3063-3078.

Cho, Y., Sloutsky, R., Naegle, K.M., and Cavalli, V. (2013). Injury-induced HDAC5 nuclear export is essential for axon regeneration. Cell *155*, 894-908.

Choe, Y., Huynh, T., and Pleasure, S.J. (2014). Migration of oligodendrocyte progenitor cells is controlled by transforming growth factor beta family proteins during corticogenesis. The Journal of neuroscience : the official journal of the Society for Neuroscience *34*, 14973-14983.

Chun, S.J., Rasband, M.N., Sidman, R.L., Habib, A.A., and Vartanian, T. (2003). Integrin-linked kinase is required for laminin-2-induced oligodendrocyte cell spreading and CNS myelination. The Journal of cell biology *163*, 397-408.

Cohen, S., Levi-Montalcini, R., and Hamburger, V. (1954). A Nerve Growth-Stimulating Factor Isolated from Sarcom as 37 and 180. Proceedings of the National Academy of Sciences of the United States of America *40*, 1014-1018.

Colman, D.R., Kreibich, G., Frey, A.B., and Sabatini, D.D. (1982). Synthesis and incorporation of myelin polypeptides into CNS myelin. The Journal of cell biology *95*, 598-608.

Colognato, H., Ramachandrappa, S., Olsen, I.M., and ffrench-Constant, C. (2004). Integrins direct Src family kinases to regulate distinct phases of oligodendrocyte development. The Journal of cell biology *167*, 365-375.

Cote, J.F., Motoyama, A.B., Bush, J.A., and Vuori, K. (2005). A novel and evolutionarily conserved PtdIns(3,4,5)P3-binding domain is necessary for DOCK180 signalling. Nature cell biology *7*, 797-807.

Cote, J.F., and Vuori, K. (2006). In vitro guanine nucleotide exchange activity of DHR-2/DOCKER/CZH2 domains. Methods in enzymology *406*, 41-57.

Cote, J.F., and Vuori, K. (2007). GEF what? Dock180 and related proteins help Rac to polarize cells in new ways. Trends in cell biology *17*, 383-393.

Cotelle, V., and Leonhardt, N. (2015). 14-3-3 Proteins in Guard Cell Signaling. Frontiers in plant science *6*, 1210.

Czopka, T., Ffrench-Constant, C., and Lyons, D.A. (2013). Individual oligodendrocytes have only a few hours in which to generate new myelin sheaths in vivo. Developmental cell *25*, 599-609.

Davare, M.A., Saneyoshi, T., Guire, E.S., Nygaard, S.C., and Soderling, T.R. (2004). Inhibition of calcium/calmodulin-dependent protein kinase kinase by protein 14-3-3. The Journal of biological chemistry *279*, 52191-52199.

DeGeer, J., Kaplan, A., Mattar, P., Morabito, M., Stochaj, U., Kennedy, T.E., Debant, A., Cayouette, M., Fournier, A.E., and Lamarche-Vane, N. (2015). Hsc70 chaperone activity underlies Trio GEF function in axon growth and guidance induced by netrin-1. The Journal of cell biology *210*, 817-832.

Del Rio-Hortega, P. (1920). Estudios sobre la neuroglía. La microglía y su transformación en células en bastoncito y cuerpos granuloadiposos. . *18*, 37-82.

Del Rio-Hortega, P. (1921). La glía de escasas radiaciones (oligodendroglía). . Boletin de la Real Sociedad Espanola de Historia Natural *21*, 30.

Del Rio-Hortega, P. (1928). Tercera aportación al conocimiento morfológico e interpretación funcional de la oligodendroglía. . *14*, 15-22.

Demarco, R.S., Struckhoff, E.C., and Lundquist, E.A. (2012). The Rac GTP exchange factor TIAM-1 acts with CDC-42 and the guidance receptor UNC-40/DCC in neuronal protrusion and axon guidance. PLoS genetics *8*, e1002665.

Dent, E.W., Gupton, S.L., and Gertler, F.B. (2011). The Growth Cone Cytoskeleton in Axon Outgrowth and Guidance. Cold Spring Harbor perspectives in biology *3*, a001800.

Diviani, D., Baisamy, L., and Appert-Collin, A. (2006). AKAP-Lbc: a molecular scaffold for the integration of cyclic AMP and Rho transduction pathways. European journal of cell biology *85*, 603-610.

Dobson, M., Ramakrishnan, G., Ma, S., Kaplun, L., Balan, V., Fridman, R., and Tzivion, G. (2011). Bimodal Regulation of FoxO3 by AKT and 14-3-3. Biochimica et biophysica acta *1813*, 1453-1464.

Domanitskaya, E., Wacker, A., Mauti, O., Baeriswyl, T., Esteve, P., Bovolenta, P., and Stoeckli, E.T. (2010). Sonic hedgehog guides post-crossing commissural axons both directly and indirectly by regulating Wnt activity. The Journal of neuroscience : the official journal of the Society for Neuroscience *30*, 11167-11176.

Domingues, H.S., Portugal, C.C., Socodato, R., and Relvas, J.B. (2016). Oligodendrocyte, Astrocyte, and Microglia Crosstalk in Myelin Development, Damage, and Repair. Frontiers in cell and developmental biology *4*, 71.

Dominici, C., Moreno-Bravo, J.A., Puiggros, S.R., Rappeneau, Q., Rama, N., Vieugue, P., Bernet, A., Mehlen, P., and Chedotal, A. (2017). Floor-plate-derived netrin-1 is dispensable for commissural axon guidance. Nature *545*, 350-354.

Dong, S., Kang, S., Lonial, S., Khoury, H.J., Viallet, J., and Chen, J. (2008). Targeting 14-3-3 sensitizes native and mutant BCR-ABL to inhibition with U0126, rapamycin and Bcl-2 inhibitor GX15-070. Leukemia *22*, 572-577.

Dransfield, D.T., Bradford, A.J., Smith, J., Martin, M., Roy, C., Mangeat, P.H., and Goldenring, J.R. (1997). Ezrin is a cyclic AMP-dependent protein kinase anchoring protein. The EMBO journal *16*, 35-43.

Dugas, J.C., Cuellar, T.L., Scholze, A., Ason, B., Ibrahim, A., Emery, B., Zamanian, J.L., Foo, L.C., McManus, M.T., and Barres, B.A. (2010). Dicer1 and miR-219 Are required for normal oligodendrocyte differentiation and myelination. Neuron *65*, 597-611.

Durand, B., and Raff, M. (2000). A cell-intrinsic timer that operates during oligodendrocyte development. BioEssays : news and reviews in molecular, cellular and developmental biology *22*, 64-71.

Ehrengruber, M.U., Hennou, S., Bueler, H., Naim, H.Y., Deglon, N., and Lundstrom, K. (2001). Gene transfer into neurons from hippocampal slices: comparison of recombinant Semliki Forest Virus, adenovirus, adeno-associated virus, lentivirus, and measles virus. Molecular and cellular neurosciences *17*, 855-871.

Emery, B., Agalliu, D., Cahoy, J.D., Watkins, T.A., Dugas, J.C., Mulinyawe, S.B., Ibrahim, A., Ligon, K.L., Rowitch, D.H., and Barres, B.A. (2009). Myelin Gene Regulatory Factor Is a Critical Transcriptional Regulator Required for CNS Myelination. Cell *138*, 172-185.

Emery, B., and Lu, Q.R. (2015). Transcriptional and Epigenetic Regulation of Oligodendrocyte Development and Myelination in the Central Nervous System. Cold Spring Harbor perspectives in biology *7*, a020461.

Erturk, A., Becker, K., Jahrling, N., Mauch, C.P., Hojer, C.D., Egen, J.G., Hellal, F., Bradke, F., Sheng, M., and Dodt, H.U. (2012). Three-dimensional imaging of solvent-cleared organs using 3DISCO. Nature protocols *7*, 1983-1995.

Evans, T.A., and Bashaw, G.J. (2010). Axon guidance at the midline: of mice and flies. Current opinion in neurobiology *20*, 79-85.

Fancy, S.P., Baranzini, S.E., Zhao, C., Yuk, D.I., Irvine, K.A., Kaing, S., Sanai, N., Franklin, R.J., and Rowitch, D.H. (2009). Dysregulation of the Wnt pathway inhibits timely myelination and remyelination in the mammalian CNS. Genes & development *23*, 1571-1585.

Fazeli, A., Dickinson, S.L., Hermiston, M.L., Tighe, R.V., Steen, R.G., Small, C.G., Stoeckli, E.T., Keino-Masu, K., Masu, M., Rayburn, H.*, et al.* (1997). Phenotype of mice lacking functional Deleted in colorectal cancer (Dcc) gene. Nature *386*, 796-804.

Feng, G., Mellor, R.H., Bernstein, M., Keller-Peck, C., Nguyen, Q.T., Wallace, M., Nerbonne, J.M., Lichtman, J.W., and Sanes, J.R. (2000). Imaging Neuronal Subsets in Transgenic Mice Expressing Multiple Spectral Variants of GFP. Neuron *28*, 41-51.

Finci, L.I., Kruger, N., Sun, X., Zhang, J., Chegkazi, M., Wu, Y., Schenk, G., Mertens, H.D.T., Svergun, D.I., Zhang, Y.*, et al.* (2014). The crystal structure of netrin-1 in complex with DCC reveals the bifunctionality of netrin-1 as a guidance cue. Neuron *83*, 839-849.

Finger, S. (1994). The Era of Cortical Localization. In The Origins of Neuroscience: A History of Explorations into Brain Function (New York: Oxford University Press), pp. 32-50.

Flores, A.I., Narayanan, S.P., Morse, E.N., Shick, H.E., Yin, X., Kidd, G., Avila, R.L., Kirschner, D.A., and Macklin, W.B. (2008). Constitutively active Akt induces enhanced myelination in the CNS. The Journal of neuroscience : the official journal of the Society for Neuroscience *28*, 7174-7183.

Fogarty, M., Richardson, W.D., and Kessaris, N. (2005). A subset of oligodendrocytes generated from radial glia in the dorsal spinal cord. Development *132*, 1951-1959.

Foote, M., Qiao, H., Graham, K., Wu, Y., and Zhou, Y. (2015). Inhibition of 14-3-3 Proteins Leads to Schizophrenia-Related Behavioral Phenotypes and Synaptic Defects in Mice. Biological psychiatry *78*, 386-395.

Freed, E., Symons, M., Macdonald, S.G., McCormick, F., and Ruggieri, R. (1994). Binding of 14-3-3 proteins to the protein kinase Raf and effects on its activation. Science *265*, 1713-1716.

Fruhbeis, C., Frohlich, D., Kuo, W.P., Amphornrat, J., Thilemann, S., Saab, A.S., Kirchhoff, F., Mobius, W., Goebbels, S., Nave, K.A.*, et al.* (2013). Neurotransmitter-

triggered transfer of exosomes mediates oligodendrocyte-neuron communication. PLoS Biol *11*, e1001604.

Fu, H., Subramanian, R.R., and Masters, S.C. (2000). 14-3-3 proteins: structure, function, and regulation. Annual review of pharmacology and toxicology *40*, 617-647.

Funfschilling, U., Supplie, L.M., Mahad, D., Boretius, S., Saab, A.S., Edgar, J., Brinkmann, B.G., Kassmann, C.M., Tzvetanova, I.D., Mobius, W.*, et al.* (2012). Glycolytic oligodendrocytes maintain myelin and long-term axonal integrity. Nature *485*, 517-521.

Fyffe-Maricich, S.L., Schott, A., Karl, M., Krasno, J., and Miller, R.H. (2013). Signaling through ERK1/2 Controls Myelin Thickness during Myelin Repair in the Adult Central Nervous System. The Journal of Neuroscience *33*, 18402-18408.

Gibson, E.M., Purger, D., Mount, C.W., Goldstein, A.K., Lin, G.L., Wood, L.S., Inema, I., Miller, S.E., Bieri, G., Zuchero, J.B.*, et al.* (2014). Neuronal activity promotes oligodendrogenesis and adaptive myelination in the mammalian brain. Science *344*, 1252304.

Gitai, Z., Yu, T.W., Lundquist, E.A., Tessier-Lavigne, M., and Bargmann, C.I. (2003). The netrin receptor UNC-40/DCC stimulates axon attraction and outgrowth through enabled and, in parallel, Rac and UNC-115/AbLIM. Neuron *37*, 53-65.

Goldman, J.S., Ashour, M.A., Magdesian, M.H., Tritsch, N.X., Harris, S.N., Christofi, N., Chemali, R., Stern, Y.E., Thompson-Steckel, G., Gris, P.*, et al.* (2013). Netrin-1 promotes excitatory synaptogenesis between cortical neurons by initiating synapse assembly. The Journal of neuroscience : the official journal of the Society for Neuroscience *33*, 17278-17289.

Gowan, K., Helms, A.W., Hunsaker, T.L., Collisson, T., Ebert, P.J., Odom, R., and Johnson, J.E. (2001). Crossinhibitory Activities of Ngn1 and Math1 Allow Specification of Distinct Dorsal Interneurons. Neuron *31*, 219-232.

Griffiths, I., Klugmann, M., Anderson, T., Yool, D., Thomson, C., Schwab, M.H., Schneider, A., Zimmermann, F., McCulloch, M., Nadon, N.*, et al.* (1998). Axonal swellings and degeneration in mice lacking the major proteolipid of myelin. Science *280*, 1610-1613.

Grinspan, J.B., and Franceschini, B. (1995). Platelet-derived growth factor is a survival factor for PSA-NCAM+ oligodendrocyte pre-progenitor cells. Journal of neuroscience research *41*, 540-551.

Grozinger, C.M., and Schreiber, S.L. (2000). Regulation of histone deacetylase 4 and 5 and transcriptional activity by 14-3-3-dependent cellular localization. Proceedings of the National Academy of Sciences of the United States of America *97*, 7835-7840.

Guilluy, C., Dubash, A.D., and Garcia-Mata, R. (2011). Analysis of RhoA and Rho GEF activity in whole cells and the cell nucleus. Nat Protocols *6*, 2050-2060.

Gunther, M.I., Gunther, M., Schneiders, M., Rupp, R., and Blesch, A. (2015). AngleJ: A new tool for the automated measurement of neurite growth orientation in tissue sections. Journal of neuroscience methods *251*, 143-150.

Halstead, J.R., Savaskan, N.E., van den Bout, I., Van Horck, F., Hajdo-Milasinovic, A., Snell, M., Keune, W.J., Ten Klooster, J.P., Hordijk, P.L., and Divecha, N. (2010). Rac controls PIP5K localisation and PtdIns(4,5)P(2) synthesis, which modulates vinculin localisation and neurite dynamics. Journal of cell science *123*, 3535-3546.

Hamburger, V. (1934). The effects of wing bud extirpation on the development of the central nervous system in chick embryos. Journal of Experimental Zoology *68*, 449-494.

Hamburger, V. (1939). Motor and sensory hyperplasia following limb-bud transplantations in chick embryos. Journal of Experimental Zoology *12*, 281.

Hardy, R.J., and Friedrich, V.L., Jr. (1996). Progressive remodeling of the oligodendrocyte process arbor during myelinogenesis. Developmental neuroscience *18*, 243-254.

He, Y., Dupree, J., Wang, J., Sandoval, J., Li, J., Liu, H., Shi, Y., Nave, K.A., and Casaccia-Bonnefil, P. (2007a). The transcription factor Yin Yang 1 is essential for oligodendrocyte progenitor differentiation. Neuron *55*, 217-230.

He, Y., Sandoval, J., and Casaccia-Bonnefil, P. (2007b). Events at the transition between cell cycle exit and oligodendrocyte progenitor differentiation: the role of HDAC and YY1. Neuron glia biology *3*, 221-231.

Helms, A.W., and Johnson, J.E. (1998). Progenitors of dorsal commissural interneurons are defined by MATH1 expression. Development *125*, 919-928.

Helms, A.W., and Johnson, J.E. (2003). Specification of dorsal spinal cord interneurons. Current opinion in neurobiology *13*, 42-49.

Hildebrand, C., and Hahn, R. (1978). Relation between myelin sheath thickness and axon size in spinal cord white matter of some vertebrate species. J Neurol Sci *38*, 421-434.

Hilpela, P., Vartiainen, M.K., and Lappalainen, P. (2004). Regulation of the actin cytoskeleton by PI(4,5)P2 and PI(3,4,5)P3. Current topics in microbiology and immunology *282*, 117-163.

Hodge, R.G., and Ridley, A.J. (2016). Regulating Rho GTPases and their regulators. Nature reviews Molecular cell biology *advance online publication*.

Huang, G.H., Sun, Z.L., Li, H.J., and Feng, D.F. (2017). Rho GTPase-activating proteins: Regulators of Rho GTPase activity in neuronal development and CNS diseases. Molecular and cellular neurosciences *80*, 18-31.

Ichimura, T., Isobe, T., Okuyama, T., Takahashi, N., Araki, K., Kuwano, R., and Takahashi, Y. (1988). Molecular cloning of cDNA coding for brain-specific 14-3-3 protein, a protein kinase-dependent activator of tyrosine and tryptophan hydroxylases. Proceedings of the National Academy of Sciences of the United States of America *85*, 7084-7088.

Ishii, A., Furusho, M., and Bansal, R. (2013). Sustained Activation of ERK1/2 MAPK in Oligodendrocytes and Schwann Cells Enhances Myelin Growth and Stimulates Oligodendrocyte Progenitor Expansion. The Journal of neuroscience : the official journal of the Society for Neuroscience *33*, 175-186.

Ishii, A., Furusho, M., Dupree, J.L., and Bansal, R. (2014). Role of ERK1/2 MAPK Signaling in the Maintenance of Myelin and Axonal Integrity in the Adult CNS. The Journal of Neuroscience *34*, 16031-16045.

Ishii, A., Fyffe-Maricich, S.L., Furusho, M., Miller, R.H., and Bansal, R. (2012). ERK1/ERK2 MAPK signaling is required to increase myelin thickness independent of

oligodendrocyte differentiation and initiation of myelination. The Journal of neuroscience : the official journal of the Society for Neuroscience *32*, 8855-8864.

Islam, S.M., Shinmyo, Y., Okafuji, T., Su, Y., Naser, I.B., Ahmed, G., Zhang, S., Chen, S., Ohta, K., Kiyonari, H.*, et al.* (2009). Draxin, a repulsive guidance protein for spinal cord and forebrain commissures. Science *323*, 388-393.

Itasaki, N., Bel-Vialar, S., and Krumlauf, R. (1999). 'Shocking' developments in chick embryology: electroporation and in ovo gene expression. Nature cell biology *1*, E203-207.

Jarjour, A.A., Bull, S.J., Almasieh, M., Rajasekharan, S., Baker, K.A., Mui, J., Antel, J.P., Di Polo, A., and Kennedy, T.E. (2008). Maintenance of axo-oligodendroglial paranodal junctions requires DCC and netrin-1. The Journal of neuroscience : the official journal of the Society for Neuroscience *28*, 11003-11014.

Jarjour, A.A., Manitt, C., Moore, S.W., Thompson, K.M., Yuh, S.J., and Kennedy, T.E. (2003). Netrin-1 is a chemorepellent for oligodendrocyte precursor cells in the embryonic spinal cord. The Journal of neuroscience : the official journal of the Society for Neuroscience *23*, 3735-3744.

Jin, J., Smith, F.D., Stark, C., Wells, C.D., Fawcett, J.P., Kulkarni, S., Metalnikov, P., O'Donnell, P., Taylor, P., Taylor, L.*, et al.* (2004). Proteomic, functional, and domain-based analysis of in vivo 14-3-3 binding proteins involved in cytoskeletal regulation and cellular organization. Curr Biol *14*, 1436-1450.

Johnson, C., Crowther, S., Stafford, M.J., Campbell, D.G., Toth, R., and MacKintosh, C. (2010). Bioinformatic and experimental survey of 14-3-3-binding sites. The Biochemical journal *427*, 69-78.

Justice, E.D., Barnum, S.J., and Kidd, T. (2017). The WAGR syndrome gene PRRG4 is a functional homologue of the commissureless axon guidance gene. PLoS genetics *13*, e1006865.

Kaplan, A., Morquette, B., Kroner, A., Leong, S., Madwar, C., Sanz, R., Banerjee, S.L., Antel, J., Bisson, N., David, S.*, et al.* (2017). Small-Molecule Stabilization of 14-3-3 Protein-Protein Interactions Stimulates Axon Regeneration. Neuron *93*, 1082-1093.e1085.

Keino-Masu, K., Masu, M., Hinck, L., Leonardo, E.D., Chan, S.S., Culotti, J.G., and Tessier-Lavigne, M. (1996). Deleted in Colorectal Cancer (DCC) encodes a netrin receptor. Cell *87*, 175-185.

Keleman, K., Rajagopalan, S., Cleppien, D., Teis, D., Paiha, K., Huber, L.A., Technau, G.M., and Dickson, B.J. (2002). Comm sorts robo to control axon guidance at the Drosophila midline. Cell *110*, 415-427.

Keleman, K., Ribeiro, C., and Dickson, B.J. (2005). Comm function in commissural axon guidance: cell-autonomous sorting of Robo in vivo. Nature neuroscience *8*, 156-163.

Kennedy, T.E., Serafini, T., de la Torre, J.R., and Tessier-Lavigne, M. (1994). Netrins are diffusible chemotropic factors for commissural axons in the embryonic spinal cord. Cell *78*, 425-435.

Kennedy, T.E., Wang, H., Marshall, W., and Tessier-Lavigne, M. (2006). Axon guidance by diffusible chemoattractants: a gradient of netrin protein in the developing spinal cord. The Journal of neuroscience : the official journal of the Society for Neuroscience *26*, 8866-8874.

Kent, C.B., Shimada, T., Ferraro, G.B., Ritter, B., Yam, P.T., McPherson, P.S., Charron, F., Kennedy, T.E., and Fournier, A.E. (2010). 14-3-3 proteins regulate protein kinase a activity to modulate growth cone turning responses. The Journal of neuroscience : the official journal of the Society for Neuroscience *30*, 14059-14067.

Kessaris, N., Fogarty, M., Iannarelli, P., Grist, M., Wegner, M., and Richardson, W.D. (2006). Competing waves of oligodendrocytes in the forebrain and postnatal elimination of an embryonic lineage. Nature neuroscience *9*, 173-179.

Kidd, T., Bland, K.S., and Goodman, C.S. (1999). Slit is the midline repellent for the robo receptor in Drosophila. Cell *96*, 785-794.

Kidd, T., Brose, K., Mitchell, K.J., Fetter, R.D., Tessier-Lavigne, M., Goodman, C.S., and Tear, G. (1998a). Roundabout controls axon crossing of the CNS midline and defines a novel subfamily of evolutionarily conserved guidance receptors. Cell *92*, 205-215.

Kidd, T., Russell, C., Goodman, C.S., and Tear, G. (1998b). Dosage-sensitive and complementary functions of roundabout and commissureless control axon crossing of the CNS midline. Neuron *20*, 25-33.

Kiernan, B.W., Gotz, B., Faissner, A., and ffrench-Constant, C. (1996). Tenascin-C inhibits oligodendrocyte precursor cell migration by both adhesion-dependent and adhesion-independent mechanisms. Molecular and cellular neurosciences *7*, 322-335.

Kim, S., Lee, S.H., and Park, D. (2001). Leucine zipper-mediated homodimerization of the p21-activated kinase-interacting factor, beta Pix. Implication for a role in cytoskeletal reorganization. The Journal of biological chemistry *276*, 10581-10584.

Ko, H.K., Guo, L.W., Su, B., Gao, L., and Gelman, I.H. (2014). Suppression of chemotaxis by SSeCKS via scaffolding of phosphoinositol phosphates and the recruitment of the Cdc42 GEF, Frabin, to the leading edge. PloS one *9*, e111534.

Koenning, M., Jackson, S., Hay, C.M., Faux, C., Kilpatrick, T.J., Willingham, M., and Emery, B. (2012). Myelin gene regulatory factor is required for maintenance of myelin and mature oligodendrocyte identity in the adult CNS. The Journal of neuroscience : the official journal of the Society for Neuroscience *32*, 12528-12542.

Kramer-Albers, E.M., and White, R. (2011). From axon-glial signalling to myelination: the integrating role of oligodendroglial Fyn kinase. Cell Mol Life Sci *68*, 2003-2012.

Kuwajima, T., Sitko, A.A., Bhansali, P., Jurgens, C., Guido, W., and Mason, C. (2013). ClearT: a detergent- and solvent-free clearing method for neuronal and non-neuronal tissue. Development *140*, 1364-1368.

Laemmli, U.K. (1970). Cleavage of structural proteins during the assembly of the head of bacteriophage T4. Nature *227*, 680-685.

Lai Wing Sun, K. (2015). Mechanisms underlying netrin-1 mediated chemoattraction. In Integrated Program in Neuroscience (McGill University), pp. 162.

Lappe-Siefke, C., Goebbels, S., Gravel, M., Nicksch, E., Lee, J., Braun, P.E., Griffiths, I.R., and Nave, K.A. (2003). Disruption of Cnp1 uncouples oligodendroglial functions in axonal support and myelination. Nature genetics *33*, 366-374.

Laurin, M., Fradet, N., Blangy, A., Hall, A., Vuori, K., and Côté, J.-F. (2008). The atypical Rac activator Dock180 (Dock1) regulates myoblast fusion in vivo. Proceedings of the National Academy of Sciences *105*, 15446-15451.

Lee, D.-H., Steinacker, P., Seubert, S., Turnescu, T., Melms, A., Manzel, A., Otto, M., and Linker, R.A. (2015). Role of glial 14-3-3 gamma protein in autoimmune demyelination. Journal of Neuroinflammation *12*, 187.

Lee, K.J., Mendelsohn, M., and Jessell, T.M. (1998). Neuronal patterning by BMPs: a requirement for GDF7 in the generation of a discrete class of commissural interneurons in the mouse spinal cord. Genes & development *12*, 3394-3407.

Leonetti, C., Macrez, R., Pruvost, M., Hommet, Y., Bronsard, J., Fournier, A., Perrigault, M., Machin, I., Vivien, D., Clemente, D.*, et al.* (2017). Tissue-type plasminogen activator exerts EGF-like chemokinetic effects on oligodendrocytes in white matter (re)myelination. Molecular neurodegeneration *12*, 20.

Levi-Montalcini, R. (1964). The Nerve Growth Factor. Annals of the New York Academy of Sciences *118*, 149-170.

Levi-Montalcini, R., and Hamburger, V. (1953). A diffusible agent of mouse sarcoma producing hyperplasia of sympathetic ganglia and hyperneurotization of viscera in the chick embryo. Journal of Experimental Zoology *123*, 233-287.

Levi-Montalcini, R., and Levi, G. (1942). Les consequences de la destruction d'un territoire d'innervation peripherique sur le developpement des centres nerveux correspondents dans embryon de poulet. Arch Biol Liege *53*, 537-545.

Li, X., Gao, X., Liu, G., Xiong, W., Wu, J., and Rao, Y. (2008). Netrin signal transduction and the guanine nucleotide exchange factor DOCK180 in attractive signaling. Nature neuroscience *11*, 28-35.

Li, X., Meriane, M., Triki, I., Shekarabi, M., Kennedy, T.E., Larose, L., and Lamarche-Vane, N. (2002a). The adaptor protein Nck-1 couples the netrin-1 receptor

DCC (deleted in colorectal cancer) to the activation of the small GTPase Rac1 through an atypical mechanism. The Journal of biological chemistry *277*, 37788-37797.

Li, X., Saint-Cyr-Proulx, E., Aktories, K., and Lamarche-Vane, N. (2002b). Rac1 and Cdc42 but not RhoA or Rho kinase activities are required for neurite outgrowth induced by the Netrin-1 receptor DCC (deleted in colorectal cancer) in N1E-115 neuroblastoma cells. The Journal of biological chemistry *277*, 15207-15214.

Li, Y., Wu, Y., and Zhou, Y. (2006). Modulation of inactivation properties of CaV2.2 channels by 14-3-3 proteins. Neuron *51*, 755-771.

Liu, D., Bienkowska, J., Petosa, C., Collier, R.J., Fu, H., and Liddington, R. (1995). Crystal structure of the zeta isoform of the 14-3-3 protein. Nature *376*, 191-194.

Liu, G., Li, W., Wang, L., Kar, A., Guan, K.L., Rao, Y., and Wu, J.Y. (2009). DSCAM functions as a netrin receptor in commissural axon pathfinding. Proceedings of the National Academy of Sciences of the United States of America *106*, 2951-2956.

Liu, X., Bates, R., Yin, D.M., Shen, C., Wang, F., Su, N., Kirov, S.A., Luo, Y., Wang, J.Z., Xiong, W.C.*, et al.* (2011). Specific regulation of NRG1 isoform expression by neuronal activity. The Journal of neuroscience : the official journal of the Society for Neuroscience *31*, 8491-8501.

Liu, Y., and Schneider, M.F. (2013). Opposing HDAC4 nuclear fluxes due to phosphorylation by beta-adrenergic activated protein kinase A or by activity or Epac activated CaMKII in skeletal muscle fibres. The Journal of physiology *591*, 3605-3623.

Liu, Y.C., Liu, Y., Elly, C., Yoshida, H., Lipkowitz, S., and Altman, A. (1997). Serine phosphorylation of Cbl induced by phorbol ester enhances its association with 14-3-3

proteins in T cells via a novel serine-rich 14-3-3-binding motif. The Journal of biological chemistry *272*, 9979-9985.

Liu, Z., Hu, X., Cai, J., Liu, B., Peng, X., Wegner, M., and Qiu, M. (2007). Induction of oligodendrocyte differentiation by Olig2 and Sox10: evidence for reciprocal interactions and dosage-dependent mechanisms. Developmental biology *302*, 683-693.

Logue, J.S., and Scott, J.D. (2010). Organizing signal transduction through A-kinase Anchoring Proteins (AKAPs). The FEBS journal *277*, 4370-4375.

Long, H., Sabatier, C., Ma, L., Plump, A., Yuan, W., Ornitz, D.M., Tamada, A., Murakami, F., Goodman, C.S., and Tessier-Lavigne, M. (2004). Conserved roles for Slit and Robo proteins in midline commissural axon guidance. Neuron *42*, 213-223.

Ly, A., Nikolaev, A., Suresh, G., Zheng, Y., Tessier-Lavigne, M., and Stein, E. (2008). DSCAM is a netrin receptor that collaborates with DCC in mediating turning responses to netrin-1. Cell *133*, 1241-1254.

Lyssiotis, C.A., Walker, J., Wu, C., Kondo, T., Schultz, P.G., and Wu, X. (2007). Inhibition of histone deacetylase activity induces developmental plasticity in oligodendrocyte precursor cells. Proceedings of the National Academy of Sciences of the United States of America *104*, 14982-14987.

Lyuksyutova, A.I., Lu, C.C., Milanesio, N., King, L.A., Guo, N., Wang, Y., Nathans, J., Tessier-Lavigne, M., and Zou, Y. (2003). Anterior-posterior guidance of commissural axons by Wnt-frizzled signaling. Science *302*, 1984-1988.

Ma, H., Zhu, J., Maronski, M., Kotzbauer, P.T., Lee, V.M., Dichter, M.A., and Diamond, S.L. (2002). Non-classical nuclear localization signal peptides for high efficiency lipofection of primary neurons and neuronal cell lines. Neuroscience *112*, 1-5.

Makinodan, M., Rosen, K.M., Ito, S., and Corfas, G. (2012). A critical period for social experience-dependent oligodendrocyte maturation and myelination. Science *337*, 1357-1360.

Mancini, M., Corradi, V., Petta, S., Barbieri, E., Manetti, F., Botta, M., and Santucci, M.A. (2011). A new nonpeptidic inhibitor of 14-3-3 induces apoptotic cell death in chronic myeloid leukemia sensitive or resistant to imatinib. The Journal of pharmacology and experimental therapeutics *336*, 596-604.

Manni, S., Mauban, J.H., Ward, C.W., and Bond, M. (2008). Phosphorylation of the cAMP-dependent protein kinase (PKA) regulatory subunit modulates PKA-AKAP interaction, substrate phosphorylation, and calcium signaling in cardiac cells. The Journal of biological chemistry *283*, 24145-24154.

Martin, H., Patel, Y., Jones, D., Howell, S., Robinson, K., and Aitken, A. (1993). Antibodies against the major brain isoforms of 14-3-3 protein: an antibody specific for the N-acetylated amino-terminus of a protein. FEBS letters *336*, 189.

Martin, H., Rostas, J., Patel, Y., and Aitken, A. (1994). Subcellular localisation of 14-3-3 isoforms in rat brain using specific antibodies. Journal of neurochemistry *63*, 2259-2265.

Martinez, E., and Tran, T.S. (2015). Vertebrate spinal commissural neurons: a model system for studying axon guidance beyond the midline. Wiley interdisciplinary reviews Developmental biology *4*, 283-297.

McCarthy, K.D., and de Vellis, J. (1978). Alpah-adrenergic receptor modulation of beta-adrenergic, adenosine and prostaglandin E1 increased adenosine 3':5'-cyclic

monophosphate levels in primary cultures of glia. Journal of cyclic nucleotide research *4*, 15-26.

McCarthy, K.D., and de Vellis, J. (1980). Preparation of separate astroglial and oligodendroglial cell cultures from rat cerebral tissue. The Journal of cell biology *85*, 890-902.

McKinsey, T.A., Zhang, C.L., and Olson, E.N. (2000). Activation of the myocyte enhancer factor-2 transcription factor by calcium/calmodulin-dependent protein kinase-stimulated binding of 14-3-3 to histone deacetylase 5. Proceedings of the National Academy of Sciences of the United States of America *97*, 14400-14405.

McPherson, R.A., Harding, A., Roy, S., Lane, A., and Hancock, J.F. (1999). Interactions of c-Raf-1 with phosphatidylserine and 14-3-3. Oncogene *18*, 3862-3869.

Megidish, T., Cooper, J., Zhang, L., Fu, H., and Hakomori, S. (1998). A novel sphingosine-dependent protein kinase (SDK1) specifically phosphorylates certain isoforms of 14-3-3 protein. The Journal of biological chemistry *273*, 21834-21845.

Megidish, T., White, T., Takio, K., Titani, K., Igarashi, Y., and Hakomori, S. (1995). The signal modulator protein 14-3-3 is a target of sphingosine- or N,N-dimethylsphingosine-dependent kinase in 3T3(A31) cells. Biochemical and biophysical research communications *216*, 739-747.

Merchan, P., Bribian, A., Sanchez-Camacho, C., Lezameta, M., Bovolenta, P., and de Castro, F. (2007). Sonic hedgehog promotes the migration and proliferation of optic nerve oligodendrocyte precursors. Molecular and cellular neurosciences *36*, 355-368.

Mi, S., Miller, R.H., Lee, X., Scott, M.L., Shulag-Morskaya, S., Shao, Z., Chang, J., Thill, G., Levesque, M., Zhang, M., *et al.* (2005). LINGO-1 negatively regulates myelination by oligodendrocytes. Nature neuroscience *8*, 745-751.

Michelsen, K., Yuan, H., and Schwappach, B. (2005). Hide and run. Arginine-based endoplasmic-reticulum-sorting motifs in the assembly of heteromultimeric membrane proteins. EMBO reports *6*, 717-722.

Mille, F., Llambi, F., Guix, C., Delloye-Bourgeois, C., Guenebeaud, C., Castro-Obregon, S., Bredesen, D.E., Thibert, C., and Mehlen, P. (2009). Interfering with multimerization of netrin-1 receptors triggers tumor cell death. Cell death and differentiation *16*, 1344-1351.

Milner, R., Anderson, H.J., Rippon, R.F., McKay, J.S., Franklin, R.J., Marchionni, M.A., Reynolds, R., and Ffrench-Constant, C. (1997). Contrasting effects of mitogenic growth factors on oligodendrocyte precursor cell migration. Glia *19*, 85-90.

Milner, R., Edwards, G., Streuli, C., and Ffrench-Constant, C. (1996). A role in migration for the alpha V beta 1 integrin expressed on oligodendrocyte precursors. The Journal of neuroscience : the official journal of the Society for Neuroscience *16*, 7240-7252.

Mire, E., Mezzera, C., Leyva-Diaz, E., Paternain, A.V., Squarzoni, P., Bluy, L., Castillo-Paterna, M., Lopez, M.J., Peregrin, S., Tessier-Lavigne, M., *et al.* (2012). Spontaneous activity regulates Robo1 transcription to mediate a switch in thalamocortical axon growth. Nature neuroscience *15*, 1134-1143.

Moore, B.W.P., V. J. (1967). Specific acidic proteins of the nervous system. In Physiological and Biochemical Aspects of Nervous Integration, F.D. Carlson, ed. (Englewood Cliffs: Prentice-Hall), pp. 343-359.

Moore, K.L., and Barr, M.L. (1954). Nuclear morphology, according to sex, in human tissues. Acta anatomica *21*, 197-208.

Moore, S.W., Correia, J.P., Lai Wing Sun, K., Pool, M., Fournier, A.E., and Kennedy, T.E. (2008). Rho inhibition recruits DCC to the neuronal plasma membrane and enhances axon chemoattraction to netrin 1. Development *135*, 2855-2864.

Moore, S.W., and Kennedy, T.E. (2001). Dissection and Culture of Embryonic Spinal Commissural Neurons. In Current Protocols in Neuroscience (John Wiley & Sons, Inc.).

Moore, S.W., and Kennedy, T.E. (2006). Protein kinase A regulates the sensitivity of spinal commissural axon turning to netrin-1 but does not switch between chemoattraction and chemorepulsion. The Journal of neuroscience : the official journal of the Society for Neuroscience *26*, 2419-2423.

Morales, D. (2017). A new model for netrin1 in commissural axon guidance. Journal of neuroscience research.

Morrison, D.K. (1995). Mechanisms regulating Raf-1 activity in signal transduction pathways. Molecular reproduction and development *42*, 507-514.

Müller, T., Brohmann, H., Pierani, A., Heppenstall, P.A., Lewin, G.R., Jessell, T.M., and Birchmeier, C. (2002). The Homeodomain Factor Lbx1 Distinguishes Two Major Programs of Neuronal Differentiation in the Dorsal Spinal Cord. Neuron *34*, 551-562.

Murray, J.A., and Blakemore, W.F. (1980). The relationship between internodal length and fibre diameter in the spinal cord of the cat. J Neurol Sci *45*, 29-41.

Muslin, A.J., Tanner, J.W., Allen, P.M., and Shaw, A.S. (1996). Interaction of 14-3-3 with signaling proteins is mediated by the recognition of phosphoserine. Cell *84*, 889-897.

Nagata, K.i., Puls, A., Futter, C., Aspenstrom, P., Schaefer, E., Nakata, T., Hirokawa, N., and Hall, A. (1998). The MAP kinase kinase kinase MLK2 co-localizes with activated JNK along microtubules and associates with kinesin superfamily motor KIF3. The EMBO journal *17*, 149-158.

Narayanan, S.P., Flores, A.I., Wang, F., and Macklin, W.B. (2009). Akt signals through the mammalian target of rapamycin pathway to regulate CNS myelination. The Journal of neuroscience : the official journal of the Society for Neuroscience *29*, 6860-6870.

Navarro-Lerida, I., Pellinen, T., Sanchez, S.A., Guadamillas, M.C., Wang, Y., Mirtti, T., Calvo, E., and Del Pozo, M.A. (2015). Rac1 nucleocytoplasmic shuttling drives nuclear shape changes and tumor invasion. Developmental cell *32*, 318-334.

Nave, K.-A., and Werner, H.B. (2014). Myelination of the Nervous System: Mechanisms and Functions. Annual Review of Cell and Developmental Biology *30*, 503-533.

Nelson, A.D., and Jenkins, P.M. (2017). Axonal Membranes and Their Domains: Assembly and Function of the Axon Initial Segment and Node of Ranvier. Frontiers in cellular neuroscience *11*, 136.

Neve, R.L., Howe, J.R., Hong, S., and Kalb, R.G. (1997). Introduction of the glutamate receptor subunit 1 into motor neurons in vitro and in vivo using a recombinant herpes simplex virus. Neuroscience *79*, 435-447.

Nishino, T.G., Miyazaki, M., Hoshino, H., Miwa, Y., Horinouchi, S., and Yoshida, M. (2008). 14-3-3 regulates the nuclear import of class IIa histone deacetylases. Biochemical and biophysical research communications *377*, 852-856.

Noack, M., Leyk, J., and Richter-Landsberg, C. (2014). HDAC6 inhibition results in tau acetylation and modulates tau phosphorylation and degradation in oligodendrocytes. Glia *62*, 535-547.

Nobes, C.D., and Hall, A. (1995). Rho, rac, and cdc42 GTPases regulate the assembly of multimolecular focal complexes associated with actin stress fibers, lamellipodia, and filopodia. Cell *81*, 53-62.

Noble, M., Murray, K., Stroobant, P., Waterfield, M.D., and Riddle, P. (1988). Platelet-derived growth factor promotes division and motility and inhibits premature differentiation of the oligodendrocyte/type-2 astrocyte progenitor cell. Nature *333*, 560-562.

Nodari, A., Zambroni, D., Quattrini, A., Court, F.A., D'Urso, A., Recchia, A., Tybulewicz, V.L.J., Wrabetz, L., and Feltri, M.L. (2007). β1 integrin activates Rac1 in Schwann cells to generate radial lamellae during axonal sorting and myelination. The Journal of cell biology *177*, 1063-1075.

Norris, A.D., Sundararajan, L., Morgan, D.E., Roberts, Z.J., and Lundquist, E.A. (2014). The UNC-6/Netrin receptors UNC-40/DCC and UNC-5 inhibit growth cone filopodial protrusion via UNC-73/Trio, Rac-like GTPases and UNC-33/CRMP. Development (Cambridge, England) *141*, 4395-4405.

Norrmen, C., and Suter, U. (2013). Akt/mTOR signalling in myelination. Biochemical Society transactions *41*, 944-950.

O'Brien, J.A., Holt, M., Whiteside, G., Lummis, S.C.R., and Hastings, M.H. (2001). Modifications to the hand-held Gene Gun: improvements for in vitro Biolistic transfection of organotypic neuronal tissue. Journal of Neuroscience Methods *112*, 57-64.

O'Toole, T.E., Bialkowska, K., Li, X., and Fox, J.E. (2011). Tiam1 is recruited to beta1-integrin complexes by 14-3-3zeta where it mediates integrin-induced Rac1 activation and motility. Journal of cellular physiology *226*, 2965-2978.

Okada, A., Charron, F., Morin, S., Shin, D.S., Wong, K., Fabre, P.J., Tessier-Lavigne, M., and McConnell, S.K. (2006). Boc is a receptor for sonic hedgehog in the guidance of commissural axons. Nature *444*, 369-373.

Omelchenko, T., Rabadan, M.A., Hernández-Martínez, R., Grego-Bessa, J., Anderson, K.V., and Hall, A. (2014). β-Pix directs collective migration of anterior visceral endoderm cells in the early mouse embryo. Genes & development *28*, 2764-2777.

Ortega, M.C., Bribian, A., Peregrin, S., Gil, M.T., Marin, O., and de Castro, F. (2012). Neuregulin-1/ErbB4 signaling controls the migration of oligodendrocyte precursor cells during development. Experimental neurology *235*, 610-620.

Pacheco, A., and Gallo, G. (2016). Actin filament-microtubule interactions in axon initiation and branching. Brain Research Bulletin *126*, 300-310.

Palmesino, E., Haddick, P.C., Tessier-Lavigne, M., and Kania, A. (2012). Genetic analysis of DSCAM's role as a Netrin-1 receptor in vertebrates. The Journal of neuroscience : the official journal of the Society for Neuroscience *32*, 411-416.

Parra, L.M., and Zou, Y. (2010). Sonic hedgehog induces response of commissural axons to Semaphorin repulsion during midline crossing. Nature neuroscience *13*, 29-35.

Payne, H.R., Hemperly, J.J., and Lemmon, V. (1996). N-cadherin expression and function in cultured oligodendrocytes. Brain research Developmental brain research *97*, 9-15.

Pérez-Cerdá, F., Sánchez-Gómez, M.V., and Matute, C. (2015). Pío del Río Hortega and the discovery of the oligodendrocytes. Frontiers in Neuroanatomy *9*.

Peschl, P., Bradl, M., Hoftberger, R., Berger, T., and Reindl, M. (2017). Myelin Oligodendrocyte Glycoprotein: Deciphering a Target in Inflammatory Demyelinating Diseases. Frontiers in immunology *8*, 529.

Pfeiffer, S.E., Warrington, A.E., and Bansal, R. (1993). The oligodendrocyte and its many cellular processes. Trends in cell biology *3*, 191-197.

Phan, K.D., Croteau, L.P., Kam, J.W., Kania, A., Cloutier, J.F., and Butler, S.J. (2011). Neogenin may functionally substitute for Dcc in chicken. PloS one *6*, e22072.

Phan, K.D., Hazen, V.M., Frendo, M., Jia, Z., and Butler, S.J. (2010). The bone morphogenetic protein roof plate chemorepellent regulates the rate of commissural axonal growth. The Journal of neuroscience : the official journal of the Society for Neuroscience *30*, 15430-15440.

Placzek, M., Tessier-Lavigne, M., Jessell, T., and Dodd, J. (1990a). Orientation of commissural axons in vitro in response to a floor plate-derived chemoattractant. Development *110*, 19-30.

Placzek, M., Tessier-Lavigne, M., Yamada, T., Dodd, J., and Jessell, T.M. (1990b). Guidance of developing axons by diffusible chemoattractants. Cold Spring Harbor symposia on quantitative biology *55*, 279-289.

Prestoz, L., Chatzopoulou, E., Lemkine, G., Spassky, N., Lebras, B., Kagawa, T., Ikenaka, K., Zalc, B., and Thomas, J.L. (2004). Control of axonophilic migration of oligodendrocyte precursor cells by Eph-ephrin interaction. Neuron glia biology *1*, 73-83.

Pulina, M.V., Rizzuto, R., Brini, M., and Carafoli, E. (2006). Inhibitory interaction of the plasma membrane Na+/Ca2+ exchangers with the 14-3-3 proteins. The Journal of biological chemistry *281*, 19645-19654.

Qian, Y., Shirasawa, S., Chen, C.-L., Cheng, L., and Ma, Q. (2002). Proper development of relay somatic sensory neurons and D2/D4 interneurons requires homeobox genes Rnx/Tlx-3 and Tlx-1. Genes & development *16*, 1220-1233.

Qiao, H., Foote, M., Graham, K., Wu, Y., and Zhou, Y. (2014). 14-3-3 proteins are required for hippocampal long-term potentiation and associative learning and memory. The Journal of neuroscience : the official journal of the Society for Neuroscience *34*, 4801-4808.

Qiu, W., Zhuang, S., von Lintig, F.C., Boss, G.R., and Pilz, R.B. (2000). Cell type-specific regulation of B-Raf kinase by cAMP and 14-3-3 proteins. The Journal of biological chemistry *275*, 31921-31929.

Quinn, C.C., Pfeil, D.S., and Wadsworth, W.G. (2008). CED-10/Rac1 mediates axon guidance by regulating the asymmetric distribution of MIG-10/lamellipodin. Current biology : CB *18*, 808-813.

Rajasekharan, S., Baker, K.A., Horn, K.E., Jarjour, A.A., Antel, J.P., and Kennedy, T.E. (2009). Netrin 1 and Dcc regulate oligodendrocyte process branching and membrane extension via Fyn and RhoA. Development *136*, 415-426.

Rama, N., Goldschneider, D., Corset, V., Lambert, J., Pays, L., and Mehlen, P. (2012). Amyloid precursor protein regulates netrin-1-mediated commissural axon outgrowth. The Journal of biological chemistry *287*, 30014-30023.

Ramshaw, H., Xu, X., Jaehne, E.J., McCarthy, P., Greenberg, Z., Saleh, E., McClure, B., Woodcock, J., Kabbara, S., Wiszniak, S.*, et al.* (2013). Locomotor hyperactivity in 14-3-3[zeta] KO mice is associated with dopamine transporter dysfunction. Translational psychiatry *3*, e327.

Rappaz, B., Lai Wing Sun, K., Correia, J.P., Wiseman, P.W., and Kennedy, T.E. (2016). FLIM FRET Visualization of Cdc42 Activation by Netrin-1 in Embryonic Spinal Commissural Neuron Growth Cones. PloS one *11*, e0159405.

Readhead, C., Popko, B., Takahashi, N., Shine, H.D., Saavedra, R.A., Sidman, R.L., and Hood, L. (1987). Expression of a myelin basic protein gene in transgenic shiverer mice: correction of the dysmyelinating phenotype. Cell *48*, 703-712.

Relucio, J., Tzvetanova, I.D., Ao, W., Lindquist, S., and Colognato, H. (2009). Laminin alters fyn regulatory mechanisms and promotes oligodendrocyte development. The Journal of neuroscience : the official journal of the Society for Neuroscience *29*, 11794-11806.

Renier, N., Wu, Z., Simon, David J., Yang, J., Ariel, P., and Tessier-Lavigne, M. (2014). iDISCO: A Simple, Rapid Method to Immunolabel Large Tissue Samples for Volume Imaging. Cell *159*, 896-910.

Richardson, W.D., Smith, H.K., Sun, T., Pringle, N.P., Hall, A., and Woodruff, R. (2000). Oligodendrocyte lineage and the motor neuron connection. Glia *29*, 136-142.

Ridley, A.J. (2006). Rho GTPases and actin dynamics in membrane protrusions and vesicle trafficking. Trends in cell biology *16*, 522-529.

Ridley, A.J., and Hall, A. (1992). The small GTP-binding protein rho regulates the assembly of focal adhesions and actin stress fibers in response to growth factors. Cell *70*, 389-399.

Ridley, A.J., Paterson, H.F., Johnston, C.L., Diekmann, D., and Hall, A. (1992). The small GTP-binding protein rac regulates growth factor-induced membrane ruffling. Cell *70*, 401-410.

Riou, P., Kjaer, S., Garg, R., Purkiss, A., George, R., Cain, R.J., Bineva, G., Reymond, N., McColl, B., Thompson, A.J.*, et al.* (2013). 14-3-3 proteins interact with a hybrid prenyl-phosphorylation motif to inhibit G proteins. Cell *153*, 640-653.

Roberts, A., Dale, N., Ottersen, O.P., and Storm-Mathisen, J. (1988). Development and characterization of commissural interneurones in the spinal cord of Xenopus laevis embryos revealed by antibodies to glycine. Development *103*, 447-461.

Rohatgi, R., Ho, H.Y., and Kirschner, M.W. (2000). Mechanism of N-WASP activation by CDC42 and phosphatidylinositol 4, 5-bisphosphate. The Journal of cell biology *150*, 1299-1310.

Rossman, K.L., Der, C.J., and Sondek, J. (2005). GEF means go: turning on RHO GTPases with guanine nucleotide-exchange factors. Nature reviews Molecular cell biology *6*, 167-180.

Roy, S., McPherson, R.A., Apolloni, A., Yan, J., Lane, A., Clyde-Smith, J., and Hancock, J.F. (1998). 14-3-3 facilitates Ras-dependent Raf-1 activation in vitro and in vivo. Molecular and cellular biology *18*, 3947-3955.

Royal, I., Lamarche-Vane, N., Lamorte, L., Kaibuchi, K., and Park, M. (2000). Activation of cdc42, rac, PAK, and rho-kinase in response to hepatocyte growth factor differentially regulates epithelial cell colony spreading and dissociation. Molecular biology of the cell *11*, 1709-1725.

Ruiz de Almodovar, C., Fabre, P.J., Knevels, E., Coulon, C., Segura, I., Haddick, P.C., Aerts, L., Delattin, N., Strasser, G., Oh, W.J.*, et al.* (2011). VEGF mediates commissural axon chemoattraction through its receptor Flk1. Neuron *70*, 966-978.

Saia-Cereda, V.M., Cassoli, J.S., Schmitt, A., Falkai, P., Nascimento, J.M., and Martins-de-Souza, D. (2015). Proteomics of the corpus callosum unravel pivotal players in the dysfunction of cell signaling, structure, and myelination in schizophrenia brains. European Archives of Psychiatry and Clinical Neuroscience *265*, 601-612.

Sampaio-Baptista, C., Khrapitchev, A.A., Foxley, S., Schlagheck, T., Scholz, J., Jbabdi, S., DeLuca, G.C., Miller, K.L., Taylor, A., Thomas, N.*, et al.* (2013). Motor skill learning induces changes in white matter microstructure and myelination. The Journal of neuroscience : the official journal of the Society for Neuroscience *33*, 19499-19503.

Santra, M., Zhang, Z.G., Yang, J., Santra, S., Santra, S., Chopp, M., and Morris, D.C. (2014). Thymosin beta4 up-regulation of microRNA-146a promotes oligodendrocyte differentiation and suppression of the Toll-like proinflammatory pathway. The Journal of biological chemistry *289*, 19508-19518.

Schnitzer, J., and Schachner, M. (1982). Cell type specificity of a neural cell surface antigen recognized by the monoclonal antibody A2B5. Cell and tissue research *224*, 625-636.

Serafini, T., Kennedy, T.E., Galko, M.J., Mirzayan, C., Jessell, T.M., and Tessier-Lavigne, M. (1994). The netrins define a family of axon outgrowth-promoting proteins homologous to C. elegans UNC-6. Cell *78*, 409-424.

Shekarabi, M., and Kennedy, T.E. (2002). The netrin-1 receptor DCC promotes filopodia formation and cell spreading by activating Cdc42 and Rac1. Molecular and cellular neurosciences *19*, 1-17.

Shekarabi, M., Moore, S.W., Tritsch, N.X., Morris, S.J., Bouchard, J.F., and Kennedy, T.E. (2005). Deleted in colorectal cancer binding netrin-1 mediates cell substrate adhesion and recruits Cdc42, Rac1, Pak1, and N-WASP into an intracellular signaling complex that promotes growth cone expansion. The Journal of neuroscience : the official journal of the Society for Neuroscience *25*, 3132-3141.

Shen, S., Li, J., and Casaccia-Bonnefil, P. (2005). Histone modifications affect timing of oligodendrocyte progenitor differentiation in the developing rat brain. The Journal of cell biology *169*, 577-589.

Sherman, D.L., and Brophy, P.J. (2005). Mechanisms of axon ensheathment and myelin growth. Nature reviews Neuroscience *6*, 683-690.

Shimada, T., Fournier, A.E., and Yamagata, K. (2013). Neuroprotective function of 14-3-3 proteins in neurodegeneration. BioMed research international *2013*, 564534.

Shirasaki, R., Katsumata, R., and Murakami, F. (1998). Change in chemoattractant responsiveness of developing axons at an intermediate target. Science *279*, 105-107.

Shirasaki, R., Tamada, A., Katsumata, R., and Murakami, F. (1995). Guidance of cerebellofugal axons in the rat embryo: directed growth toward the floor plate and subsequent elongation along the longitudinal axis. Neuron *14*, 961-972.

Simon, K., Hennen, S., Merten, N., Blattermann, S., Gillard, M., Kostenis, E., and Gomeza, J. (2016). The Orphan G Protein-coupled Receptor GPR17 Negatively Regulates Oligodendrocyte Differentiation via Galphai/o and Its Downstream Effector Molecules. The Journal of biological chemistry *291*, 705-718.

Simons, M., and Lyons, D.A. (2013). Axonal selection and myelin sheath generation in the central nervous system. Current opinion in cell biology *25*, 512-519.

Simons, M., and Nave, K.A. (2015). Oligodendrocytes: Myelination and Axonal Support. Cold Spring Harbor perspectives in biology *8*, a020479.

Sloan, T.F.W., Qasaimeh, M.A., Juncker, D., Yam, P.T., and Charron, F. (2015). Integration of Shallow Gradients of Shh and Netrin-1 Guides Commissural Axons. PLOS Biology *13*, e1002119.

Snaidero, N., Mobius, W., Czopka, T., Hekking, L.H., Mathisen, C., Verkleij, D., Goebbels, S., Edgar, J., Merkler, D., Lyons, D.A.*, et al.* (2014). Myelin membrane wrapping of CNS axons by PI(3,4,5)P3-dependent polarized growth at the inner tongue. Cell *156*, 277-290.

Snaidero, N., and Simons, M. (2014). Myelination at a glance. Journal of cell science *127*, 2999-3004.

Sommer, I., and Schachner, M. (1981). Monoclonal antibodies (O1 to O4) to oligodendrocyte cell surfaces: an immunocytological study in the central nervous system. Dev Biol *83*, 311-327.

Spassky, N., de Castro, F., Le Bras, B., Heydon, K., Queraud-LeSaux, F., Bloch-Gallego, E., Chedotal, A., Zalc, B., and Thomas, J.L. (2002). Directional guidance of

oligodendroglial migration by class 3 semaphorins and netrin-1. The Journal of neuroscience : the official journal of the Society for Neuroscience *22*, 5992-6004.

Sperber, B.R., Boyle-Walsh, E.A., Engleka, M.J., Gadue, P., Peterson, A.C., Stein, P.L., Scherer, S.S., and McMorris, F.A. (2001). A unique role for Fyn in CNS myelination. The Journal of neuroscience : the official journal of the Society for Neuroscience *21*, 2039-2047.

Sperry, R.W. (1943). Visuomotor coordination in the newt (*Triturus viridescens*) after regeneration of the optic nerve. Journal of Comparative Neurology *79*, 33-55.

Sperry, R.W. (1963). Chemoaffinity in the Orderly Growth of Nerve Fiber Patterns and Connections. Proceedings of the National Academy of Sciences of the United States of America *50*, 703-710.

Sperry, R.W., and Miner, N. (1949). Formation within sensory nucleus V of synaptic associations mediating cutaneous localization. The Journal of comparative neurology *90*, 403-423.

Stein, E., and Tessier-Lavigne, M. (2001). Hierarchical organization of guidance receptors: silencing of netrin attraction by slit through a Robo/DCC receptor complex. Science *291*, 1928-1938.

Stoeckli, E. (2017). Where does axon guidance lead us? F1000Research *6*, 78.

Sun, S., Wong, E.W., Li, M.W., Lee, W.M., and Cheng, C.Y. (2009). 14-3-3 and its binding partners are regulators of protein-protein interactions during spermatogenesis. The Journal of endocrinology *202*, 327-336.

Syed, Y.A., Abdulla, S.A., and Kotter, M.R. (2017). Studying the Effects of Semaphorins on Oligodendrocyte Lineage Cells. Methods in molecular biology (Clifton, NJ) *1493*, 363-378.

Taoufiq, Z., Eguchi, K., and Takahashi, T. (2013). Rho-kinase accelerates synaptic vesicle endocytosis by linking cyclic GMP-dependent protein kinase activity to phosphatidylinositol-4,5-bisphosphate synthesis. The Journal of neuroscience : the official journal of the Society for Neuroscience *33*, 12099-12104.

Taveggia, C., Zanazzi, G., Petrylak, A., Yano, H., Rosenbluth, J., Einheber, S., Xu, X., Esper, R.M., Loeb, J.A., Shrager, P*., et al.* (2005). Neuregulin-1 type III determines the ensheathment fate of axons. Neuron *47*, 681-694.

Tep, C., Kim, M.L., Opincariu, L.I., Limpert, A.S., Chan, J.R., Appel, B., Carter, B.D., and Yoon, S.O. (2012). Brain-derived neurotrophic factor (BDNF) induces polarized signaling of small GTPase (Rac1) protein at the onset of Schwann cell myelination through partitioning-defective 3 (Par3) protein. The Journal of biological chemistry *287*, 1600-1608.

Tessier-Lavigne, M., Placzek, M., Lumsden, A.G., Dodd, J., and Jessell, T.M. (1988). Chemotropic guidance of developing axons in the mammalian central nervous system. Nature *336*, 775-778.

Theurkauf, W.E., and Vallee, R.B. (1982). Molecular characterization of the cAMP-dependent protein kinase bound to microtubule-associated protein 2. The Journal of biological chemistry *257*, 3284-3290.

Thiry, L., Lemieux, M., O, D.L., and Bretzner, F. (2016). Role of DSCAM in the development of the spinal locomotor and sensorimotor circuits. Journal of neurophysiology *115*, 1338-1354.

Tinti, M., Madeira, F., Murugesan, G., Hoxhaj, G., Toth, R., and Mackintosh, C. (2014). ANIA: ANnotation and Integrated Analysis of the 14-3-3 interactome. Database : the journal of biological databases and curation *2014*, bat085.

Tzivion, G., Dobson, M., and Ramakrishnan, G. (2011). FoxO transcription factors; Regulation by AKT and 14-3-3 proteins. Biochimica et biophysica acta *1813*, 1938-1945.

Uesaka, N., Hayano, Y., Yamada, A., and Yamamoto, N. (2007). Interplay between laminar specificity and activity-dependent mechanisms of thalamocortical axon branching. The Journal of neuroscience : the official journal of the Society for Neuroscience *27*, 5215-5223.

Umahara, T., Uchihara, T., Tsuchiya, K., Nakamura, A., and Iwamoto, T. (2007). Intranuclear localization and isoform-dependent translocation of 14-3-3 proteins in human brain with infarction. Journal of the Neurological Sciences *260*, 159-166.

Vallstedt, A., Klos, J.M., and Ericson, J. (2005). Multiple dorsoventral origins of oligodendrocyte generation in the spinal cord and hindbrain. Neuron *45*, 55-67.

van Rheenen, J., Song, X., van Roosmalen, W., Cammer, M., Chen, X., Desmarais, V., Yip, S.C., Backer, J.M., Eddy, R.J., and Condeelis, J.S. (2007). EGF-induced PIP2 hydrolysis releases and activates cofilin locally in carcinoma cells. The Journal of cell biology *179*, 1247-1259.

Varadarajan, S.G., and Butler, S.J. (2017). Netrin1 establishes multiple boundaries for axon growth in the developing spinal cord. Developmental biology.

Varadarajan, S.G., Kong, J.H., Phan, K.D., Kao, T.J., Panaitof, S.C., Cardin, J., Eltzschig, H., Kania, A., Novitch, B.G., and Butler, S.J. (2017). Netrin1 Produced by Neural Progenitors, Not Floor Plate Cells, Is Required for Axon Guidance in the Spinal Cord. Neuron *94*, 790-799.e793.

Vokes, M.S., and Carpenter, A.E. (2008). Using CellProfiler for automatic identification and measurement of biological objects in images. Current protocols in molecular biology *Chapter 14*, Unit 14.17.

Vulliemoz, S., Raineteau, O., and Jabaudon, D. (2005). Reaching beyond the midline: why are human brains cross wired? Lancet neurology *4*, 87-99.

Waggener, C.T., Dupree, J.L., Elgersma, Y., and Fuss, B. (2013). CaMKIIbeta regulates oligodendrocyte maturation and CNS myelination. The Journal of neuroscience : the official journal of the Society for Neuroscience *33*, 10453-10458.

Wake, H., Lee, P.R., and Fields, R.D. (2011). Control of local protein synthesis and initial events in myelination by action potentials. Science *333*, 1647-1651.

Wang, B., Yang, H., Liu, Y.C., Jelinek, T., Zhang, L., Ruoslahti, E., and Fu, H. (1999). Isolation of high-affinity peptide antagonists of 14-3-3 proteins by phage display. Biochemistry *38*, 12499-12504.

Wang, C., Rougon, G., and Kiss, J.Z. (1994). Requirement of polysialic acid for the migration of the O-2A glial progenitor cell from neurohypophyseal explants. The Journal of neuroscience : the official journal of the Society for Neuroscience *14*, 4446-4457.

Wang, P.S., Wang, J., Xiao, Z.C., and Pallen, C.J. (2009). Protein-tyrosine phosphatase alpha acts as an upstream regulator of Fyn signaling to promote

oligodendrocyte differentiation and myelination. The Journal of biological chemistry *284*, 33692-33702.

Wang, S., Sdrulla, A.D., diSibio, G., Bush, G., Nofziger, D., Hicks, C., Weinmaster, G., and Barres, B.A. (1998). Notch receptor activation inhibits oligodendrocyte differentiation. Neuron *21*, 63-75.

Watari-Goshima, N., Ogura, K., Wolf, F.W., Goshima, Y., and Garriga, G. (2007). C. elegans VAB-8 and UNC-73 regulate the SAX-3 receptor to direct cell and growth-cone migrations. Nature neuroscience *10*, 169-176.

Watkins, T.A., Emery, B., Mulinyawe, S., and Barres, B.A. (2008). Distinct stages of myelination regulated by gamma-secretase and astrocytes in a rapidly myelinating CNS coculture system. Neuron *60*, 555-569.

Wei, J.Y., Lu, Q.N., Li, W.M., and He, W. (2015). Intracellular translocation of histone deacetylase 5 regulates neuronal cell apoptosis. Brain research *1604*, 15-24.

Weng, C., Ding, M., Fan, S., Cao, Q., and Lu, Z. (2017). Transcription factor 7 like 2 promotes oligodendrocyte differentiation and remyelination. Molecular medicine reports *16*, 1864-1870.

Westphal, R.S., Soderling, S.H., Alto, N.M., Langeberg, L.K., and Scott, J.D. (2000). Scar/WAVE-1, a Wiskott–Aldrich syndrome protein, assembles an actin-associated multi-kinase scaffold. The EMBO journal *19*, 4589-4600.

Wilson, R.S., Swatek, K.N., and Thelen, J.J. (2016). Regulation of the Regulators: Post-Translational Modifications, Subcellular, and Spatiotemporal Distribution of Plant 14-3-3 Proteins. Frontiers in plant science *7*, 611.

Winkler, D.G., Cutler, R.E., Jr., Drugan, J.K., Campbell, S., Morrison, D.K., and Cooper, J.A. (1998). Identification of residues in the cysteine-rich domain of Raf-1 that control Ras binding and Raf-1 activity. The Journal of biological chemistry *273*, 21578-21584.

Woodcock, J.M., Murphy, J., Stomski, F.C., Berndt, M.C., and Lopez, A.F. (2003). The dimeric versus monomeric status of 14-3-3zeta is controlled by phosphorylation of Ser58 at the dimer interface. The Journal of biological chemistry *278*, 36323-36327.

Woodcock, S.A., Jones, R.C., Edmondson, R.D., and Malliri, A. (2009). A modified tandem affinity purification technique identifies that 14-3-3 proteins interact with Tiam1, an interaction which controls Tiam1 stability. Journal of proteome research *8*, 5629-5641.

Wu, C.Y., Lin, M.W., Wu, D.C., Huang, Y.B., Huang, H.T., and Chen, C.L. (2014). The role of phosphoinositide-regulated actin reorganization in chemotaxis and cell migration. British journal of pharmacology *171*, 5541-5554.

Xiao, B., Smerdon, S.J., Jones, D.H., Dodson, G.G., Soneji, Y., Aitken, A., and Gamblin, S.J. (1995). Structure of a 14-3-3 protein and implications for coordination of multiple signalling pathways. Nature *376*, 188-191.

Xiao, L., Hu, C., Yang, W., Guo, D., Li, C., Shen, W., Liu, X., Aijun, H., Dan, W., and He, C. (2013). NMDA receptor couples Rac1-GEF Tiam1 to direct oligodendrocyte precursor cell migration. Glia *61*, 2078-2099.

Xu, K., Wu, Z., Renier, N., Antipenko, A., Tzvetkova-Robev, D., Xu, Y., Minchenko, M., Nardi-Dei, V., Rajashankar, K.R., Himanen, J.*, et al.* (2014). Structures of Netrin-1 Bound to two Receptors Provide Insight into its Axon Guidance Mechanism. Science (New York, NY) *344*, 1275-1279.

Xu, X., Jaehne, E.J., Greenberg, Z., McCarthy, P., Saleh, E., Parish, C.L., Camera, D., Heng, J., Haas, M., Baune, B.T.*, et al.* (2015). 14-3-3ζ deficient mice in the BALB/c background display behavioural and anatomical defects associated with neurodevelopmental disorders. *5*, 12434.

Yaffe, M.B., Rittinger, K., Volinia, S., Caron, P.R., Aitken, A., Leffers, H., Gamblin, S.J., Smerdon, S.J., and Cantley, L.C. (1997). The structural basis for 14-3-3:phosphopeptide binding specificity. Cell *91*, 961-971.

Yam, P.T., Kent, C.B., Morin, S., Farmer, W.T., Alchini, R., Lepelletier, L., Colman, D.R., Tessier-Lavigne, M., Fournier, A.E., and Charron, F. (2012). 14-3-3 proteins regulate a cell-intrinsic switch from sonic hedgehog-mediated commissural axon attraction to repulsion after midline crossing. Neuron *76*, 735-749.

Yam, P.T., Langlois, S.D., Morin, S., and Charron, F. (2009). Sonic hedgehog guides axons through a noncanonical, Src-family-kinase-dependent signaling pathway. Neuron *62*, 349-362.

Yang, L., Garbe, D.S., and Bashaw, G.J. (2009). A frazzled/DCC-dependent transcriptional switch regulates midline axon guidance. Science *324*, 944-947.

Yang, T., and Terman, J.R. (2012). 14-3-3epsilon couples protein kinase A to semaphorin signaling and silences plexin RasGAP-mediated axonal repulsion. Neuron *74*, 108-121.

Yang, X., Lee, W.H., Sobott, F., Papagrigoriou, E., Robinson, C.V., Grossmann, J.G., Sundstrom, M., Doyle, D.A., and Elkins, J.M. (2006). Structural basis for protein-protein interactions in the 14-3-3 protein family. Proceedings of the National Academy of Sciences of the United States of America *103*, 17237-17242.

Ye, F., Chen, Y., Hoang, T., Montgomery, R.L., Zhao, X.H., Bu, H., Hu, T., Taketo, M.M., van Es, J.H., Clevers, H., *et al.* (2009). HDAC1 and HDAC2 regulate oligodendrocyte differentiation by disrupting the beta-catenin-TCF interaction. Nature neuroscience *12*, 829-838.

Young, K.M., Psachoulia, K., Tripathi, R.B., Dunn, S.J., Cossell, L., Attwell, D., Tohyama, K., and Richardson, W.D. (2013). Oligodendrocyte dynamics in the healthy adult CNS: evidence for myelin remodeling. Neuron *77*, 873-885.

Yu, Y., Chen, Y., Kim, B., Wang, H., Zhao, C., He, X., Liu, L., Liu, W., Wu, L.M., Mao, M., *et al.* (2013). Olig2 targets chromatin remodelers to enhancers to initiate oligodendrocyte differentiation. Cell *152*, 248-261.

Zatorre, R.J., Fields, R.D., and Johansen-Berg, H. (2012). Plasticity in gray and white: neuroimaging changes in brain structure during learning. Nature neuroscience *15*, 528-536.

Zeger, M., Popken, G., Zhang, J., Xuan, S., Lu, Q.R., Schwab, M.H., Nave, K.A., Rowitch, D., D'Ercole, A.J., and Ye, P. (2007). Insulin-like growth factor type 1 receptor signaling in the cells of oligodendrocyte lineage is required for normal in vivo oligodendrocyte development and myelination. Glia *55*, 400-411.

Zenke, F.T., Krendel, M., DerMardirossian, C., King, C.C., Bohl, B.P., and Bokoch, G.M. (2004). p21-activated kinase 1 phosphorylates and regulates 14-3-3 binding to GEF-H1, a microtubule-localized Rho exchange factor. The Journal of biological chemistry *279*, 18392-18400.

Zhang, H., Vutskits, L., Calaora, V., Durbec, P., and Kiss, J.Z. (2004). A role for the polysialic acid-neural cell adhesion molecule in PDGF-induced chemotaxis of oligodendrocyte precursor cells. Journal of cell science *117*, 93-103.

Zhang, H., Vutskits, L., Pepper, M.S., and Kiss, J.Z. (2003). VEGF is a chemoattractant for FGF-2-stimulated neural progenitors. The Journal of cell biology *163*, 1375-1384.

Zhao, X., He, X., Han, X., Yu, Y., Ye, F., Chen, Y., Hoang, T., Xu, X., Mi, Q.S., Xin, M.*, et al.* (2010). MicroRNA-mediated control of oligodendrocyte differentiation. Neuron *65*, 612-626.

Zhou, Z., Wan, L., Wang, C., and Zhou, K. (2015). Integration of Shh and Wnt Signaling Pathways Regulating Hematopoiesis. DNA and cell biology *34*, 710-716.

Zhu, G., Fan, Z., Ding, M., Zhang, H., Mu, L., Ding, Y., Zhang, Y., Jia, B., Chen, L., Chang, Z.*, et al.* (2015). An EGFR/PI3K/AKT axis promotes accumulation of the Rac1-GEF Tiam1 that is critical in EGFR-driven tumorigenesis. Oncogene *34*, 5971-5982.